2009

Inhibition of the Calcium Plateau Following In Vitro Status Epilepticus Prevents the Development of Spontaneous Recurrent Epileptiform Discharges

Nisha Nagarkatti
Virginia Commonwealth University

School of Medicine
Virginia Commonwealth University

This is to certify that the dissertation prepared by Nisha Nagarkatti entitled Inhibition of the Calcium Plateau Following In Vitro Status Epilepticus Prevents the Development of Spontaneous Recurrent Epileptiform Discharges has been approved by his or her committee as satisfactory completion of the dissertation requirement for the degree of Doctor of Philosophy

Robert J. DeLorenzo, M.D., Ph.D., M.P.H., Director of Dissertation

John Bigbee, Ph.D., School of Medicine

Robert Blair, Ph.D., School of Medicine

Sandra Welch, Ph.D., School of Medicine

Jenny Wiley, Ph.D., School of Medicine

Jerome F. Strauss, III, M.D., Ph.D., Dean, School of Medicine

Dr. F. Douglas Boudinot, Dean of the Graduate School

[Click here and type the Month, Day and Year this page was signed.]

INHIBITION OF THE CALCIUM PLATEAU FOLLOWING IN VITRO STATUS EPILEPTICUS PREVENTS THE DEVELOPMENT OF SPONTANEOUS RECURRENT EPILEPTIFORM DISCHARGES

A Dissertation submitted in partial fulfillment of the requirements for the degree of Doctor of Philosophy at Virginia Commonwealth University.

by

NISHA NAGARKATTI
Artium Baccalaureus, Harvard University, 2004

Director: Robert J. DeLorenzo
Professor
Departments of Neurology, Pharmacology & Toxicology, Biochemistry & Molecular Biophysics

Virginia Commonwealth University
Richmond, Virginia
September, 2009

Acknowledgments

I would like to thank my parents, Drs. Prakash and Mitzi Nagarkatti, and my husband, Davíd Nagarkatti-Gude. Together, these three people have provided continuous support and encouragement in all aspects of my life. My parents have shown by example what it truly means to excel—they continue to be absolutely selfless parents, amazing researchers, and the most loving individuals. I am thankful for their indefatigable support and am constantly in awe of how lucky I have been to have them guide me through life. And somehow, I have found a life companion who possesses these same wonderfully selfless qualities. My husband has provided me with unwavering love and brings to my life not only extraordinary amounts of intelligence and thoughtfulness, but also fills my days with laughter, joy, excitement, and enthusiastic hopefulness about the future. His unfaltering commitment to me and my success has been a tremendous source of strength. I remain perpetually grateful to him and for our time together. I would also like to thank "mi familia"—David, Luti, Danny, Megan, and Marika—I couldn't ask for a more loving extended family! I cannot adequately thank these individuals as they have filled my life with more than words can describe.

I want to also offer special thanks to my advisor, Dr. Robert DeLorenzo. His mentorship has been invaluable and he is a terrific role model for aspiring physician-scientists. I continue to marvel at how he manages to balance it all. He has made himself available to me at all times and exudes a contagious enthusiasm for science and life, which I deeply appreciate. His guidance has been crucial both to my research and my development as a scientist and for this, I am grateful.

I would also like to thank members of the DeLorenzo lab. Drs. Robert Blair, Sompong Sombati, Dawn Carter, Laxmikant Deshpande, and Katherine Falenski for being excellent mentors both in and out of the lab. They bring a great deal of wisdom and knowledge to the lab, from which I have benefitted greatly. Thanks to Elisa Attkisson, her cell culture techniques and assistance in pilocarpine preps have made the work in this dissertation possible. A special thanks to Julie Ziobro, who has shared in all aspects of this experience with me and is not only good at commiserating but is also a great friend. Lastly, thanks to Kristin Fenton, Brendan McKay, and Vasudha Surampudi—it has been a pleasure interacting with each of you over the last few years.

My committee members deserve thanks for all their input and guidance. Drs. Robert Blair, John Bigbee, Sandy Welch, and Jenny Wiley have always been extremely supportive and have not only asked great questions but helped provide me with many answers that have steered my research. Dr. Bigbee, as head of the Neuroscience

program, has been a terrific mentor and has very positively affected my course of study. Finally, I would like to thank Dr. Gordon Archer for his tireless support of us M.D./Ph.D. students. I appreciate that his door has always been open to me and am thankful that the program has such a supportive advocate.

Table of Contents

List of Tables

Page

List of Figures

Page

List of Abbreviations

AED	anti-epileptic drug(s)
AM	acetoxymethylester
ANOVA	analysis of variance
BAPTA	1,2-bis(2-aminophenoxy)ethane-*N,N,N′,N′*-tetraacetate
CA1	cornu ammonis area 1
Ca^{2+}	calcium ion
$[Ca^{2+}]_i$	free intracellular calcium concentration
CaMKII	calcium/calmodulin kinase II
CICR	calcium-induced calcium release
CNQX	6-cyano-7-nitroquinoxaline-2,3-dione
CNS	central nervous system
DIV	day(s) in vitro
DMSO	dimethyl sulfoxide
EEG	electroencephalogram
EGTA	ethylene glycol-bis (β-aminoethyl ether)-N,N,N',N'-tetraacetic acid
ER	endoplasmic reticulum
FBS	fetal bovine serum
GABA	γ-aminobutyric acid
HEPES	N-2-hydroxyethylpiperazine-N'-2-ethanesulfonic acid
HS	horse serum
IP3	inositol 1,4,5-tris-phosphate
IP3R	inositol 1,4,5-tris-phosphate receptor
LEV	levetiracetam
Mg^{2+}	magnesium ion
MK-801	(+)-5-methyl-10,11- dihydro-5*H*-dibenzo[*a*,*d*]cyclohepten-5,10-imine maleate
MΩ	mega-ohm
MEM	minimal essential media
min	minute(s)
mL	milliliter
mM	millimolar
mV	millivolt
n	sample size
Na^{+}	sodium ion
NMDA	N-methyl-D-aspartate
NMDAR	N-methyl-D-aspartate receptor
pBRS	physiological basal recording solution
PBS	phosphate buffered saline
RyR	ryanodine receptor
SE	status epilepticus

SEM	standard error of the mean
TTX	tetrodotoxin
V	voltage

Abstract

INHIBITION OF THE CALCIUM PLATEAU FOLLOWING IN VITRO STATUS EPILEPTICUS PREVENTS THE DEVELOPMENT OF SPONTANEOUS RECURRENT EPILEPTIFORM DISCHARGES

By Nisha Nagarkatti, A.B.

A Dissertation submitted in partial fulfillment of the requirements for the degree of Doctor of Philosophy at Virginia Commonwealth University.

Virginia Commonwealth University, 2009

Major Director: Robert J. DeLorenzo, M.D., Ph.D., M.P.H.
Professor, Departments of Neurology, Pharmacology & Toxicology, and Biochemistry & Molecular Biophysics

Status epilepticus (SE) is a major clinical emergency resulting in continuous seizure activity that can cause brain injury and many molecular and pathophysiologic changes leading to neuronal plasticity. The neuronal plasticity following SE-induced brain injury can initiate epileptogenesis and lead to the ultimate expression of acquired epilepsy (AE), characterized clinically by spontaneous, recurrent seizures. Epileptogenesis is the process wherein healthy brain tissue is transformed into hyperexcitable neuronal networks

that produce AE. Understanding these alterations induced by brain injury is an important clinical challenge and can lend insight into possible new therapeutic targets to halt the development of AE. Currently there are no means to prevent epileptogenesis following brain injury; thus, the elucidation of mechanisms of epileptogenesis will be useful in preventing the long-term clinical sequela. It has been demonstrated in vivo that calcium (Ca^{2+}) dynamics are severely altered during SE and that elevations in intracellular Ca^{2+} ($[Ca^{2+}]_i$) in hippocampal neurons are maintained well past the duration of the injury itself (Ca^{2+} plateau). Here we report that similar changes in $[Ca^{2+}]_i$ are observed in the hippocampal neuronal culture model of SE-induced AE. As an important second messenger, the maintenance of a Ca^{2+} plateau following injury can lead to several changes in gene expression, neurotransmitter release, and overall, neuronal plasticity. Thus, changes in post-SE $[Ca^{2+}]_i$ and Ca^{2+} homeostasis may be important in understanding epileptogenesis and eventually preventing the progression to chronic epilepsy. This dissertation examines the development and maintenance of the Ca^{2+} plateau after SE and demonstrates the novel finding that pharmacological modulation of $[Ca^{2+}]_i$ following SE may inhibit epileptogenesis in vitro.

Chapter 1: General Introduction

Status Epilepticus and Acquired Epilepsy

Epilepsy is one of the most common neurological conditions, affecting about 50 million people worldwide [1] and approximately 2.7 million Americans [2]. It results in an estimated annual cost of $15.5 billion [3] and thus, represents a significant clinical challenge. The condition is characterized by the presence of recurrent, spontaneous seizures, which stem from sudden neuronal hyperexcitability. Approximately 60% of all cases of epilepsy are idiopathic, while the remaining 40% occur following neuronal injury and are thus, classified as acquired. Acquired epilepsy (AE) is a neurological condition characterized by the development of spontaneous, recurrent seizures following a Central Nervous System (CNS) injury such as status epilepticus (SE), stroke, or traumatic brain injury (TBI) [4,5]. The process by which healthy brain tissue is transformed into a hyperexcitable circuit of neurons giving rise to seizures is called epileptogenesis [6,7]. The focus of these studies will be on AE following SE, as 20-40 percent of all cases of SE develop this chronic condition [7,8]. Moreover, experimental models of SE-induced AE remain the most widely studied and best characterized examples of epileptogenesis. Ultimately, the AE produced in these models closely resembles the pathology observed in humans and has provided tremendous insight into molecular mechanisms of

epileptogenesis. Understanding the pathophysiological mechanisms through which SE causes the development of AE would lend insight into mechanisms of neuronal plasticity and also aid in the elucidation of new therapeutic targets to prevent epileptogenesis.

SE has been defined as a medical emergency constituting convulsive or non-convulsive seizures lasting for at least 30 minutes, or multiple seizures without regaining consciousness lasting the same duration of time [9,10]. The seizures can be behavioral or electrographic, which can be determined through electrophysiological monitoring using electroencephalograms (EEG). This particular definition of SE, as described above, was reached following reports in experimental animal models that correlated seizure duration with degree of permanent brain injury; after 30 minutes, animal data indicated significant declines in brain oxygenation and increases in cardiovascular distress and refractoriness to treatment. However, this definition has been revisited because from a treatment standpoint, after 5 minutes of ongoing seizures there is a high likelihood that the seizure will continue for at least 30 minutes and become increasingly difficult to treat [11]. In the United States, the frequency of SE is approximately 100,000-150,000 cases annually with almost 55,000 deaths per year [12]. Various processes can cause SE including metabolic disorders, drug toxicity, head trauma, hypoxia, and stroke. Often chronic conditions such as pre-existing epilepsy, alcohol abuse, or CNS tumors can also precipitate SE [12-15]. Therefore, experimental models are needed to study both SE and SE-induced AE to better understand mechanisms and develop treatments.

Models of SE-Induced AE Provide Important Tools to Study Epileptogenesis

In vivo

There are several different models utilized to study SE-induced AE (Table 1-1). The development of these models has made SE-induced AE more accessible to study than AE caused by other brain injuries, such as stroke and TBI. Moreover, models of AE following SE have provided insight into general mechanisms of neuronal injury [16]. Chemoconvulsants such as pilocarpine and kainic acid, as well as prolonged hippocampal stimulation leading to the spontaneous development of epileptiform activity, are most commonly used to induce SE in animals [17,18]. Electrical stimulation can also be used to trigger SE and is often utilized as a model of epileptogenesis following SE. The pilocarpine model has been used most often in the studies described in this dissertation; thus, in order to understand the model, it is useful to explore the experimental design. Briefly, rats are injected intra-peritoneally with scopolamine to block the peripheral effects of pilocarpine, a muscarinic agonist. 30 minutes later, the animals are treated intra-peritoneally with pilocarpine to trigger SE. The animals are allowed to seize for 1 hr before the seizures are terminated with a benzodiazepine, diazepam. The animals are video-EEG monitored approximately 1 month following SE for the development of recurrent seizures, or epilepsy.

The animal models that utilize chemicals such as pilocarpine follow a progression that correlates closely with the clinical presentation of SE in man. Following SE-induced brain injury, there is a latency period characterized by a lack of seizure activity [4,19,20]. This

period is then followed by the development of spontaneous, recurrent seizures. The progression from SE to AE is thus, often divided into three stages [19,20]: induction or injury (the episode of SE), a latent period of epileptogenesis, and finally the development and chronic occurrence of AE (Figure 1-1, Figures from Chapter 1 are adapted from Nagarkatti et al. [21]). The animal models also share several other characteristics with the human condition. In the pilocarpine model, similarities including hippocampal neuronal death, astrocyte proliferation, and microglial activation are observed [18,22]. Although the in vivo models have the advantage of representing the clinical presentation in an intact animal, they also provide challenges in studying the mechanisms of epileptogenesis, since it is difficult to control many of the variables needed to conduct molecular biological studies in these complex, multi-dimensional systems. Thus, the development of an in vitro model of epileptogenesis has proven to be a useful addition to understanding this clinical condition.

In vitro

Our laboratory has developed an in vitro cell culture model of SE and SE-induced AE using cultured hippocampal neurons plated on glial beds [23]. This model offers a powerful tool to evaluate potential molecular mechanisms underlying epileptogenesis, but has the disadvantage of not representing clinical epilepsy in an intact brain. The in vitro model utilizes a buffer solution with no added magnesium (Mg^{2+}), referred to as "low Mg^{2+}" to trigger epileptiform discharges, the in vitro correlate to SE. These cultures are treated with low Mg^{2+} for three hours (hrs), during which time they manifest continuous

epileptiform discharges as a result of removing the Mg^{2+} block on N-methyl d-aspartate receptor (NMDAR). These discharges occur at a frequency greater than three hertz, consistent with the frequency and characteristics of seizure activity observed in clinical, electrographic SE.

When the neurons are returned to normal, Mg^{2+}-containing maintenance media and patched using whole-cell current clamp electrophysiology, they no longer manifest SE-like continuous epileptiform discharges, the neurons instead show only occasional depolarizations and short epileptiform discharges. By 12 hrs post-low Mg^{2+}, the neurons consistently exhibit spontaneous, recurrent epileptiform discharges (SREDs), characterized by bursts of action potentials over-riding paroxysmal depolarization shifts. At this and all later time points, between six to nine distinct SRED episodes are observed per hour. These SREDs meet the electrophysiological characteristics of seizure discharges observed in patients exhibiting seizure activity. The SREDs persist for the life of the neurons in culture and are synchronous events between networked neurons. Thus, this model utilizes an inciting injury that resembles SE to cause the subsequent development of SREDs, an in vitro correlate to AE. The model exhibits several features consistent with the development of AE in both in vivo models and the clinical condition, including pharmacoresistance to anticonvulsants, cell death, homeostatic changes in Ca^{2+}, and spike frequency [23,24]. Moreover, the cell injury observed in the in vitro and in vivo models correspond to that seen in clinical studies documenting the relationship between SE and neuronal injury [25-27].

The low Mg^{2+} in vitro model and the in vivo models of SE-induced AE are useful tools to study potential molecular mechanisms underlying the induction of AE; however, it is important to note that there are several limitations in these models. Clear differences between the experimental models and the human condition include: duration of latency between SE and the development of epilepsy, percentage of SE cases that develop epilepsy, and comorbidities associated with the pathology [28]. Yet, despite these differences, these models have provided much insight on molecular mechanisms of epileptogenesis and have been useful tools in the elucidation of new therapeutic modalities.

Ca^{2+} Dynamics in the Rat Pilocarpine Model of SE-Induced AE

Both in vivo and in vitro models of SE-induced AE have provided tremendous insights into the molecular and cellular changes that occur during and following SE. This research is important since the characterization of mechanisms that cause AE after brain injuries has significant implications on the development of new treatments to prevent the progression to AE. Recently, several studies have highlighted the novel observation that intracellular Ca^{2+} ($[Ca^{2+}]_i$) dynamics change during an injury such as SE, stroke, or TBI [29-31].

SE causes elevations in $[Ca^{2+}]_i$

One landmark paper demonstrated changes in hippocampal neuronal Ca^{2+} during pilocarpine-induced SE and at various time points post-SE [32]. In brief, rats were treated with the muscarinic agonist, pilocarpine to induce SE. The SE lasted for 1 hr before being

terminated by diazepam, a benzodiazepine. Representative EEG recordings generated from control animals show 'normal' brain activity, whereas traces from animals in SE demonstrate the high frequency epileptiform discharges observed following treatment with pilocarpine (Figure 1-2 A). Using this model, it was possible to evaluate hippocampal neuronal Ca^{2+} levels during and after SE. Thus, during and immediately following SE, the rats were sacrificed, hippocampal tissue was acutely isolated, various regions were dissected out, and neurons were dissociated. $[Ca^{2+}]_i$ levels were evaluated in these neurons using Ca^{2+} indicator dyes. Significant elevations in $[Ca^{2+}]_i$ were observed in hippocampal neurons from the CA1 region immediately following pilocarpine-induced SE but not in those isolated from vehicle-control animals, 850±59 nM and 90 ± 22 nM, respectively (Figure 1-2 B). This represented a 9.4-fold increase in $[Ca^{2+}]_i$ between post-SE neurons and control neurons. These studies suggest that $[Ca^{2+}]_{i,}$ increases during SE.

The Ca^{2+} plateau following SE: Long-term elevations in $[Ca^{2+}]_i$

This same paper identified the presence of a "Ca^{2+} plateau" that is maintained well past the duration of the injury itself in the same rat pilocarpine model of SE-induced AE [32]. $[Ca^{2+}]_i$ was evaluated at 1, 2, 6, 10, and 30 days following SE in acutely isolated CA1 hippocampal neurons (Figure 1-3). Neurons from animals in the SE group exhibited markedly elevated $[Ca^{2+}]_i$ at each of these time points. $[Ca^{2+}]_i$ does decrease over time from the levels observed in neurons isolated from animals immediately after SE. By 6 days post-SE, the $[Ca^{2+}]_i$ has leveled out but interestingly, is still significantly higher than concentrations recorded from neurons in the control group. More studies are being

conducted to better characterize the Ca^{2+} plateau in this model so as to aid in our ability to understand the mechanisms responsible for this novel observation.

SE causes long-term neuroplasticity changes including AE, elevated $[Ca^{2+}]_i$, and altered Ca^{2+} homeostatic mechanisms

To determine whether the changes in Ca^{2+} dynamics were transient or more long-lasting, animals were treated with pilocarpine or vehicle to induce SE and were then maintained for one year post-SE [32]. These animals were evaluated for epilepsy using video-EEG and spontaneous, recurrent seizures were observed only in the pilocarpine group, as shown in representative EEG recordings from control and epileptic animals (Figure 1-4 A). Hippocampal neurons isolated from epileptic animals one year post-pilocarpine demonstrated markedly elevated $[Ca^{2+}]_i$ (325 ± 35 nM)—more than double the values observed in control neurons (Figure 1-4 B).

Neurons from animals displaying the epileptic phenotype were acutely isolated at one-year post-SE and also challenged with glutamate to evaluate whether homeostatic mechanisms were intact. Glutamate, as an excitatory neurotransmitter, stimulates neurons so that Ca^{2+} is released into the cell. Under normal conditions, neurons can recover from this challenge and restore $[Ca^{2+}]_i$ to the concentration observed prior to the stimulation. Neurons from epileptic animals were unable to restore $[Ca^{2+}]_i$ to baseline levels as effectively as control neurons, therefore suggesting persistent alterations in homeostatic mechanisms at this time point (Figure 1-4 C). The observation that neurons in animals from the pilocarpine-treated

group exhibited marked changes in both $[Ca^{2+}]_i$ and Ca^{2+} homeostatic mechanisms one year after the initial injury suggests that Ca^{2+} dynamics post-SE affect plasticity changes and, ultimately, contribute to the maintenance of the chronic, epileptic phenotype.

These studies demonstrated that $[Ca^{2+}]_i$ was elevated and Ca^{2+} homeostatic mechanisms were altered well past the duration of neuronal injury. These changes appear to play a significant role in the maintenance of the epileptic phenotype. The elucidation of the specific mechanisms behind such long-lasting alterations remains an important area of research; moreover, understanding how these changes lead to development or maintenance of chronic epilepsy could provide new information for the development of better treatments or new preventative measures to halt epileptogenesis.

Role of Ca^{2+} in Normal Cellular Physiology

The importance of altered Ca^{2+} dynamics is largely based on Ca^{2+} being an important divalent, cationic charge carrier that serves as a second messenger in cell signaling [33]. Under standard conditions, extracellular Ca^{2+} concentration is significantly higher than intracellular Ca^{2+} concentration ($[Ca^{2+}]_i$) at approximately 1-2 mM and 100 nM, respectively. Regulators of intracellular Ca^{2+} and of Ca^{2+} efflux pathways are primarily responsible for maintaining such low concentrations inside the cell [34].

The large concentration gradient between extracellular and intracellular spaces allows for a high signal to noise ratio and thus, enables Ca^{2+} to serve as a second messenger even upon

the smallest of changes in its intracellular concentration. Transient increases in $[Ca^{2+}]_i$ are required for higher functions such as learning and memory consolidation through the cellular phenomenon of long-term potentiation (LTP) [35]. In addition, such ephemeral elevations are necessary for basic neuronal processes, and thereby play a significant role in synaptic activity and gene expression (Figure 1-5). Moderate to severe injuries can lead to more sustained elevations in $[Ca^{2+}]_i$ resulting in prolonged and often permanent alterations in cellular function—such increases can overwhelm the cell and regulators of cellular homeostasis, leading to the initiation of pro-apoptotic pathways and, ultimately, to cell death [4]. While it is well known that severe elevations in neuronal $[Ca^{2+}]_i$ following injury can lead to both acute and delayed neuronal death [36], studies from our laboratory have demonstrated that the sustained elevations in $[Ca^{2+}]_i$ observed in surviving neurons lead to altered neuronal function and induce neuronal plasticity [4].

Ca^{2+}, through second messenger effects, can alter gene expression, neurotransmitter release, basic cellular functions, and plasticity. Thus, it is important to examine the implications of altered Ca^{2+} dynamics on the development and maintenance of AE in light of recent discoveries in this evolving field. Further elucidating how the observed post-SE Ca^{2+} plateau contributes both to epileptogenesis and the maintenance of AE remains an important area of research. Understanding the mechanisms responsible for the Ca^{2+} plateau may lead to therapeutic approaches to block this long-term elevation in Ca^{2+} after injuries such as SE, therefore leading to the prevention of AE. Thus, learning more about the mechanisms responsible for altered Ca^{2+} dynamics after brain injury has potentially

important implications for both basic scientists and clinicians. The following presents an overview of evidence documenting the development of altered Ca^{2+} dynamics and what is known on how the Ca^{2+} plateau following SE contributes to epileptogenesis and AE.

Mechanisms Underlying Ca^{2+} Changes After SE

Glutamate and NMDA receptors

SE is an excitotoxic injury, meaning it triggers the release of large amounts of the amino acid neurotransmitter glutamate [37-39]. The degree and duration of SE directly affects the concentration of glutamate, which has been reported to exist at extracellular concentrations ranging from 1-5 μM under normal conditions. Excess glutamate following excitotoxic neuronal injuries such as SE causes the over-stimulation of glutamate receptors, including the NMDA receptor that is coupled with a Ca^{2+}-permeable ion channel, thus leading to the excess movement of Ca^{2+} across the cell membrane into the cell (Figure 1-6). While glutamate acts at several receptors, it appears that the NMDA receptor contributes most significantly to the neuronal pathology and to Ca^{2+} changes observed post-injury, as confirmed by the ability of NMDA antagonists to offer neuroprotection when administered prior to injury despite an undiminished SE [40-42]. Several studies have demonstrated that these elevations in glutamate cause neuronal death and that the inhibition of Ca^{2+} overload through the use of NMDA antagonists can prevent both the cognitive sequelae and epileptogenesis [41,43].

A majority of the work demonstrating that epileptogenesis is Ca^{2+}-dependent was performed in the hippocampal neuronal culture model of epilepsy as various pharmacological inhibitors were able to be utilized to tease out which systems were involved in the process. One study correlated electrophysiological activity with intracellular Ca^{2+} imaging in the presence of various Ca^{2+} channel inhibitors in order to determine if any of these channels were contributing to the development of SREDs (Table 1-2) [44]. During the 3 hour low Mg^{2+} treatment, cells were in the presence of either low Ca^{2+} (0.2 mM), 1,2-bis(2-aminophenoxy)ethane-*N,N,N′,N′*-tetraacetate (BAPTA) (100μM), MK-801 (10μM), APV (25μM), 6-cyano-7-nitroquinoxaline-2,3-dione (CNQX) (10μM), 2,3-dihydroxy-6-nitro-7-sulfamoylbenzo[*f*]quinoxaline (NBQX) (10μM), or nifedipine (5μM). No significant changes in spike frequency, intensity, or epileptic discharge duration were observed during in vitro SE under each condition [44]. However, both the Ca^{2+} chelating agent, BAPTA and the low-Ca^{2+} conditions prevented the development of SREDs 48 hrs post-in vitro SE, [44] demonstrating the overall importance of Ca^{2+} in causing SREDs. Furthermore, NMDA receptor antagonists, including MK-801 and APV, exhibited similar effects wherein SE was unaffected but SREDs failed to develop 48 hrs following low Mg^{2+}[44]. In contrast, the AMPA receptor antagonists CNQX and NBQX, as well as the antagonist of L-type voltage gated Ca^{2+} channels, nifedipine, failed to inhibit SREDs at this time-point [44]. Moreover, when Ca^{2+} imaging was performed on the neurons under each condition while the cells were in low Mg^{2+} it was demonstrated that only low extracellular Ca^{2+}, NMDA antagonists, and BAPTA were able to prevent or diminish Ca^{2+} entry during SE [44]. Thus, this study demonstrated in vitro that Ca^{2+} is a

necessary component in the generation of SREDs post-SE and that the NMDA receptor in particular contributes to the Ca^{2+} entry involved in epileptogenesis.

Intracellular regulators of Ca^{2+}

Neurons have a network of endoplasmic reticulum (ER) which contributes to the overall levels of $[Ca^{2+}]_i$ by acting to either release or sequester Ca^{2+} [45]. Ca^{2+} that is stored in the ER can be released through activation of the inositol triphosphate receptors (IP3R) or ryanodine receptors (RyR) [45,46]. These receptors gauge cytoplasmic Ca^{2+} and mediate Ca^{2+}-induced Ca^{2+} release (CICR) from the ER; thus, the channels amplify the Ca^{2+} signal coming from outside the cell. IP3 and cyclic ADP ribose, levels of Ca^{2+} in the ER, and other messengers can influence the sensitivity of these receptors. The ER also has a sequestration mechanism through the sarco/endoplasmic reticulum Ca^{2+} ATPase (SERCA), which pumps Ca^{2+} back into the ER from the cytosol [46]. The ER is able to sequester large amounts of Ca^{2+} under normal conditions.

Thus, SE causes glutamate release that stimulates Ca^{2+} entry into the cell, triggering the activation of CICR wherein RyR and IP3R are activated to release more Ca^{2+} from ER stores [47,48]. During the Ca^{2+} plateau, epileptic neurons show upregulation of CICR mechanisms when compared to control neurons [48]. Interestingly, one study demonstrated that the intracellular injection of IP3 causes epileptiform discharges in hippocampal neurons [49]. Therefore, several groups have examined the ability of anti-epileptic drugs to inhibit IP3 or IP3R as a means to prevent epileptiform activity [50,51].

Moreover, it has also been demonstrated that SERCA is unable to effectively sequester Ca^{2+} in "epileptic" neurons, [48] thus suggesting that this mechanism may contribute to the Ca^{2+} plateau. Future studies should further examine this relationship between SERCA uptake and CICR as they are interdependent processes.

Ca^{2+} binding proteins

Ca^{2+} binding proteins also play an important role in basic physiology further contributing to the maintenance of basal $[Ca^{2+}]_i$. It has been hypothesized that the down-regulation of Ca^{2+} binding proteins also contributes to the elevated $[Ca^{2+}]_i$ maintained during the Ca^{2+} plateau following SE [52]. Several studies utilizing human epileptic hippocampal tissue showed that calbindin levels in the dentate granule cells were diminished [53,54]. The pilocarpine model has yielded similar results wherein it has been demonstrated that at one month after pilocarpine-induced SE, epileptic animals demonstrated a 50% reduction in calbindin protein expression in the hippocampus [52]. These changes were observed up to two years after the initial SE [52]; moreover, calbindin mRNA expression was also decreased in these animals.

These observations have also been noted a few months post-initial injury in other models of epilepsy including those utilizing kindling and kainic acid [55,56]. However, some studies have also shown that following kainic acid or electrically stimulated seizures, calbindin mRNA levels are unchanged or even increased [57-59]. Therefore, these data suggest that following a glutamate-induced Ca^{2+} influx, there is a transient compensatory

up-regulation in calbindin expression, but the long-term elevations in $[Ca^{2+}]_i$ observed in epileptic animals may be attributed to overall down-regulation in protein expression. This suggests that the maintenance of the post-SE Ca^{2+} plateau may be mediated in part by a decrease in Ca^{2+} binding proteins, which normally buffer elevations in Ca^{2+}.

Ca^{2+} regulated enzymes

Ca^{2+}/calmodulin-dependent protein kinase II (CaM kinase II) is an enzyme that plays a major role in the modulation of neuronal excitability through its actions on Ca^{2+}-dependent neuronal processes [60,61]. CaM kinase II has a widespread distribution throughout the nervous system and interestingly, comprises up to 2% of total hippocampal protein [62].

Genetic studies have demonstrated that mice with a null mutation of the alpha-subunit of CaM kinase II show gene dose-dependent neuronal hyperexcitability and seizures [18]. In vitro molecular approaches have yielded supporting data by the demonstration that reduction of α-CaM kinase II levels through antisense oligonucleotides causes spontaneous epileptic discharges in culture [63]. While these studies have provided tremendous insight on CaM kinase II as a means of neuronal excitability, they have not examined whether CaM kinase II expression or activity was actually altered in neurons from epileptic animals or from cultures exhibiting in vitro epilepsy.

In whole animal and slice models that use repeated hippocampal stimulation to elicit SE, decreased CaM kinase II activity has been shown to trigger epileptiform activity [64]. Both

pilocarpine and kainic acid models of SE-induced AE have shown decreased CaM kinase II activity and these results have also been observed in the low Mg^{2+} in vitro hippocampal culture model [65-67]. Interestingly, reduced CaM kinase II activity can be stopped by NMDA receptor antagonists administered prior to SE [61,67]. Thus, the change in CaM kinase II activity appears to be a consequence of NMDA receptor activation. Paradoxically, short-term NMDA receptor activation and the resulting elevations in intracellular Ca^{2+} lead to increased CaM kinase II activation and the translocation of the enzyme from the cytosol to excitatory synapses [68]. The precise role for CaM kinase II in the induction and development of epilepsy is being actively pursued and several studies have discussed in great detail the paradoxical nature of its interactions with NMDA receptors versus the hyperexcitability observed in CaM kinase II knockdown studies [68]. In pentylenetetrazol or electroconvulsive shock studies it has been demonstrated that seizures cause CaM kinase II to translocate from the synapse to the cytosol [65,69]. Therefore, in distancing the enzyme from its substrate, the translocation may serve to further reduce the effective enzymatic activity.

Effects of Elevated $[Ca^{2+}]_i$ on Cellular Function

Cellular Ca^{2+} signaling is a complex process that is difficult to elucidate due to the interdependence of Ca^{2+} handling/regulatory systems. However, clear links between Ca^{2+} levels and membrane excitability, protein phosphorylation, and gene regulation have been demonstrated [70]. Moreover, elevated $[Ca^{2+}]_i$ also has a profound effect on the neuronal circuit, cell death, and glial function. Several studies have demonstrated that this increase

in Ca^{2+} concentration triggers hypertrophy of glia and expression of proteins on glia that are not normally observed [71]. In addition, the elevations in $[Ca^{2+}]_i$ have been shown to activate genes for growth factors, including brain-derived neurotrophic factor and fibroblast growth factor, induce changes in glutamate receptors, and cause altered expression of cytoskeletal proteins [71]. All of these alterations significantly affect the development or maintenance of the epileptic circuit [72]. Developing efficacious therapeutic strategies may be aided by a more thorough understanding of Ca^{2+} dynamics in neurons and how these alterations in Ca^{2+} can affect glia and the neuronal circuit.

Generally, the degree of Ca^{2+} influx contributes greatly to the level of injury sustained by the neurons and impacts the overall fate of the cell. Severely injured cells exhibit an irreversible Ca^{2+} overload that leads to cell death through various means, some of which include: the disruption of cytoskeletal organization, formation of cell membrane blebs, activation of Ca^{2+}-dependent endonuclease leading to chromatin cleavage, and mitochondrial impairment resulting in loss of ATP synthesis [73]. Notably, cell death is a prominent manifestation immediately after SE where $[Ca^{2+}]_i$ increases dramatically with a percentage cell death of approximately 10-15% in vivo [41] and 15% in vitro [24]. Interestingly, epilepsy itself did not cause more cell death in vitro, in vivo, or in human studies [24,74-78]. Thus, although the elevated Ca^{2+} plateau is maintained, the levels are not high enough to induce significant cell death, but can cause permanent alterations in neuronal homeostasis.

The neurons that survive SE undergo altered Ca^{2+} homeostasis but not necessarily an irreversible Ca^{2+} overload; therefore, since dead neurons do not seize, it is these injured but surviving neurons that serve as the substrate for epileptogenesis. These neurons sustain reversible elevations in $[Ca^{2+}]_i$ that are maintained over days or weeks [32]—these increases mediate changes in synaptic plasticity, gene expression, and neuronal function. Therefore, the overall increased $[Ca^{2+}]_i$ directly affects nuclear Ca^{2+} levels and leads to the induction of gene transcription of several pro-apoptotic or epileptogenic genes and alters neuronal functions including excitability, transmitter release, and neurotoxicity [79]. One effect is that increases in $[Ca^{2+}]_i$ activate an enzyme, calcineurin, leading to a downstream cascade of events including an accelerated internalization of $GABA_A$ receptors, resulting in decreased inhibitory neurotransmission [18,80]. Thus, it is the injured neurons and these molecular changes that become potential targets for future therapies to prevent AE. The ability to target these intracellular changes and reduce the Ca^{2+} load may prevent the development of the epileptic phenotype following SE or other neuronal injuries.

Summary and Rationale

Epilepsy is a common condition affecting 1-2% of the world's population and can significantly impact an individual's quality of life. While much progress has been made in the development of treatments that can inhibit seizures, still approximately 30% of all people with epilepsy are resistant to anti-convulsant therapies [72,81]. Moreover, 40% of all cases of epilepsy are acquired following neuronal injury [81]. The development of AE can be divided into three phases: the injury itself (in this case, SE), followed by a latency

period during which the neurons are undergoing the changes that lead to the final phase, the chronic epileptic phase wherein an individual displays recurrent seizures. This transformation from healthy brain tissue to hyperexcitable neuronal networks responsible for seizure activity is called epileptogenesis. Thus, studying the pathophysiological changes that occur during epileptogenesis could not only bolster our understanding of plasticity following brain injury but also aid in the development of anti-epileptogenic agents. Currently, many anti-epileptic drugs (AEDs) exist that inhibit or dampen seizures in epileptic individuals; however, no therapeutics exist that can be given immediately after an injury to prevent the ultimate development of epilepsy. Thus, the latency period between the injury and the development of AE represents a therapeutic window of opportunity in preventing epileptogenesis.

Recently, several studies have demonstrated that Ca^{2+} dynamics are severely altered during SE and remain altered in those animals that develop AE following SE [4,32]. In the in vivo rat pilocarpine model of SE-induced AE, $[Ca^{2+}]_i$ increases during SE and remains elevated for at least one year post-SE in those animals that later develop epilepsy [32]. Moreover, hippocampal neurons from epileptic animals also demonstrate persistent alterations in homeostatic mechanisms, which may contribute to the altered phenotype [32]. Thus, the modulation of $[Ca^{2+}]_i$ and Ca^{2+} regulatory systems by pharmacological agents immediately following neuronal injuries such as SE may help to prevent epileptogenesis.

The animal model utilized in many of the studies described above, while closely resembling the human condition, remains a challenging tool to study pharmacological effects or discern molecular mechanisms because of the difficulties in manipulating the system and controlling for variables. Therefore, we were interested in testing whether similar changes as we observed in vivo also occurred in the in vitro low Mg^{2+} model of SE-induced AE. If so, this well-characterized model would serve as an ideal tool to better elucidate molecular mechanisms as well as to perform high throughput screening tests on various pharmacological compounds.

Central Hypothesis

Studies utilizing the rat pilocarpine model of SE-induced AE have demonstrated that $[Ca^{2+}]_i$ in hippocampal neurons increases during SE, and that these elevations are maintained only in those animals that go on to develop epilepsy. Ca^{2+} is an important second messenger; therefore, changes in its concentration may be responsible for alterations in cellular function, neurotransmitter release, and, ultimately, neuronal plasticity. Therefore, modulation of calcium post-injuries represents an interesting approach to understanding and potentially preventing epileptogenesis. Our central hypothesis is that increases in $[Ca^{2+}]_i$ that are triggered by neuronal injury play a role in mediating epileptogenesis and neuronal plasticity. To test this hypothesis we have employed the in vitro low Mg^{2+} model, as hippocampal neuronal cultures provide an appropriate model to test both pharmacological and molecular modifications as external

variables are more easily controlled. In order to address this hypothesis we will focus on the following aims:

1) Evaluate whether changes in $[Ca^{2+}]_i$ observed in the in vivo model of SE-induced AE are also present in the low Mg^{2+} hippocampal neuronal culture model

2) Develop pharmacological means to lower $[Ca^{2+}]_i$ post-injury (SE)

3) Evaluate whether lowering $[Ca^{2+}]_i$ can prevent the expression of spontaneous recurrent epileptiform discharges, the in vitro correlate to epilepsy

The conclusions reached from this dissertation demonstrate that similar alterations in $[Ca^{2+}]_i$ are observed in the low Mg^{2+} model as were demonstrated in vivo. Various pharmacological agents have been tested to determine both which Ca^{2+} regulatory systems are contributing to the Ca^{2+} plateau and whether overall lowering Ca^{2+} can inhibit epileptogenesis in the in vitro model of SE-induced AE.

Table 1-1. Models of SE-induced AE.

	Inciting Agent	Name of Model
In Vitro Models		
Hippocampal Neuronal Culture	3 hr treatment with low Mg^{2+} containing solution to mimic SE	Low Mg^{2+} model
In Vivo Models		
Rat/Mouse		
Chemical:	SE induced by treatment with pilocarpine	Pilocarpine model
	SE induced by treatment with kainic acid	Kainic acid model
Electrical:	SE induced by electrical stimulation	Electrical stimulation model

Figure 1-1. The progression to AE: Phases of epileptogenesis.
Injuries to the Central Nervous system such as SE (down arrow) can elicit permanent changes in neurons, resulting in the development of epilepsy. The period between the inciting injury (down arrow) and the manifestation of recurrent seizures or epilepsy (black) is called epileptogenesis (gray). This gray period may provide a therapeutic window of opportunity wherein the use of pharmacological agents or molecular tools can prevent the transition of healthy brain tissue to a hyperexcitable network manifesting spontaneous recurrent epileptiform discharges.

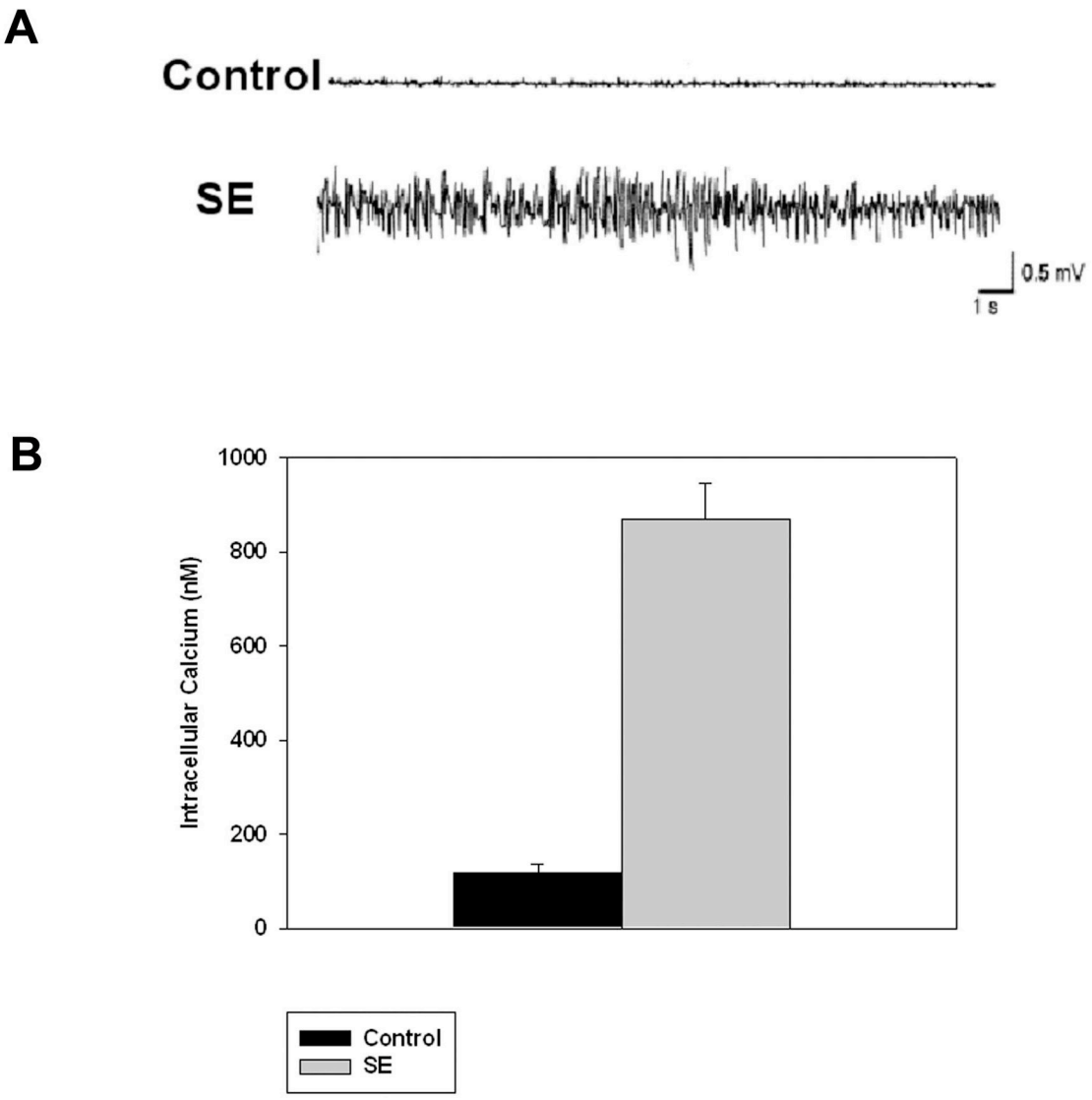

Figure 1-2. SE causes increased $[Ca^{2+}]_i$ acutely in the in vivo pilocarpine model. **A,** representative EEG recording from control (vehicle) rats and rats in pilocarpine-induced SE. **B,** bar graph demonstrating that $[Ca^{2+}]_i$ is higher in neurons from animals immediately following SE when compared to those from animals in the control group—850 ± 59 nM and 90 ± 22 nM, respectively (data expressed as mean ± SEM).

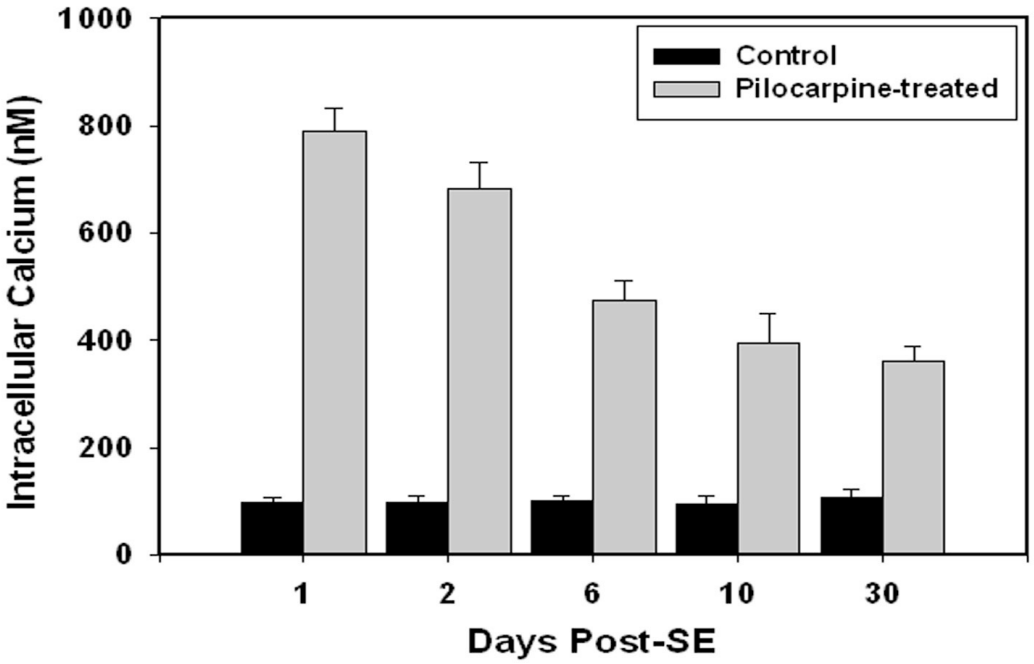

Figure 1-3. The Ca^{2+} plateau following SE. At one day post-SE, $[Ca^{2+}]_i$ are significantly elevated when compared to controls, 790 ± 43 nM and 98 ± 10 nM, respectively (all data expressed as mean ± SEM). Two days post-SE the $[Ca^{2+}]_i$ is 684 ± 47 nM, which is significantly higher than the 96 ± 14 nM observed in the control. At six days following SE, the $[Ca^{2+}]_i$ is still markedly elevated when compared to controls yet has fallen slightly from earlier timepoints, 475 ± 36 nM and 100 ± 10 nM, respectively. $[Ca^{2+}]_i$ falls slightly at 10 days post-SE to 395 ± 56 nM but is still significantly elevated when compared to the controls with $[Ca^{2+}]_i$ of 95 ± 14 nM. Finally, at 30 days post-SE the $[Ca^{2+}]_i$ is 361 ± 28 nM versus 106 ± 16 nM in controls. The persistent elevation in $[Ca^{2+}]_i$ represents the Ca^{2+} plateau.

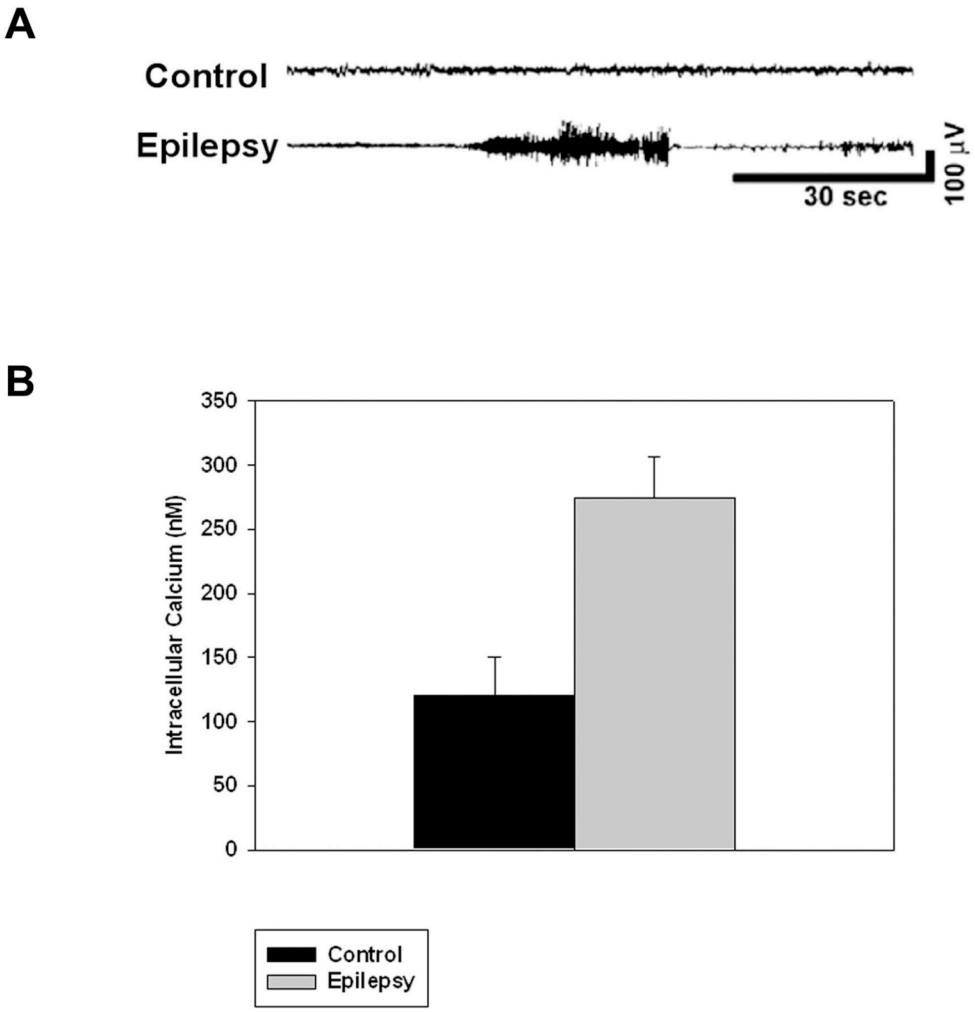

Figure 1-4. AE is associated with alterations in $[Ca^{2+}]_i$ and Ca^{2+} homeostatic mechanisms one year post-in vivo SE. A, representative EEG recording from control (vehicle) rats and epileptic rats (following pilocarpine-induced SE). **B,** bar graph with neurons from epileptic animals at one year post-SE demonstrating $[Ca^{2+}]_i$ of 325 ± 35 nM (data represented as mean ± SEM), which is significantly higher than neurons from control group. **C,** upon glutamate stimulation, the $[Ca^{2+}]_i$ increases and then returns to baseline in neurons from the control group, unlike neurons from the epileptic group which also peak but then fail to return to baseline.

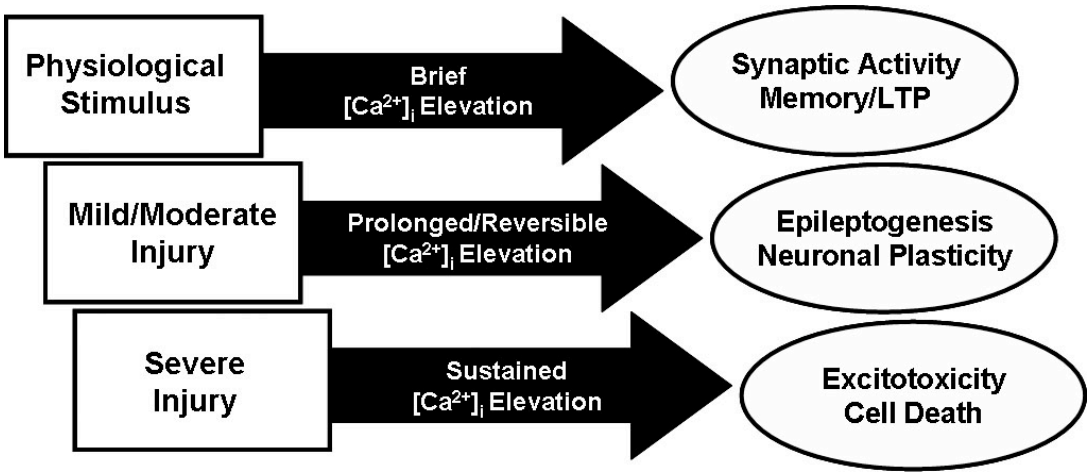

Figure 1-5. Effect of elevated $[Ca^{2+}]_i$ on neurons. Normal stimuli cause transient elevations in $[Ca^{2+}]_i$ that control synaptic activity and are responsible for learning and memory (top arrow). Mild to moderate injuries may cause prolonged elevations in $[Ca^{2+}]_i$ that are ultimately reversible (middle arrow). Such elevations are not substantial enough to initiate cell death but are able to cause plasticity changes in neurons, leading to epileptogenesis. Finally, severe injury causes sustained, massive increases in $[Ca^{2+}]_i$ that lead to cell death (bottom arrow).

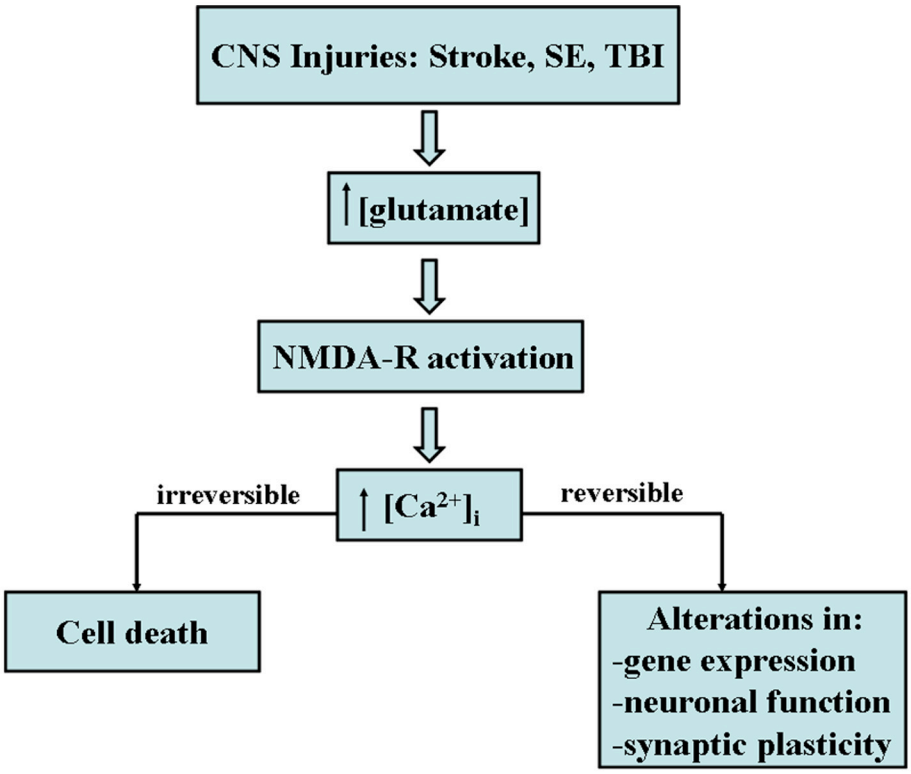

Figure 1-6. CNS injuries cause death or plasticity changes in neurons. CNS injuries such as stroke, SE, and TBI can lead to one of two fates for affected neurons. First, all injuries cause increases in glutamate concentration, which leads to the over-stimulation of glutamatergic receptors, including NMDA receptors (NMDAR). The activation of these receptors trigger an influx of Ca^{2+} across the cell membrane and cause a Ca^{2+} overload. This elevation in $[Ca^{2+}]_i$ can be irreversible and overwhelm cellular processes, resulting in cell death. In contrast, neurons that are less severely injured exhibit a sustained but reversible increase in $[Ca^{2+}]_i$ that leads to alterations in gene expression, neuronal function, and synaptic plasticity through second messenger systems.

Table 1-2. Effect of Ca^{2+} Inhibitors on SE and SREDs. The first column shows the various conditions including control and low Mg^{2+} treated neurons as well low Mg^{2+} neurons that were then treated with Ca^{2+} channel inhibitors. The second column shows $[Ca^{2+}]_i$ levels observed in each condition. The third and fourth columns show whether or not the neurons developed SREDs (epilepsy) or whether the frequency of SE was changed under each condition, respectively. Data is represented as mean ± SEM for $[Ca^{2+}]_i$ and SE spike frequency and as all or none effects for the development of epilepsy.

Condition	$[Ca^{2+}]_i$, nM	Epilepsy	SE spike frequency
Control	165 ± 10	No	0
Low-Mg^{2+} (SE)	577 ± 35	Yes	12 ± 4.4
+ Low Ca^{2+} (0.2 mM)	177 ± 18	No	10 ± 3.2
+ BAPTA (100 µM)	160 ± 8	No	14 ± 5.1
+ APV (25 µM)	293 ± 24	No	16 ± 3.8
+MK-801 (10 µM)	287 ± 25	No	11 ± 2.9
+CNQX (10 µM)	433 ± 10	Yes	9 ± 3
+NBQX (10 µM)	422 ± 56	Yes	8 ± 2.4
+Nifedipine (5 µM)	441 ± 19	Yes	13 ± 4.1
+TTX (1 µM)	157 ± 17	No	0

Chapter 2: Characterization of the Calcium Plateau In Vitro

Introduction

It has been demonstrated in the in vivo pilocarpine model of SE-induced AE that Ca^{2+} dynamics are significantly altered during SE and that these alterations are maintained well past the duration of the injury itself [4,32]. As an important second messenger that is highly regulated so as to maintain low intracellular levels, such alterations could have tremendous implications in terms of plasticity and ultimately, in the development of epilepsy following SE. One study published the novel finding that intracellular Ca^{2+} ($[Ca^{2+}]_i$) is elevated almost 8-fold in hippocampal neurons acutely isolated from animals immediately following SE when compared to those isolated from controls [32]. Interestingly, this elevation exists in hippocampal neurons, particularly those from the Cornu Ammonis area 1 (CA1) region, but not in frontal or occipital neurons. This result corresponds to the well-recognized observation that the hippocampus is often most vulnerable to seizure activity [82] and likely to exhibit increased plasticity changes following injury. Moreover, this same study evaluated $[Ca^{2+}]_i$ at various time points post-SE to determine whether the elevations observed acutely were more long-lasting or ephemeral. It was demonstrated that $[Ca^{2+}]_i$ falls gradually over the course of the week following SE. However, at all latter time points (days 6, 10, 30, and 1 year) post-SE, the

$[Ca^{2+}]_i$ remains significantly elevated when compared to levels recorded in neurons from either control animals or those animals that fail to develop AE following SE [32]. This study suggests that SE causes elevations in $[Ca^{2+}]_i$ and these sustained elevations may be involved in the pathophysiology of epileptogenesis. Therefore, it follows that modulation or inhibition of $[Ca^{2+}]_i$ immediately after SE, may potentially prevent the development of AE. However, since the precise mechanisms through which increased $[Ca^{2+}]_i$ are maintained following SE remain unclear, it would be beneficial to study the pathophysiologic changes in an in vitro model wherein the system is more easily manipulated through molecular biological or pharmacological means.

The purpose of this study is to evaluate $[Ca^{2+}]_i$ in an in vitro model of SE-induced AE to determine if the changes observed in vivo also occur in this model. If so, the model would be a tremendous tool in the evaluation of new therapeutic modalities aimed at restoring Ca^{2+} homeostasis post-injury. The hippocampal neuronal culture model of SE-induced AE is a well-characterized model that utilizes a solution with no added Mg^{2+} (low-Mg^{2+}) to simulate SE [23]. Once the Mg^{2+} is restored to these cultures and the cells are later evaluated by whole-cell current clamp electrophysiology, spontaneous, recurrent epileptiform discharges (SREDs) are observed for their life in culture. These SREDs are the in vitro correlate to epilepsy. The hippocampal neuronal culture model is an excellent in vitro model in that it closely corresponds to the human condition in several ways. The spike frequency of epileptiform discharges during in vitro SE is greater than 3 Hz, which meets the clinical definition of SE [83]. Moreover, the in vitro SREDs manifested in this

culture model mimic the electrographic features observed in epilepsy. Due to similarities between the human condition and this model, the model has been employed to characterize electrophysiological, cellular, and molecular mechanisms underlying SE and epileptogenesis [4,67,83]. Similarities in pharmacoresistance, changes in biochemical markers, and cell death have also been demonstrated between the clinical condition and both in vivo and in vitro models [24,84]. Thus, the hippocampal neuronal culture model provides a useful tool to evaluate changes in Ca^{2+} dynamics post-in vitro SE.

Materials and Methods

Hippocampal neuronal culture preparation

Hippocampal tissue was harvested from 2-day postnatal Sprague-Dawley rats (Harlan, Indianapolis, IN) in phosphate buffered saline (PBS) with sucrose, N-[2-Hydroethyl]piperazine-N'[2-ethanesulfonic acid] (HEPES), and penicillin (10,000 units/mL) but no added Ca^{2+} or Mg^{2+}. The dissection PBS was maintained at 4◦ and the dissection itself was performed at room temperature. Hippocampal tissue was separated from vasculature and meninges under a dissection microscope and was subjected to 0.25% trypsin at 37°C for 30 minutes, followed by mechanical trituration using fire-polished Pasteur pipettes. Cells were counted on a hemocytometer (Scientific Apparatus, Philadelphia, PA) using the trypan blue dye exclusion method to estimate the concentration of cells in suspension. The single cell suspension was diluted to a concentration of $1x10^5$ cells/mL in either glial feed (minimal essential media (MEM) with Earle's Salts (Invitrogen, Carlsbad, CA), 25 mM HEPES, 2 mM L-glutamine, 3 mM glucose, and 10%

fetal bovine serum (FBS)) or neuronal feed (MEM with Earle's Salts, 25 mM HEPES, 2 mM L-glutamine, 3 mM glucose, 100 µg/ml transferrin, 5 µg/mL insulin, 100 µM putrescine, 3 nM sodium selenite, 200 nM progesterone, 1 mM sodium pyruvate, 0.1% ovalbumin, 0.2 ng/mL triiodothyroxine, and 0.4 ng/mL corticosterone) supplemented with 5% horse serum (HS).

To grow glial cultures, $1x10^5$ or $5x10^4$ cells in glial feed were plated onto 35 mm plastic culture dishes or Lab-Tek 2-well glass chambers (Nunc, Naperville, IL), respectively, that were previously coated with 0.05 mg/ml poly-L-lysine. The cultures were maintained at 37°C in a 5% CO_2/95% O_2 atmosphere and culture media was replaced three times per week with fresh glial feed. The glia were grown until confluent and were then treated with 5 µM cytosine arabinoside for two days to halt cell division. On the 10^{th} day in vitro (DIV), the culture media was replaced with glial feed supplemented with 5% HS instead of FBS. Then, on the 13^{th} DIV, the glial feed supplemented with HS was replaced with neuronal feed supplemented with 5% HS.

On the 14^{th} DIV, cells ($8.75x10^4$ for glass slides; $2x10^5$ for 35 mm culture dishes) suspended in neuronal feed plus 5% HS were plated onto the confluent glial beds. Cultures were maintained under standard conditions at 37°C in a 5% CO_2/95% air atmosphere and were fed twice weekly with neuronal feed containing 20% conditioned media. Neurons were allowed to mature and all experiments were performed 14-18 days

following plating of neurons to allow formation of networks, adequate neuronal maturation, and development of NMDA receptors.

Whole-cell current clamp electrophysiology

Hippocampal neuronal cultures were transferred to the temperature-controlled stages of either a Nikon Diaphot inverted microscope (Garden City, NY) or Olympus IX-70 (Olympus, Center Valley, PA) in order to perform electrophysiological recordings. A Flaming-Brown P-80C electrode puller (Sutter Instruments, Sarasota, FL) was utilized to pull patch microelectrodes from thin borosilicate glass capillaries (World Precision Instruments, Inc., Sarasota, FL). Only microelectrodes with a resistance of 3-7 MΩ were used to patch cells. These microelectrodes were filled with an internal solution consisting of (in mM): 140 K^+ gluconate, 1 $MgCl_2$, 10 HEPES, 1.1 ethylene glycol tetraacetic acid (EGTA), adjusted to pH 7.2, 310 mOsm.

An Axopatch 200A amplifier or an Axoclamp-2A amplifier (Axon Instruments, Foster City, CA) in current clamp mode was used to obtain recordings from phase-bright pyramidal-shaped neurons. The filled microelectrode was secured to the amplifier headstage and moved using the course-manipulators until the tip is above the neuron to be patched. Offset potentials were nulled and fine-adjustment manipulators were then used to position and lower the microelectrode so that it made contact with the surface of the neuron of interest. Negative pressure was gently applied through the microelectrode to form a giga-ohm seal and rupture the membrane in the microelectrode tip. Compensation

for capacitance was performed and recording was initiated. Together, the Neuro-corder DR-890 (Neurodata Instruments Corp, New York, NY) and Sony Videocassette Recorder allowed for digitization and storage of data on videocassettes. Acquired data were then analyzed by playing recordings back through a Dash IV chart recorder (Astro-Med Inc., Warwick, RI) or to a computer via a Digidata 1322A (Axon Instruments, Foster City, CA). Perfusions of drugs into the system were performed using a six-valve perfusion system (Warner Instrument Corp., Hamden, CT) at a rate of 1 mL/minute.

Calcium microfluorometry

To determine $[Ca^{2+}]_i$ in hippocampal neuronal cultures, cells were loaded with Fura-2-acetoxymethyl ester (AM) (Molecular Probes, Eugene, OR), a high affinity (K_d=145nM) Ca^{2+} indicator dye. Fura-2AM is able to cross cell membranes and once inside the cell, the AM groups are cleaved by intracellular esterases leaving the cell-impermeant Fura-2 inside the cell. Once the dye binds to Ca^{2+}, Fura-2 exhibits an absorption shift that can be observed by exciting the dye at 340 nm instead of 380 nm, the excitation wavelength used to measure unbound Fura-2. The emission generated by either of these wavelengths can be measured at 510 nm. Therefore, alternating excitation wavelengths of 340 nm and 380 nm are utilized to quantify the relative concentration of Ca^{2+}-bound Fura-2 and Ca^{2+}-free Fura-2. Thus, the resulting 340/380 ratio recorded corresponds directly to the total concentration of Ca^{2+} inside the cell and can be used to determine changes in $[Ca^{2+}]_i$. Moreover, the utilization of the 340/380 ratio is important in that it accounts for potential

confounders such as unequal loading for Fura-2 or variable cell thickness from interfering with the measurements.

Hippocampal neuronal cultures were loaded with 1μM Fura-2AM dissolved in 0.1% dimethyl sulfoxide (DMSO) and incubated at 37˚C in 5% CO_2/95% air for 30 min. The cultures were then washed so as to terminate dye-loading. Following the wash, the cells incubated for another 15 minutes to maximize cleavage of the AM moiety by intracellular esterases. The cultures were then transferred a heated stage (Harvard Apparatus, Holliston, MA) wherein the temperature of the cultures could be maintained at 37°C. Pyramidal, phase-bright neurons were visualized through the 20X, 0.7 numerical aperture fluorite water immersion objective on an Olympus IX-70 inverted microscope. The Fura-2 was excited by alternating excitation wavelengths of 340 nm and 380 nm, created through filtering light from a 75 W xenon arc lamp through optical filters on a Lambda 10-2 wheel (Sutter Instruments Co., Novato, CA). Emissions were captured at 510 nm through a 400 nm dichroic mirror in a Fura filter cube (Olympus, Center Valley, PA) by using a Hamamatsu ORCA-ER digital, charged-coupled device (CCD) camera (Hamamatsu, Bridgewater, NJ). This system is connected to the fluorescent imaging software, MetaFluor (Olympus, Center Valley, PA), which allows for image acquisition and analysis. Images were acquired from any given field at various time intervals depending on the specific experiment and background fluorescence was subtracted from all acquired data by imaging hippocampal neuronal cultures that were not loaded with Fura-2. Ratio

values can be converted to $[Ca^{2+}]_i$ using calibration curves described [85] or can be left as ratio values, which correlate directly with $[Ca^{2+}]_i$.

In vitro SE and SREDs in hippocampal neuronal cultures

In vitro SE was generated using the low Mg^{2+} model [18] that was developed in the DeLorenzo lab. Maintenance media (neuronal feed plus conditioned media) was removed from the hippocampal neuronal cultures and replaced with physiological basal recording solution (pBRS) consisting of: 145 mM NaCl, 2.5 mM KCl, 10 mM HEPES, 10 mM glucose, 2 mM $CaCl_2$, 1 mM $MgCl_2$, 0.002 mM glycine, adjusted to pH 7.3, 325 mOsm or pBRS without the $MgCl_2$ (hereafter referred to as, low Mg^{2+}). The cells then incubated at 37 °C under 5% CO_2/95% air atmosphere for 3 hours (hrs). During this time, neurons were patched using whole-cell current clamp electrophysiology to determine whether cells in low Mg^{2+} demonstrated high frequency spiking of greater than 3 Hertz (Hz) in frequency, which is characterized as the in vitro correlate to SE. The neurons treated with pBRS served as the controls for the low Mg^{2+}-treated group.

After 3 hrs of low Mg^{2+} or pBRS treatment, the cells were returned to normal, Mg^{2+}-containing maintenance media and were evaluated using whole-cell current clamp electrophysiology at least 12 hrs post-in vitro SE to determine expression of in vitro epilepsy, or SREDs. SREDs are characterized by bursts of action potentials over-riding paroxysmal depolarization shifts. The 3 hr treatment duration was determined after it was demonstrated that 1 and 2 hrs of low Mg^{2+} exposure did not produce consistent

epileptogenecity [23]; whereas, following 3 hrs, greater than 95% of all neurons sampled expressed permanent alterations in excitability. Interestingly, a 4 hr exposure produced more extensive cell death, leading to greater variability in the results, as network connectivity is important in the development of SREDs [23].

Glutamate challenge: Assessing Ca^{2+} homeostatic mechanisms

In order to assess Ca^{2+} homeostatic mechanisms, neurons were loaded with Fura-2AM and challenged with 50 μM glutamate for 2 minutes. After this time, the cultures were washed with pBRS to remove the glutamate. 340/380 ratio images were captured every 30 seconds to record both the response to and recovery from glutamate exposure.

Statistical analysis

To determine statistical significance of Ca^{2+} imaging data, a one-way Analysis of Variance (ANOVA) test was employed, followed by Fisher's post-hoc test when appropriate. A p-value<0.05 was considered statistically significant. Statistical analysis will be performed using SigmaStat 3.0 or SigmaPlot (Systat Software, San Jose, CA).

Results

In order to determine if the in vitro model of SE-induced AE resembles the in vivo pilocarpine model in terms of changes in $[Ca^{2+}]_i$, neurons were treated with low Mg^{2+} and then evaluated at various time points through both whole-cell current clamp

electrophysiology to determine activity as well as calcium imaging to quantify changes in Ca^{2+}.

Treatment of hippocampal neuronal cultures with low Mg^{2+} causes in vitro SE

Similarly to previous results published by our laboratory [23], replacing neuronal maintenance media with low Mg^{2+} produced continuous, high frequency epileptiform activity consistent with SE (Figure 2-1 B). This frequency of epileptiform discharges was recorded to be greater than 3 Hz, which is in accordance with the frequency of SE discharges observed in humans. The high frequency discharges were observed immediately after replacing the maintenance media with the low Mg^{2+} solution and were quickly abolished (within ~1 min) upon restoration of $MgCl_2$. This activity observed in neurons treated with low Mg^{2+} was in contrast to control neurons that were treated with Mg^{2+}-containing pBRS. These control neurons showed only occasional action potentials (Figure 2-1 A), consistent with the activity observed in naïve neurons.

In vitro SE causes a significant elevation in $[Ca^{2+}]_i$

While the neurons were still in low Mg^{2+}, the cultures were loaded with the Ca^{2+} indicator, Fura-2AM. Fluorescent ratio values were obtained using alternating excitation wavelengths of 340 nm and 380 nm. The resulting 340/380 ratios correspond directly to $[Ca^{2+}]_i$. Moreover, pseudocolor images were generated wherein individual pixels from the captured image are assigned a color based on the associated grayscale values, which correspond to Ca^{2+} levels. Red is associated with a higher grayscale value and thus, more

Ca^{2+}; whereas, at the other end of the colorimetric spectrum, blue is associated with lower grayscale values and less Ca^{2+}. Pseudocolor allows for better visualization of changes in $[Ca^{2+}]_i$. An increase from control, baseline $[Ca^{2+}]_i$ was observed while the neurons were in the low Mg^{2+} solution (in vitro SE). The Fura-2 340/380 ratios increased from 0.39±0.05 in control neurons to 0.78±0.05 in neurons after 3 hrs of low Mg^{2+} (Figure 2-2 A). Pseudocolor images confirmed these changes in Fura-2 ratios with increased ratios in neurons post-low Mg^{2+} (Figure 2-2 B, right panel) but not in the sham controls (Figure 2-2 B, left panel). Previous studies have shown with high speed simultaneous electrophysiological and Ca^{2+} imaging that each epileptiform spike was associated with increases in $[Ca^{2+}]_i$.

Three hours of low Mg^{2+} treatment leads to the development of in vitro epilepsy (SREDs)

To evaluate Ca^{2+} dynamics following SE, cultured hippocampal neurons were patch-clamped to study electrophysiological activity and also imaged for evidence of alterations in Fura-2 ratios 24 hrs post-low Mg^{2+} treatment [23,86]. When patched using whole-cell current clamp techniques, the low-Mg^{2+} treated cells consistently displayed SREDs (Figure 2-3 B) unlike the sham-control neurons, which failed to show SREDs (Figure 2-3 A). Each event was spontaneous and on average, 8 events were observed per hour. In accordance with previous studies in our lab, most SREDs lasted for ~30 sec with some extending for 1-2 min in duration [23]. These SREDs recorded in cultures that were

treated with low Mg^{2+} resembled what is generally observed in clinical epilepsy, with the in vitro seizure episodes consisting of paroxysmal depolarization shifts.

Elevations in $[Ca^{2+}]_i$ are maintained for at least 24 hours post-in vitro SE

At the same time time-point upon which neurons were patched to look for SREDs, neurons were also loaded with Fura-2 to determine $[Ca^{2+}]_i$. In brief, hippocampal neuronal cultures were treated with low Mg^{2+} for 3 hrs, returned to Mg^{2+}-containing maintenance media, and then loaded with Fura-2 24 hrs post-in vitro SE. 340/380 ratios were recorded as a direct indicator of $[Ca^{2+}]_i$. Ratio values in low Mg^{2+} treated cells appeared significantly elevated when compared to control neurons even at 24 hrs post-in vitro SE. This was indicated by an increase in Fura-2 340/380 ratios from 0.40±0.02 in control neurons to 0.46±0.02 in low Mg^{2+} neurons (Figure 2-4).

Neurons displaying SREDs exhibit alterations in Ca^{2+} homeostatic mechanisms

In addition, SE caused permanent changes in plasticity as demonstrated by alterations in Ca^{2+} homeostatic mechanisms. Neurons were briefly stimulated with 50μM glutamate for 2 minutes to test the ability of Ca^{2+} homeostatic mechanisms to compensate for brief excitatory challenges. These cells demonstrated a markedly diminished ability to recover from the insult (Figure 2-5) suggesting that the homeostatic mechanisms, which under normal conditions maintain tight control of Ca^{2+} influx, efflux, and sequestration are altered or diminished following SE. Stimulation with glutamate resulted in an increase in $[Ca^{2+}]_i$ both in control and post-SE neurons; however, in neurons treated with low Mg^{2+},

Ca^{2+} never returned to basal levels and showed a decreased rate of recovery when compared to controls.

Discussion

These results demonstrate that the low Mg^{2+} hippocampal neuronal culture model of SE-induced AE may prove to be a useful tool in studying epileptogenesis. The in vitro SE that was produced resembled the human condition in spike frequency and the model reproducibly caused SREDs, the in vitro correlate to epilepsy. Finally, and most interestingly, several pathophysiological features observed in the rat pilocarpine model of SE-induced AE also exist in this culture model, making it a useful tool to better understand molecular/cellular changes and develop new therapeutics before testing in the animal model. We demonstrated in this study that, much like the in vivo model, increases in $[Ca^{2+}]_i$ were observed during SE and that these elevations were maintained for at least 24 hrs post-SE. Moreover, as observed in hippocampal neurons acutely isolated from epileptic animals, cultured neurons that displayed SREDs also showed a decreased ability to recover from a glutamate challenge. This suggests that epilepsy alters Ca^{2+} homeostatic mechanisms and that this may contribute either to the development or maintenance of the chronic epileptic phenotype.

These studies demonstrated that well past the duration of in vitro SE, $[Ca^{2+}]_i$ was elevated and Ca^{2+} homeostatic mechanisms were altered in the low Mg^{2+} culture model of SE-induced AE. In the in vivo model wherein approximately 2/3 of the animals develop

epilepsy following SE, only the animals that have increased hippocampal $[Ca^{2+}]_i$ develop epilepsy [32]. This finding suggests that the changes in Ca^{2+} appear to play a significant role in the maintenance of the epileptic phenotype. Moreover, it has also been demonstrated in stroke-induced epileptogenesis that increases in $[Ca^{2+}]_i$ are not simply triggered by the seizure activity itself, because in vitro treatment of neurons showing SREDs with tetradotoxin to block all action potentials does not completely inhibit the elevation in $[Ca^{2+}]_i$ [87]. The elucidation of the specific mechanisms behind such long-lasting alterations remains an important area of research; moreover, understanding how these changes lead to the development or maintenance of chronic epilepsy could provide new information for the design of efficacious treatments or new preventative measures to halt epileptogenesis.

In the pilocarpine model of SE-induced AE, it is well established that the elevations in $[Ca^{2+}]_i$ are maintained post-injury in animals that develop epilepsy. However, other conditions including stroke and TBI can also lead to the development of epilepsy. Finding common pathophysiologic mechanisms behind how excitotoxic injuries can lead to the epileptic condition will bolster efforts to design new therapeutics to prevent epileptogenesis. Thus, the examination of Ca^{2+} dynamics in other models of injury-induced epilepsy may be of great clinical importance and represent an important area to study in the future. As a ubiquitous second messenger, alterations in $[Ca^{2+}]_i$ and Ca^{2+} homeostatic mechanisms have significant repercussions on gene expression, neurotransmitter release, and hence, neuronal plasticity. Therefore, the development and

use of myriad models of acquired epilepsy to better understand the relationship between Ca^{2+} and epileptogenesis may offer an important tool in the future.

It should be noted that the modulation of $[Ca^{2+}]_i$ is a challenging pursuit in that Ca^{2+} is a ubiquitous second messenger that affects everything from neurotransmission to gene expression and has important functions in most cells of the body. This means that modulation of Ca^{2+} has the potential to cause many unwanted side effects until more specific methods of drug delivery/Ca^{2+} targeting are developed. Despite these difficulties in the modulation of Ca^{2+}, many studies have utilized Ca^{2+} channel antagonists or Ca^{2+}-chelating agents with varying degrees of success. Perhaps the most promising study is a Phase II clinical trial that utilized DP-BAPTA, a Ca^{2+}-chelating agent, to patients following stroke and found that this treatment did not cause vascular or neurological side effects, but did improve the National Institutes of Health stroke scores [88]. Moreover, patients with Alzheimer's disease are being treated with the NMDA antagonist, Memantine, which affects Ca^{2+} influx into the cell [89].

Despite these cases wherein Ca^{2+}-modifying agents have been used to improve outcomes from various neurological pathologies without significant deleterious effects, there is both positive and negative data regarding whether or not Ca^{2+} channel antagonists can be used as anti-convulsants or to potentiate the effects of other AEDs [90,91]. However, a good AED does not necessarily exhibit anti-epileptogenic properties and very little work has explored whether Ca^{2+}-modifying agents can affect epileptogenesis. The few studies that

exist have predominately used the NMDA antagonist, MK-801. One study demonstrated that this drug could effectively decrease the number of animals that developed epilepsy following electrically-stimulated SE [43], while another study showed that in the kainic acid model of SE-induced AE, MK-801 did not prevent the development of epilepsy [92]. Such conflicting results between models have underscored the need for many different types of models to be utilized [93] and have demonstrated that common pathophysiologic features need to be understood so as to develop better targets for anti-epileptogenic agents. Thus, the in vitro hippocampal neuronal culture model provides a useful tool in preliminary tests to determine anti-epileptogenic effects prior to screening in more complex systems. Moreover, the presence of these alterations in $[Ca^{2+}]_i$ and Ca^{2+} homeostatic mechanisms in both the pilocarpine and low Mg^{2+} model suggest that these may be common pathophysiologic features of epileptogenesis; therefore, understanding these changes may aid in the development of anti-epileptogenic agents.

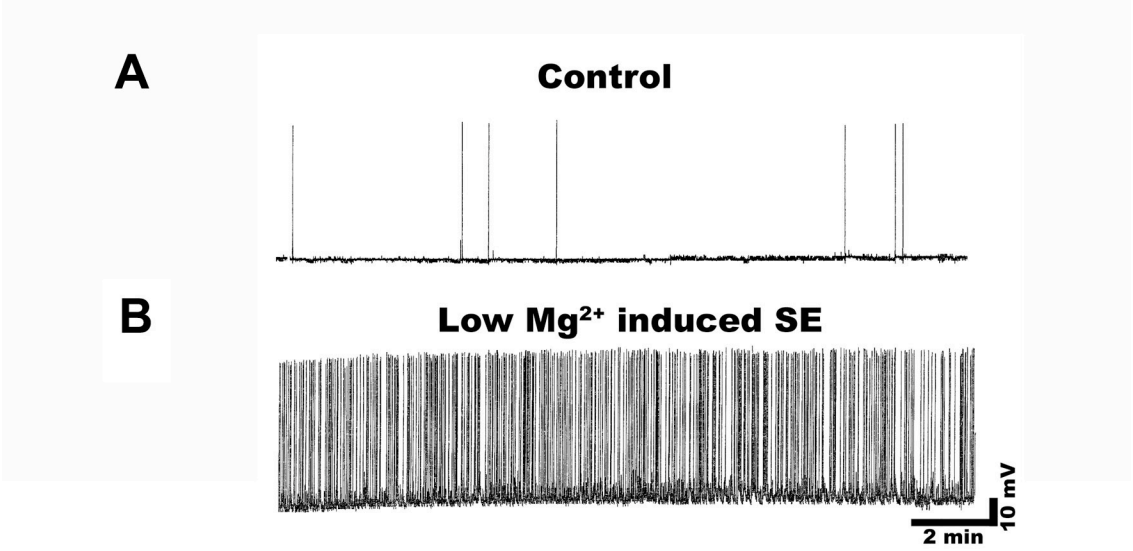

Figure 2-1. Treatment of hippocampal neuronal cultures with low Mg^{2+} causes in vitro SE. **A**, representative whole-cell current-clamp electrophysiological recordings obtained from a control neuron and **B**, a neuron in low Mg^{2+}, or in vitro SE. The neuron in low Mg^{2+} shows epileptiform discharges at a frequency greater than 3 Hertz. In contrast, the control neuron shows action potentials intermittently, consistent with baseline firing activity. Resting membrane potential= -62 mV; duration of trace shown= 18 min.

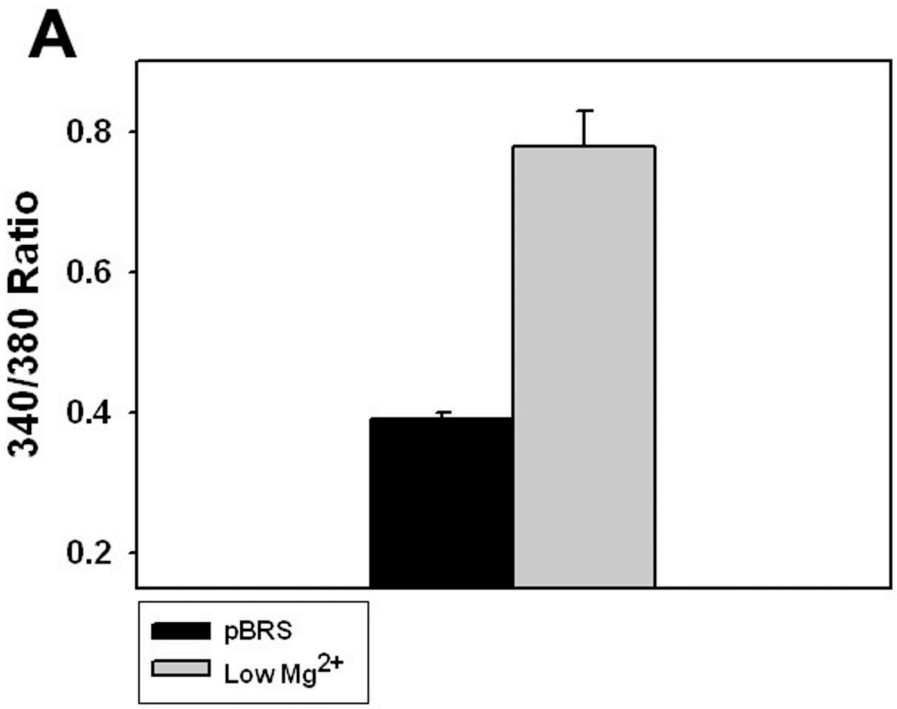

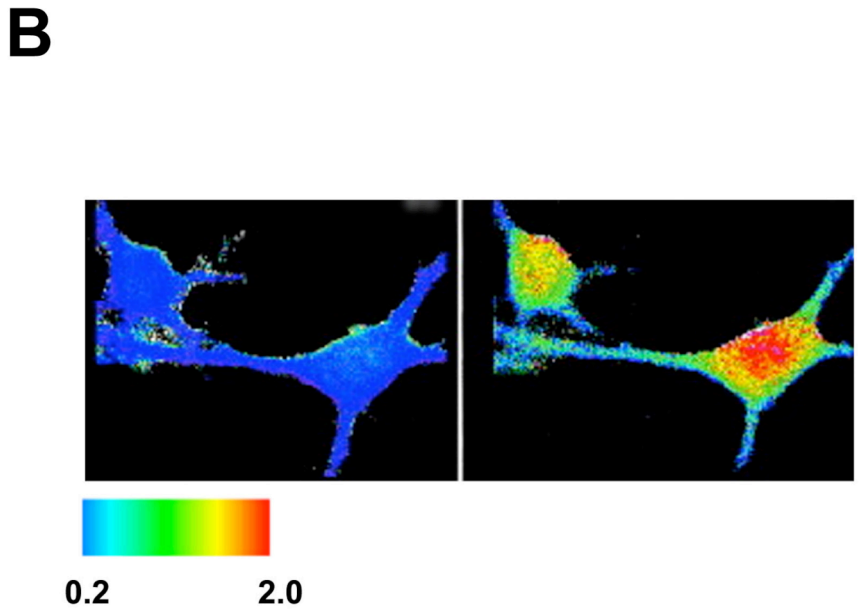

Figure 2-2. In vitro SE causes a significant elevation in $[Ca^{2+}]_i$. **A**, bar graph comparing Fura-2 340/380 ratios in control neurons versus neurons immediately following 3 hrs of low Mg^{2+}. The low Mg^{2+}-treated cells exhibit ratio values of 0.78±0.05 as compared to the control neurons with values of 0.39±0.01 (data expressed as mean ± SEM). **B**, representative pseudocolor ratio images obtained from control (left panel) and low Mg^{2+}-treated (right panel) neurons. Neurons from the low Mg^{2+} group show an increased 340/380 ratio immediately following treatment.

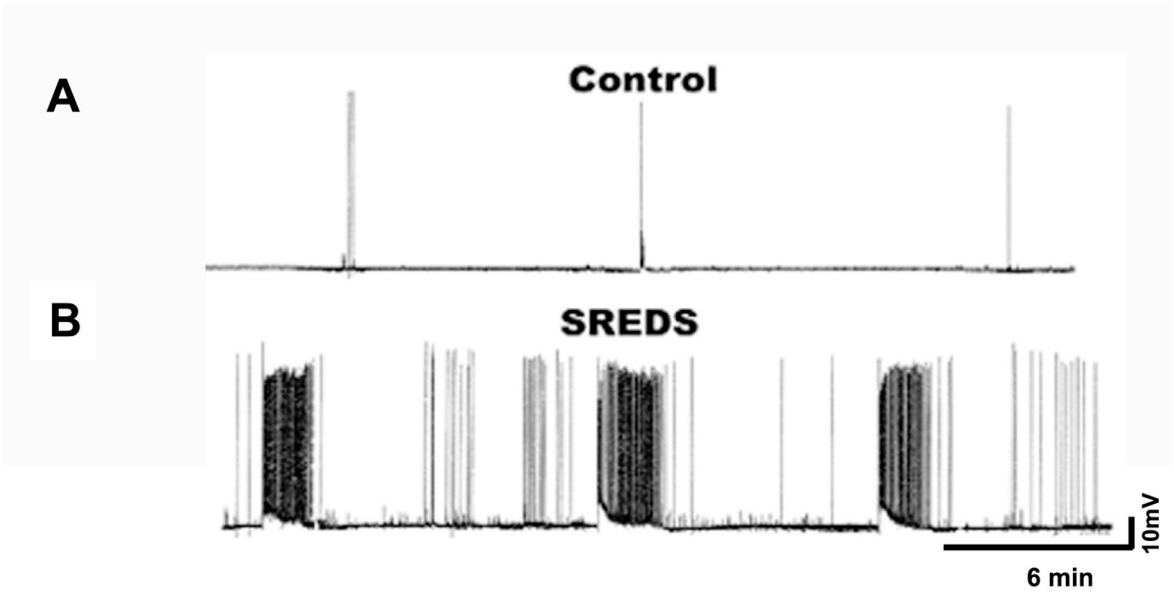

Figure 2-3. Low Mg^{2+} treatment leads to the development of in vitro epilepsy (SREDs). **A**, electrophysiological traces using current-clamp technique demonstrate baseline activity in control neurons and **B,** spontaneous, recurrent epileptiform discharges (SREDs) in neurons that had been treated in low Mg^{2+} for 3 hrs and then returned to normal maintenance media. Resting membrane potential= -61.5 mV; duration of shown trace= 30 min.

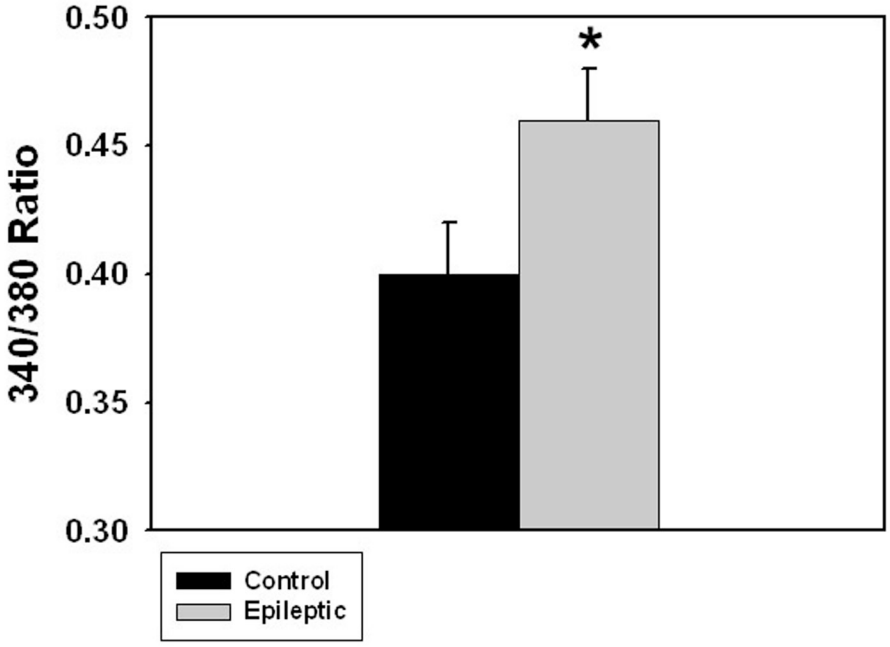

Figure 2-4. Elevations in $[Ca^{2+}]_i$ are maintained for at least 24 hours post-in vitro SE. Bar graph comparing 340/380 ratio values in control versus SE groups 24 hrs after treatment with Mg^{2+}-containing buffer solution or low Mg^{2+}, respectively. Neurons in the SE group exhibit a 340/380 ratio of 0.46±0.02 (mean ratio ± SEM). The ratio from control group neurons is significantly lower at 0.40±0.02.

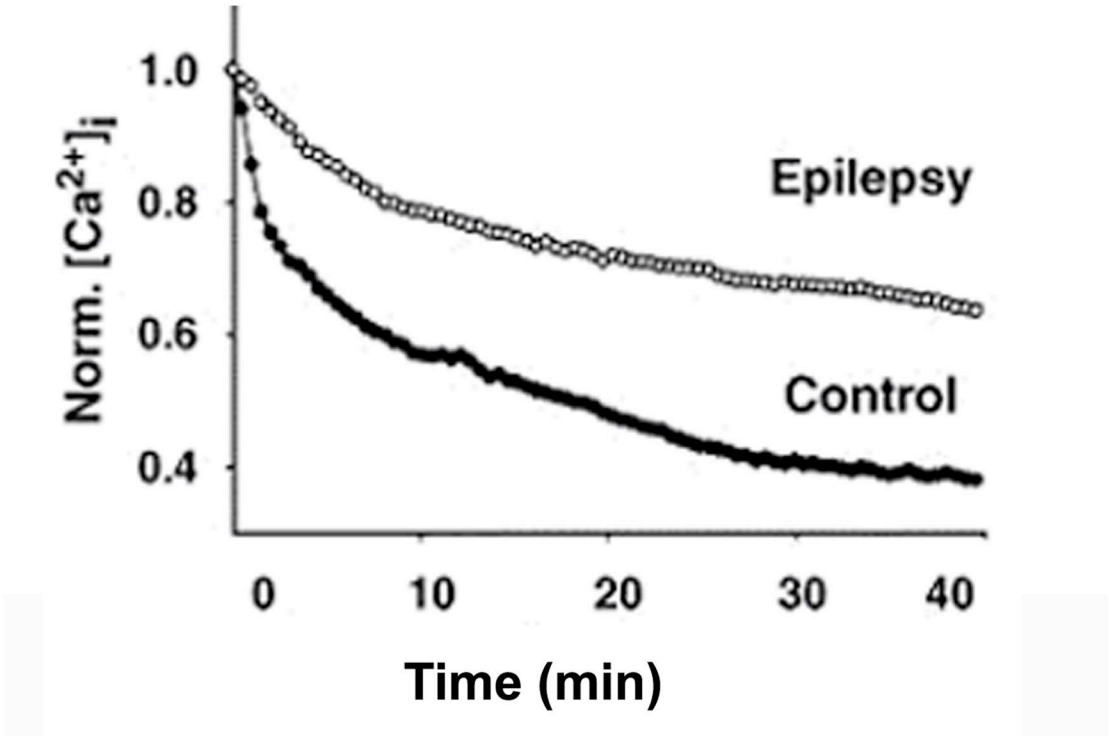

Figure 2-5. Neurons displaying SREDs exhibit alterations in Ca^{2+} homeostatic mechanisms. Glutamate stimulation causes increased $[Ca^{2+}]_i$. Peak ratios following glutamate are normalized to 1.0. Recovery from this challenge is hindered in epileptic neurons when compared to controls.

Chapter 3: Dantrolene Inhibits the SE-Induced Calcium Plateau and Prevents the Development of Spontaneous Recurrent Epileptiform Discharges in Hippocampal Neuronal Cultures

Introduction

Epilepsy is a common neurological condition that is characterized by spontaneous, recurrent seizures and affects 1-2% of the population worldwide [2,81]. Acquired epilepsy (AE) is one form of epilepsy that occurs following a brain injury such as status epilepticus (SE), traumatic brain injury (TBI), stroke, or infections of the central nervous system (CNS) [4,5]. AE represents approximately 40% of all cases of epilepsy [81]; thus, it remains an important public health concern. The transformation of healthy brain tissue into hyperexcitable networks of neurons that manifest epileptiform discharges is called epileptogenesis. Characterization of this process may help in elucidating particular targets to which potential anti-epileptogenic agents can be directed. Currently, only anti-epileptic drugs (AEDs) exist, which limit the occurrence of seizures once an individual has epilepsy. However, there are no anti-epileptogenic agents to prevent the process of epileptogenesis.

In order to better understand the process of epileptogenesis, many divide the development of AE into three stages: the injury itself, a period of latency or epileptogenesis, and finally, the maintenance of chronic epilepsy [19,20]. The period between the injury and the development of epilepsy could provide a therapeutic window of opportunity wherein pharmacological agents could be administered to prevent epileptogenesis. Thus, characterization of the pathophysiological changes that occur following neuronal injury is necessary in order to find new therapeutic targets.

It was demonstrated in the pilocarpine model of SE-induced AE that SE causes significant changes in $[Ca^{2+}]_i$ and Ca^{2+} homeostatic mechanisms in hippocampal neurons [32]. As far out as 1 year post-SE, animals that demonstrated epilepsy showed significant elevations in hippocampal neuronal Ca^{2+} levels (Ca^{2+} plateau), in contrast to those animals that failed to develop epilepsy post-SE [32]. As a ubiquitous second messenger, changes in $[Ca^{2+}]_i$ can affect everything from neurotransmitter release to gene transcription. Therefore, studying these alterations in Ca^{2+} and the underlying regulatory systems that control these changes is important not only in understanding plasticity but also in developing anti-epileptogenic strategies.

It was also demonstrated in the rat pilocarpine model of SE-induced AE that the N-methyl-D-aspartic acid (NMDA) antagonist, MK-801, when administered prior to SE, does not diminish SE but is able to prevent both the Ca^{2+} plateau as well as, the development of

epilepsy [32]. This study provided evidence that NMDA receptors (NMDAR) are involved in initiating the Ca^{2+} plateau during SE. However, little is known regarding what systems contribute to the long-term maintenance of these elevations in intracellular Ca^{2+} ($[Ca^{2+}]_i$) and whether inhibiting this elevation after the injury could prevent epileptogenesis. We hypothesized that the calcium-induced calcium release (CICR) system was activated by the massive influx of Ca^{2+} into the cell through NMDAR. Ryanodine receptors (RyR), along with inositol triphosphate receptors (IP3R), are part of the CICR mechanisms and control $[Ca^{2+}]_i$ inside of the cell by acting to either release or sequester Ca^{2+}. These receptors gauge cytoplasmic Ca^{2+} and mediate CICR from internal stores; therefore, these channels can either amplify or dampen the Ca^{2+} signal coming from outside the cell [45,46]. In these studies, dantrolene, a pharmacological inhibitor of RyR, was used to better elucidate the role of these receptors in the development of the Ca^{2+} plateau.

While the rat pilocarpine model has provided a great deal of information regarding potential pathophysiologic changes that occur during epileptogenesis, the whole-animal model is far too complex to be useful in preliminary pharmacological screenings. Thus, this study utilizes the hippocampal neuronal culture model wherein low Mg^{2+} is used to induce SE-like activity that leads to the development of spontaneous, recurrent epileptiform discharges (SREDs), the in vitro correlate to epilepsy. We assessed whether the changes in $[Ca^{2+}]_i$ observed in the rat pilocarpine model also existed in this model. If such changes existed, this model could provide a useful tool in further characterizing these

pathophysiological mechanisms behind epileptogenesis in a less complex system. Furthermore, we examined whether giving the RyR inhibitor, dantrolene, post-in vitro SE could prevent the development of SREDs.

Materials and Methods

Reagents

All the reagents were purchased from Sigma Chemical Co. (St Louis, MO) unless otherwise noted. Cell culture media was purchased from Invitrogen (Carlsbad, CA).

Hippocampal neuronal culture preparation

All animal use procedures were in strict accordance with the National Institutes of Health Guide for the Care and Use of Laboratory Animals and approved by Virginia Commonwealth University's Institutional Animal Care and Use Committee. As described previously [23], hippocampal neurons were harvested from 2-day postnatal Sprague-Dawley rats (Harlan, Indianapolis, IN) and grown on a glial support layer that was previously plated onto poly-L-lysine (0.05 mg/mL) coated plates. The cultures were maintained at 37°C in a 5% CO_2/95% air atmosphere and neuronal cultures were fed twice a week with minimal essential media containing: Earle's Salts, 25 mM HEPES, 2 mM l-Glutamine, 3 mM Glucose, 100 µg/mL transferrin, 5 µg/mL insulin, 100 µM putrescine, 3 nM sodium selenite, 200 nM progesterone, 1 mM sodium pyruvate, 0.1% ovalbumin, 0.2 ng/mL triiodothyroxine, and 0.4 ng/mL corticosterone supplemented with 20% conditioned media. Neurons were allowed to mature and all experiments were performed 14-18 days

following plating of neurons to allow formation of networks, adequate neuronal maturation, and development of NMDA receptors.

Whole-cell current clamp electrophysiology

Whole-cell current clamp electrophysiology was performed according to previously described procedures [23,84]. In short, hippocampal neuronal culture media was replaced with physiological basal recording solution (pBRS) containing (in mM): 145 NaCl, 2.5 KCl, 10 HEPES, 2 $CaCl_2$, 1 $MgCl_2$, 10 glucose, and 0.002 glycine, pH 7.3, and osmolarity adjusted to 325 ± 5 mOsm with sucrose. The plates were transferred to the temperature-controlled stages of either a Nikon Diaphot inverted microscope (Garden City, NY) or Olympus IX-70 (Olympus, Center Valley, PA) in order to perform electrophysiological recordings. A Flaming-Brown P-80C electrode puller (Sutter Instruments, Sarasota, FL) was utilized to pull patch microelectrodes with resistances of 3-7 MΩ from thin borosilicate glass capillaries (World Precision Instruments, Inc., Sarasota, FL). These microelectrodes were filled with an internal solution consisting of (in mM): 140 K^+ gluconate, 1 $MgCl_2$, 10 HEPES, and 1.1 ethylene glycol tetraacetic acid (EGTA), adjusted to pH 7.2, and osmolarity of 310 mOsm.

An Axopatch 200A amplifier or an Axoclamp-2A amplifier (Axon Instruments, Foster City, CA) in current clamp mode was used to obtain recordings from phase-bright pyramidal-shaped neurons. Together, the Neuro-corder DR-890 (Neurodata Instruments Corp, New York, NY) and Sony Videocassette Recorder allowed for digitization and

storage of data on videotapes. Acquired data were then analyzed by playing recordings back through a DC-500 Hz chart recorder (Astro-Med Inc., Warwick, RI) or to a computer via a Digidata 1322A (Axon Instruments, Foster City, CA).

Calcium microfluorometry

To determine $[Ca^{2+}]_i$ in hippocampal neuronal cultures, cells were loaded with 1μM Fura-2-acetoxymethyl ester (AM) (Molecular Probes, Eugene, OR) for 30 min at 37˚C in 5% CO_2/95% O_2, as described previously [50]. The plates were then transferred a temperature-controlled stage (Harvard Apparatus, Holliston, MA) on an Olympus IX-70 inverted microscope. Ratio images were acquired using alternating excitation wavelengths (340 and 380 nm) with a filter wheel (Sutter Instruments, Novato, CA) and fura filter cube at 510/540 nm emissions with a dichroic mirror at 400 nm [94]. Thus, the resulting 340/380 ratio recorded corresponds directly to the total concentration of Ca^{2+} inside the cell and can be used to determine changes in $[Ca^{2+}]_i$. The utilization of the 340/380 ratio is important in that it accounts for potential confounders such as unequal loading for Fura-2AM or variable cell thickness from interfering with the measurements. This system is connected to the fluorescent imaging software, MetaFluor (Olympus, Center Valley, PA), which allows for image acquisition and analysis. Images were acquired from any given field at various time intervals depending on the specific experiment and background fluorescence was subtracted from all acquired data by imaging hippocampal neuronal cultures that were not loaded with Fura-2AM.

In vitro SE and SREDs in hippocampal neuronal cultures

In vitro SE was generated using a low Mg^{2+}-containing solution [18]. Maintenance media was replaced with low Mg^{2+} (pBRS without any added $MgCl_2$). The cells then incubated at 37 °C under 5% CO_2/95% O_2 atmosphere for 3 hrs. During this time, when the neurons were patch-clamped using whole-cell current clamp electrophysiology, they demonstrated high frequency spiking, characterized as in vitro SE. Neurons treated with pBRS for 3 hrs served as the sham-controls.

After 3 hrs of low Mg^{2+} or pBRS treatment, the cells were returned to normal, Mg^{2+}-containing maintenance media and were evaluated using whole-cell current clamp electrophysiology at least 12 hrs post-in vitro SE to determine expression of in vitro epilepsy, or SREDs. Each episode of SREDs is characterized by paroxysmal depolarization shifts and generally, 5-9 SREDs are observed per hour.

Cell death assay

Neuronal death was assessed using the dye, Propidium Iodide (PI) as well as, Annexin V conjugated to fluorescein isothiocyanate (FITC). PI binds DNA in membrane-compromised neurons, whereas, Annexin V binds phosphotidylserines that translocate to the outer cell membrane in the early stages of apoptosis. Several randomly selected fields from each plate were marked and both phase and fluorescent images were captured using MetaMorph (Olympus, Center Valley, PA). Fraction of neuronal death was calculated as the number of neurons labeled with only Annexin V plus the number of neurons labeled

with Annexin V and PI, divided by the total number of neurons. The data was subjected to an outlier test wherein all values outside of two standard deviations from the mean were considered outliers.

Pilocarpine preparation

All animal use procedures were in strict accordance with the National Institutes of Health Guide for the Care and Use of Laboratory Animals and were approved by Virginia Commonwealth University's Animal Use Committee. Sprague-Dawley rats, weighing between 185-235 g, were injected intra-peritoneally (i.p.) with the muscarinic agonist, pilocarpine (375 mg/kg). 20 minutes prior to this injection, the animals were given methyl-scopolamine nitrate (1mg/kg) i.p. to block the systemic effects of pilocarpine. Both of these drugs were dissolved in 0.9% saline and filter-sterilized. Behavioral seizures generally began within 20 minutes of injection with pilocarpine. Animals were allowed to seize for 1 hr before SE was terminated by the i.p. administration of 4 mg/kg diazepam (DZP) at 1, 3, and 5 hrs post-SE. Sham animals were injected with all of the drugs described above except pilocarpine, instead they received equal volumes of 0.9% saline i.p. When appropriate, animals received either dantrolene (10 mg/kg) or vehicle (DMSO) i.p. at the end of 1 hr of SE for studies related to epileptogenesis.

Acute isolation of hippocampal neurons

Animals were sacrificed 24 hrs post-SE to determine $[Ca^{2+}]_i$ in hippocampal neurons from the sham, pilo-vehicle, and pilo-dantrolene treated groups. Briefly, as described previously

[85], hippocampal slices were cut and incubated for 1 hr following dissection in oxygenated artificial cerebrospinal fluid (aCSF). Slices were exposed to 8 mg/ml Type XXIII protease (Sigma Chemical Co, St. Louis, MO) for 6 minutes, and then washed to abolish protease activity. Mechanical dissociation of tissue was accomplished through trituration in N-2-hydroxyethylpiperazine-N'-2-ethanesulfonic acid (HEPES) buffer using a series of fire polished Pasteur pipettes. Dispersed neurons were plated in buffer containing Fura-2AM onto poly-L-lysine and Cell-Tak (BD Biosciences, Franklin Lakes, NJ) coated culture dishes allowing the appropriate adherence to conduct $[Ca^{2+}]_i$ imaging.

Racine score

To evaluate severity of behavioral seizures during SE, the Racine scoring method was used [95]. The Racine scale scores various behavioral traits during SE and in doing so, serves as a quantitative tool to measure seizure severity. The scale rates behaviors on a scale from 0-6, with 0=no SE to 6=severe tonic-clonic seizures resulting in death.

Isolation and homogenization of hippocampal tissue

At various time points either during or after SE, animals were anesthetized by inhalation of isoflurane until the righting reflex was lost and respiration rate slowed and were then rapidly decapitated. The brain was quickly removed and dissected. Hippocampal tissue was separated from the rest of the brain and flash-frozen in liquid nitrogen. The frozen hippocampus was homogenized using a motorized homogenizer in 750 µL of modified, ice-cold RIPA buffer consisting of: 1% NP-40, 10 mM Tris-HCl (pH 7.4), 150 mM

NaCl, and 1% Triton- X100, as well as, phenylmethanesulphonylfluoride (PMSF), and Halt Phosphatase Inhibitor Cocktail (Pierce, Rockford, IL) to inhibit protease and phosphatase activity, respectively. The homogenates were stored at -80°C and protein concentration was measured using the Bradford reagent (BioRad, Hercules, CA) and a spectrophotometer (595 nm).

Western blotting

Western blotting of hippocampal homogenates was performed as described previously [52]. In brief, protein (10 μg /lane) was resolved on SDS-PAGE and transferred to a polyvinylidene fluoride (PVDF) membrane (Millipore, Bedford, MA) at 100 V, 4°C. Membranes were blocked using 5% bovine serum albumin (BSA) made up in tris-buffered saline containing 0.1% Tween-20 (TBST) for 1 hr at room temperature (RT). Primary antibodies were made up in this 5% BSA solution. The membrane incubated in the RyR2 primary antibody (1:200) (Alamone Labs #ARR-002, Jerusalem, Israel) overnight at 4°C or phospho-RyR2 (1:5,000, Serine-2809) (Badrilla #P010-30, Leeds, United Kingdom) for 1 hr at RT. To assess whether there was equal loading of protein, blots were cut and incubated in actin (1:8000) (Chemicon #MAB1501, Billerica, MA) or β-tubulin (1:4000) (AbCam #ab6046, Cambridge, MA) for 1 hr at RT. The membranes were washed with TBST 5 times following incubation with primary antibody and incubated for 1 hr with goat anti-rabbit (1:10,000, for phospho-RyR2, RyR2, β-tubulin antibodies) (Chemicon #AP132P) or goat anti-mouse (1:10,000, for actin antibody) (Chemicon #AP124P) secondary antibodies conjugated to horseradish peroxidase. The blots were washed 5

times with TBST and washed in enhanced chemiluminescence reagent (SuperSignal, Pierce, Rockford, IL) prior to exposing Kodak X-Omat Blue XB-1 X-ray film (Eastman Kodak, Rochester, NY) for detection of protein.

Data analyses

Data were expressed as mean ± SEM. To determine significance between treatment groups for Ca^{2+} imaging, SREDs, and neuronal death assays, one-way analysis of variance (ANOVA) tests were employed, followed by Fisher's post-hoc test when appropriate. For the Ca^{2+} imaging and cell death experiments, at least 6 plates were used per treatment group. For electrophysiology experiments, 2-3 neurons are patch-clamped from each plate with a minimum of 5 plates used for each treatment group. All experiments were performed over the period of several weeks so that the results were representative of multiple cultures. A p-value<0.05 was considered statistically significant. Statistical analysis was performed using StatView 5.0.1 and graphs were drawn using SigmaPlot (Systat Software, San Jose, CA).

Results

In the rat pilocarpine model of SE-induced AE, hippocampal neuronal $[Ca^{2+}]_i$ increases during SE and significant elevations in $[Ca^{2+}]_i$ are maintained for at least one year post-SE in those animals that go on to develop epilepsy. Thus, our first aim was to evaluate whether similar long-term changes in $[Ca^{2+}]_i$ are observed in the in vitro, low Mg^{2+} model.

In vitro SE causes significant, long-lasting elevations in $[Ca^{2+}]_i$ (Ca^{2+} plateau)

Neurons were treated for 3 hrs with either low Mg^{2+} to simulate in vitro SE or pBRS as a sham control, in accordance with previously described methodology [23]. The cells were loaded with the Ca^{2+} indicator, Fura-2AM to determine 340/380 ratios both at the end of this treatment and at various time points following the treatment (Figure 3-1). These fluorescent ratio values were obtained using alternating excitation wavelengths of 340 nm and 380 nm, and the resulting 340/380 ratios correspond directly to $[Ca^{2+}]_i$. There was no significant difference in 340/380 ratios between the sham control neurons that were treated with pBRS at any of the time points tested. In contrast, neurons treated with low Mg^{2+} displayed ratio values of 0.78±0.05 acutely at the end of this 3 hr treatment, approximately double the ratio values observed in sham controls.

In order to end in vitro SE, $MgCl_2$ was restored to these cultures by washing them with pBRS. The same neurons were imaged for the first hour post-restoration of $MgCl_2$. Within 10 min of restoring the $MgCl_2$ to the low Mg^{2+}-treated plates, the 340/380 ratio dropped from 0.78±0.01 to 0.67±0.05. At 30 min post-in vitro SE, the ratios fell slightly to 0.66±0.06 and at 60 min post-SE to 0.60±0.07. At the 3 hr and 6 hr time points, the 340/380 ratios had dropped further to 0.46±0.01 and 0.43±0.01, respectively. Finally, at 24 hrs post-in vitro SE, the low Mg^{2+}-treated cells exhibited 340/380 ratios of 0.46±0.02. n= 6 plates at each time point tested with 52-134 neurons imaged in total per treatment group. The recorded ratios in the low Mg^{2+}-treated group were significantly elevated when compared to the controls at each of the time points tested. This suggests that low Mg^{2+}-

induced in vitro SE triggers long-lasting elevations in $[Ca^{2+}]_i$, as evidenced by maintenance of increased 340/380 ratios for at least 24 hrs.

Dantrolene lowers $[Ca^{2+}]_i$ to baseline levels following in vitro SE

We next wanted to test whether these persistent elevations in $[Ca^{2+}]_i$ following low Mg^{2+}-induced SE-like activity could be inhibited pharmacologically and whether doing so, would prevent the expression of SREDs. Dantrolene, an inhibitor of RyR, was utilized immediately post-in vitro SE to determine whether inhibition of RyR-mediated CICR could lower the elevated $[Ca^{2+}]_i$. To test this, hippocampal neuronal cultures were treated for 3 hrs with low Mg^{2+} and were then loaded with Fura-2AM. As shown in Figure 3-2, following 3 hrs of in vitro SE (time 0 on x-axis), neurons showed elevations in 340/380 ratios that were normalized to the peak ratio. These neurons were then treated with either dantrolene (50 μM) or vehicle (0.1% DMSO). At 5 min post-treatment, vehicle-treated cells showed a slight decrease in 340/380 ratio; in contrast, dantrolene-treated cells exhibited 340/380 ratios that were 47% of the peak observed at the end of in vitro SE. At 10 min post-treatment, the 340/380 ratio values were 83% and 43% of the post-SE peak in vehicle- and dantrolene-treated groups, respectively. At 15 min post-treatment, the 340/380 ratio values were 82% and 40% of the post-SE peak in vehicle- and dantrolene-treated groups, respectively. In the cells that were exposed to dantrolene after the low Mg^{2+} treatment, $[Ca^{2+}]_i$ returned to the baseline levels observed in the naïve controls (data not shown) within 20 minutes. In contrast, the vehicle controls showed elevated $[Ca^{2+}]_i$ at all time points tested—the 340/380 ratios fell by only 18% over the first 20 minutes

following in vitro SE, consistent with the data reported in Figure 3-1. There was a significant difference in the 340/380 ratios between the dantrolene and vehicle treated groups at each time point after 1 min of treatment, with the dantrolene-treated group showing marked enhancement in the ability to rapidly lower the $[Ca^{2+}]_i$. n=6 plates were used per treatment group with ~60 neurons imaged in total per condition. These experiments demonstrated that dantrolene was able to lower $[Ca^{2+}]_i$ when administered acutely after in vitro SE; thus, suggesting that RyR may play a role in mediating the post-SE elevations in $[Ca^{2+}]_i$.

In vitro SE is not inhibited by dantrolene

This in vitro hippocampal neuronal culture model of SE is, much like the clinical condition, difficult to treat because it is highly refractory to anticonvulsant treatment. Thus, we sought to determine if dantrolene could act to block this low Mg^{2+}-induced, high frequency spiking. Using whole-cell current clamp electrophysiology, we observed that naïve cultured hippocampal neurons exhibited infrequent spontaneous action potentials while in normal pBRS (Figure 3-3 A). Upon replacing the culture media with low Mg^{2+}, the neurons demonstrated continuous, high frequency epileptiform discharges (Figure 3-3 B). The spike frequency observed in cultures treated with low Mg^{2+} was greater than 3 Hz. This frequency is consistent with the criteria for clinical SE. We demonstrated that treatment with dantrolene (50 μM) failed to slow down the low Mg^{2+}-induced high frequency spiking (Figure 3-3 C). No change in mean membrane potential or mean input resistance was observed between groups. There was no significant difference in spike

frequency between neurons treated with low Mg^{2+} plus dantrolene versus low Mg^{2+} alone—this suggests that dantrolene is unable to inhibit low Mg^{2+}-induced in vitro SE.

Dantrolene maintaines baseline Ca^{2+} levels 24 and 48 hours post-SE

In order to evaluate whether the dantrolene-mediated changes in $[Ca^{2+}]_i$ that were observed acutely were more long-lasting, we treated neurons with low Mg^{2+} followed by dantrolene or vehicle and imaged the cells 24 (Figure 3-4 A) and 48 hrs (Figure 3-4 B) post-treatment. Neurons treated with low Mg^{2+} and then vehicle exhibited significantly elevated 340/380 ratios when compared to the control, these numbers were consistent with data collected in Figure 3-1. Interestingly, in neurons treated with low Mg^{2+} and then dantrolene, 340/380 ratios were not significantly different from those observed in the control. Thus, 24 hrs post-SE, dantrolene was able to maintain $[Ca^{2+}]_i$ at baseline levels (96.25 ± 5.13% of the control). Whereas, hippocampal neuronal cultures treated with low Mg^{2+} and then vehicle demonstrated significant elevations in $[Ca^{2+}]_i$ (120.47 ± 6.95% of the control). n=10 or more plates with ~100 cells imaged per treatment group at this time point.

At 48 hrs post-treatment, $[Ca^{2+}]_i$ in the dantrolene-treated neurons was comparable to concentrations observed in controls (96.23 ± 3.45% of the control). In contrast, neurons treated with low Mg^{2+} and then vehicle, showed significant elevations in 340/380 ratios compared to both the drug-treated and the control neurons (120.74 ± 3.58% of the control). n=5 plates with ~60 cells imaged per treatment group at 48 hr time point. Therefore,

dantrolene appears to be able to maintain $[Ca^{2+}]_i$ for at least 48 hrs post-in vitro SE at the baseline concentrations observed in control neurons.

Dantrolene prevents the development of SREDs 24 and 48 hours post-SE but does not inhibit SREDs acutely

Also at 24 and 48 hrs post-in vitro SE, neurons were patched using current-clamp electrophysiology to evaluate for the expression of SREDs. Control neurons demonstrated "normal" activity consisting of sporadic firing of action potentials (Figure 3-5 A). In contrast, 84% and 100% of neurons treated with low Mg^{2+} showed SREDs at 24 and 48 hrs post-in vitro SE, respectively. A representative trace is shown that highlights the characteristics of the observed SREDs (Figure 3-5 B). These episodes consisted of paroxysmal depolarization shifts and occurred at a frequency of 5-8 episodes per hour with each SRED lasting 1-3 minutes. Neurons from the plates that were treated with low Mg^{2+} followed by dantrolene showed a marked inhibition in the expression of SREDs 24 hrs (Figure 3-5 C) and 48 hrs (Figure 3-5 D) post-treatment. Only 10% and 20% showed SREDs at 24 and 48 hrs post-SE, respectively. Of this small percentage, the SRED frequency was 1.7/hr at the 24 hr time point and 1.9/hr at the 48 hr time point, a marked reduction when compared to the SRED frequency observed in cells treated with low Mg^{2+} but no drug.

To test for potential anti-convulsant properties, we studied whether acutely adding dantrolene (50μM) to neurons already demonstrating SREDs could inhibit these episodes.

Dantrolene did not inhibit SREDs when administered acutely (line over Figure 3-5 B represents treatment with dantrolene); in fact, there was no change in the frequency or duration of the SREDs. No change in mean resting membrane potential or mean input resistance was observed between groups.

Dantrolene is neuroprotective

While several studies have demonstrated in other models of epilepsy that dantrolene exhibits some neuroprotective properties [96-98], we wanted to evaluate whether it could be neuroprotective when given after the SE-related injury in the hippocampal culture model. We treated cells with low Mg^{2+} for 3 hrs followed by drug or vehicle and determined cell viability 24 and 48 hrs later (Figure 3-6). Cell viability was ascertained using PI and Annexin V-FITC. At the 24 hr time point, sham control cultures that had been subjected to 3 hrs of pBRS instead of low Mg^{2+} had a fraction cell death of 0.141 ± 0.013. Neurons treated with low Mg^{2+} and then dantrolene (50 μM) had an average fraction cell death of 0.138 ± 0.012, consistent with levels observed in the sham control. Lastly, cultures exposed to 3 hrs of low Mg^{2+} and then vehicle had an average cell death fraction of 0.180 ± 0.013, which was significantly higher than the cell death observed in both drug and control groups. This demonstrated that at 24 hrs post-treatment with low Mg^{2+} or pBRS, dantrolene was able to reduce cell death to levels observed in the sham controls.

Data was also collected at 48 hrs post-SE. There was no significant difference in fraction cell death between sham and low Mg^{2+} plus dantrolene groups; however, low Mg^{2+} plus vehicle neurons showed a significant increase from the other two groups. Fraction cell death was 0.139 ± 0.019, 0.208 ± 0.022, and 0.128 ± 0.028 in sham, low Mg^{2+} plus vehicle, and low Mg^{2+} plus dantrolene treated neurons, respectively. n=7 or more plates per treatment group and time point. Thus, these results showed that dantrolene-treated neurons exhibited decreased fraction cell death, which suggests that dantrolene may be neuroprotective when administered after in vitro SE.

In the rat pilocarpine model of SE-induced AE, dantrolene is able to lower hippocampal neuronal Ca^{2+} post-SE

In order to test whether our in vitro observations were valid in a whole animal model, we utilized the rat pilocarpine model of SE-induced AE. Long-lasting elevations in $[Ca^{2+}]_i$ following SE were first demonstrated in this model [32]. We tested whether dantrolene was able to lower hippocampal neuronal $[Ca^{2+}]_i$ when administered following 1 hr of pilocarpine-induced SE. Animals were given pilocarpine and allowed to seize for 1 hr, upon which time they were administered diazepam to terminate the SE and then either dantrolene (10 mg/kg) or vehicle (DMSO). Then, 24 hrs post-SE, the animals were sacrificed and hippocampal neurons were acutely isolated and imaged to determine $[Ca^{2+}]_i$. As demonstrated in Figure 3-7, in the neurons isolated from the naïve control animals, an average 340/380 ratio of 0.615 ± 0.019 was observed. Neurons from animals in the SE group had an average 340/380 ratio of 0.763 ± 0.047, which was significantly higher than

the ratios observed in the naïve control. In contrast, neurons from animals that were in SE and then treated with dantrolene had an average 340/380 ratio of 0.571 ± 0.014, which was consistent with that observed in the control but significantly lower than the SE alone neurons. n=2 or more animals in each group with approximately 30 cells imaged per animal. This suggests that dantrolene, when administered immediately following SE, may lower $[Ca^{2+}]_i$ in hippocampal neurons in vivo.

Dantrolene does not affect the severity of pilocarpine-induced SE

To ensure that dantrolene was decreasing the $[Ca^{2+}]_i$ by directly inhibiting Ca^{2+} rather than simply abolishing SE more efficiently and thus, decreasing the severity of the insult, we quantified the robustness of pilocarpine-induced seizures in animals pre-treated with either vehicle (DMSO) or dantrolene (10 mg/kg). A modified Racine scale was used that ranged from 0-6, with no response scored as a 0 and death scored as a 6. Two trained observers independently scored the SE and scores were averaged for each animal. The severity of the seizures in pilocarpine plus vehicle scored a 3.5 ± 0.20 and in pilocarpine plus dantrolene a 3.75 ± 0.25; thus, no significant difference was observed between the two groups (Figure 3-8). n=4 animals per group. The results from this experiment demonstrated that dantrolene does not affect the severity of seizures induced by pilocarpine.

The Ca^{2+} plateau may be maintained in vivo by "leaky" ryanodine receptors

It has been demonstrated in a cardiac model of ventricular arrhythmias, phosphorylation of the RyR leads to increased dissociation of a protein, calstabin [99,100]. Dissociation of this protein is associated with increased Ca^{2+} leak from the receptor, leading to ventricular arrhythmias [99,100]. It can be hypothesized that if RyR are contributing to the Ca^{2+} plateau post-SE, they are either upregulated or simply more active, allowing for increases in $[Ca^{2+}]_i$. Western blot analysis was carried out at several time points both during and after SE. The most interesting change in expression noted was at 1 wk post-SE. At this time point, no significant difference was observed in quantity of RyR2; however, the phosphorylated (at serine-2809) form of the receptor was significantly upregulated in the SE animals when compared to both the naïve and sham controls (Figure 3-9). At 1 hr and 1 day post-SE there does not appear to be an upregulation in either RyR or the phosphorylated form of this receptor (data not shown). This suggests that 'leaky' RyR, which increase in expression only during the period of epileptogenesis, may contribute to the ultimate phenotype.

Discussion

This study demonstrated that neuronal injuries such as SE can cause an increase in $[Ca^{2+}]_i$ that is sustained well past the duration of the injury itself in the hippocampal neuronal culture model of SE-induced AE. Moreover, dantrolene, a RyR inhibitor, is able to both lower $[Ca^{2+}]_i$ to levels observed in control neurons and prevent the development of SREDs when used after in vitro SE. The observation that an injury-triggered, sustained elevation in $[Ca^{2+}]_i$ (the calcium plateau) exists in vitro correlates closely to findings reported in

Raza et al [32]. This group demonstrated in the rat pilocarpine model of SE-induced AE that hippocampal neuronal $[Ca^{2+}]_i$ increases during injury and remains elevated only in those animals that later develop epilepsy [32]. This study suggests that changes in $[Ca^{2+}]_i$ and Ca^{2+} homeostatic mechanisms lead to a Ca^{2+} plateau, which may be a pathophysiological characteristic of neuronal injury and epileptogenesis. Understanding various cellular and molecular changes that occur either during or following neuronal injuries is important in developing new therapeutics to prevent the ultimate development of AE. Therefore, the finding that the changes in $[Ca^{2+}]_i$ that were observed in vivo are also seen in vitro suggests that this culture model may provide a useful tool in screening various pharmacological agents and performing new molecular modulations in order to prevent epileptogenesis.

The in vitro model utilizing low Mg^{2+} to elicit SE-like activity and ultimately, SREDs is a commonly used model to study various characteristics of both SE and epilepsy such as pharmacoresistance, plasticity changes, mechanisms of epileptogenesis, and cell death [18,24,84]. The model exhibits several features consistent with the development of AE in both animal models and the clinical condition, which make it a useful tool in elucidating the underlying mechanisms of epileptogenesis and seizures [23,24]. Moreover, the cell injury observed in the in vitro and in vivo models correspond to that seen in clinical studies documenting the relationship between SE and neuronal injury [25-27]. It should be noted that the hippocampal neuronal cultures do not have the true anatomical connections maintained in slice preparations or the intact brain. However, the cultures are an essential

tool in the development of new drugs and the study of molecular mechanisms because they provide a controlled environment to do high-throughput screenings and are more easily manipulated for molecular studies.

While currently there are several anti-epileptic drugs, there are no anti-epileptogenic drugs. Such therapeutic agents that can be administered immediately following injury so as to prevent long-term sequelae, namely the development of AE, would be extremely important clinically. In this study, we demonstrated that dantrolene, when given post-SE inhibited the Ca^{2+} plateau and prevented the development of SREDs in the in vitro low Mg^{2+} model. Our results also highlighted that dantrolene did not stop SE or serve as an anti-convulsant but is neuroprotective in the low Mg^{2+} model even when used following the neuronal injury. The ability to offer neuroprotection following a neuronal injury is an important strategy to prevent the development of injury-related chronic neurological conditions [101,102]. In this study, many of the in vitro experiments were also replicated in the rat pilocarpine model and the novel finding that dantrolene was able to lower $[Ca^{2+}]_i$ when administered following SE without diminishing the SE itself was demonstrated. This finding affirms that the in vitro model may prove to be an effective tool in preliminary pharmacological studies. Studies have been initiated to determine whether this drug has anti-epileptogenic properties in vivo, as this would have tremendous clinical implications.

It should be noted that the pharmacological modulation of Ca^{2+} in vivo is a challenge in that the ubiquitous nature of this ion suggests that systemic inhibition would potentially

have numerous side effects [103]. However, a recent clinical trial has utilized a Ca^{2+}-chelating agent in patients following stroke and the unpublished results have indicated that not only are stroke outcome scores improved, but the patients experienced no significant negative cardiovascular or neurological side effects [88].

The data also suggest that the RyR, a regulator of CICR, may contribute to the maintenance of the calcium plateau. Much of what is currently known regarding the role of RyR in epilepsy is based on studies using dantrolene either as a prophylactic neuroprotective agent before injury so as to prevent the development of AE or as an anti-convulsant after the full development of AE. It has been demonstrated that pre-treatment with dantrolene blocks the induction phase in hippocampal slice preparation [104]. Another study confirmed these results in the kindling model of epilepsy, showing that animals pre-treated with dantrolene require significantly greater stimuli to generate seizures [105]. Moreover, after the animals are kindled, during the chronic phase of epilepsy, dantrolene has no anti-convulsant effects [91,105]. Thus, while such studies have suggested that treatment with dantrolene could provide tremendous benefits when administered before the inciting injury, there is still a need for studies to examine its effects when administered after the injury, as this would be more clinically relevant. It remains plausible that during an excitotoxic neuronal injury, the massive release of glutamate activates NMDAR leading to increased $[Ca^{2+}]_i$. However, following the injury, CICR mechanisms controlled by the RyR may play a role in maintaining the long-lasting elevations observed both in the rat pilocarpine model and in the in vitro model used in this

study. This hypothesis is supported by western blot experiments performed in this study demonstrating that at 1 week post-SE, during the period of epileptogenesis, there is an increase in phospho-RyR2 and no change in RyR2 expression in the hippocampus. Phospho-RyR2 has been associated with increased Ca^{2+} leak from the RyR, therefore, this may contribute to the maintenance of a Ca^{2+} plateau [99,100].

Thus, this study is the first to demonstrate the novel finding that in vitro SE causes long-lasting elevations in $[Ca^{2+}]_i$, which can lowered post-injury by treatment with dantrolene in both in vitro and in vivo models of SE-induced AE. More studies are needed to better understand and characterize the post-SE Ca^{2+} plateau, as this may be a useful tool in the development of anti-epileptogenic targets. Lowering the post-SE Ca^{2+} plateau may prevent the second messenger effects that lead to epileptogenesis and the development of chronic epilepsy.

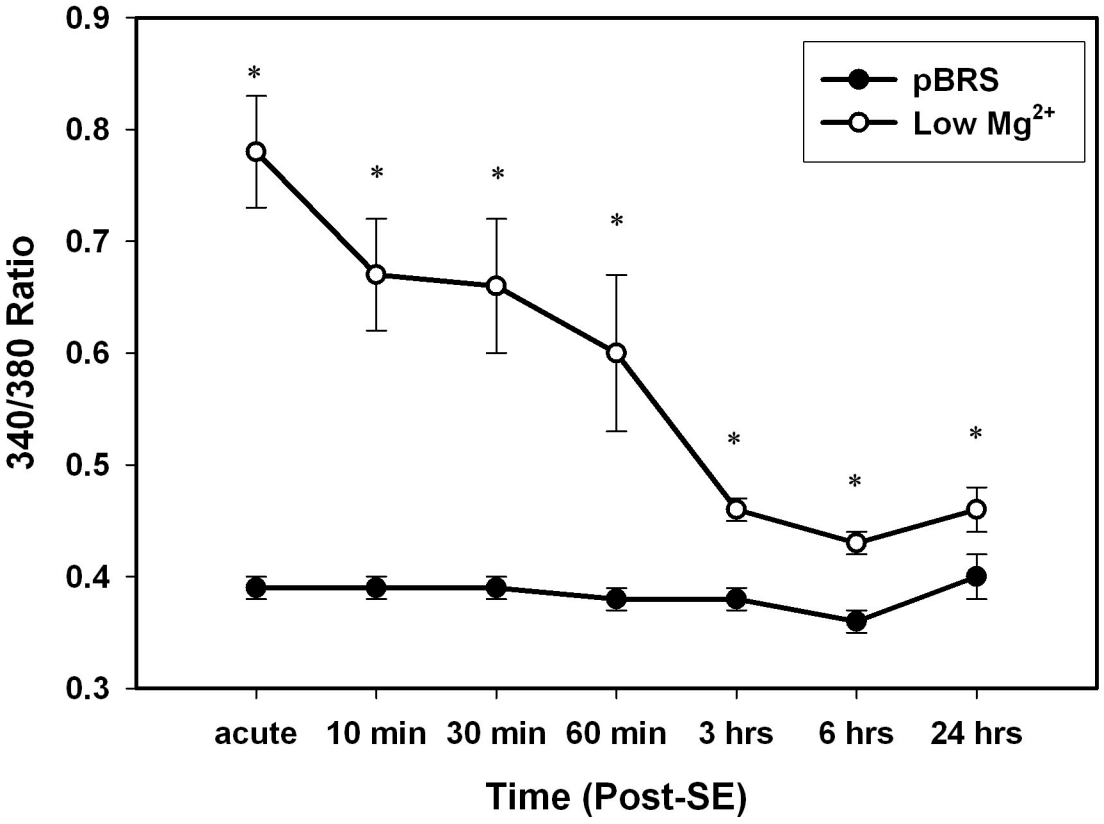

Figure 3-1. In vitro SE causes significant, long-lasting elevations in $[Ca^{2+}]_i$ (Ca^{2+} plateau). Time course comparing sham controls treated with pBRS (solid black circles) versus neurons treated with low Mg^{2+} (clear circles) at the end of in vitro SE (acute) and at various time points following in vitro SE (10 min, 30 min, 60 min, 3 hrs, 6 hrs, 24 hrs). All data represented as average 340/380 ratio ± standard error of the mean (SEM). *$p<0.05$, n= 6 or more plates with 52-134 neurons imaged per condition at each time point studied.

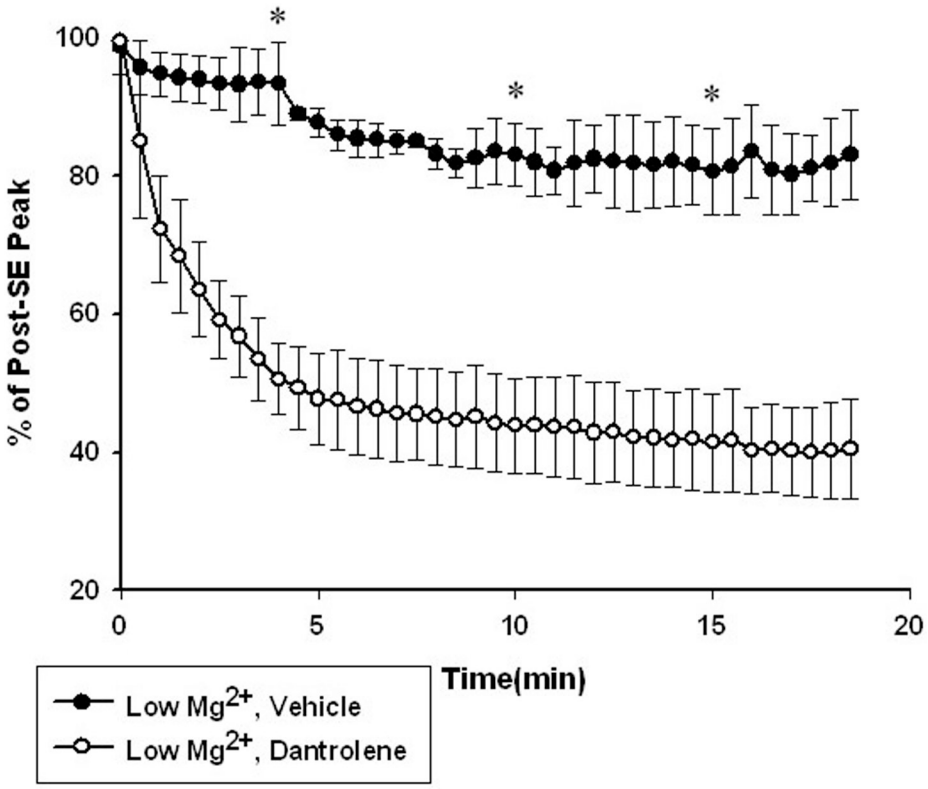

Figure 3-2. Dantrolene lowers $[Ca^{2+}]_i$ to baseline levels following in vitro SE. Following 3 hours of in vitro SE (time=0), cells were treated with either dantrolene (50 μM, clear circles) or vehicle (solid black circles). 340/380 ratios were recorded every 30 seconds for 20 minutes and normalized to percent of the peak ratio observed at time=0. *$p<0.05$, n=6 plates per treatment group with ~60 neurons imaged per condition.

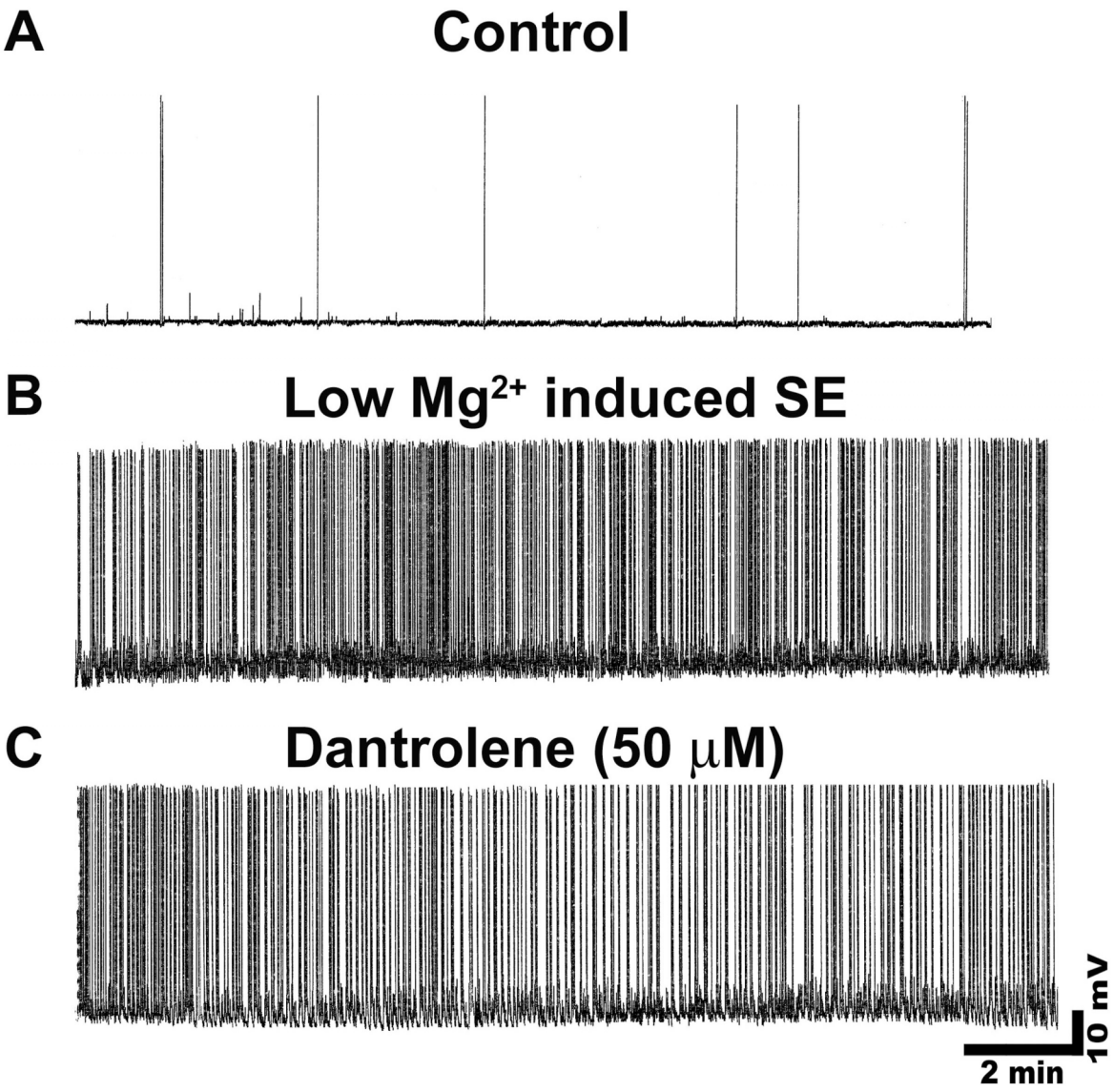

Figure 3-3. In vitro SE is not inhibited by dantrolene. **A**, representative current-clamp trace from control neuron **B**, neuron in low Mg^{2+} or in vitro SE and **C**, neuron in low Mg^{2+} plus dantrolene (50 μM).

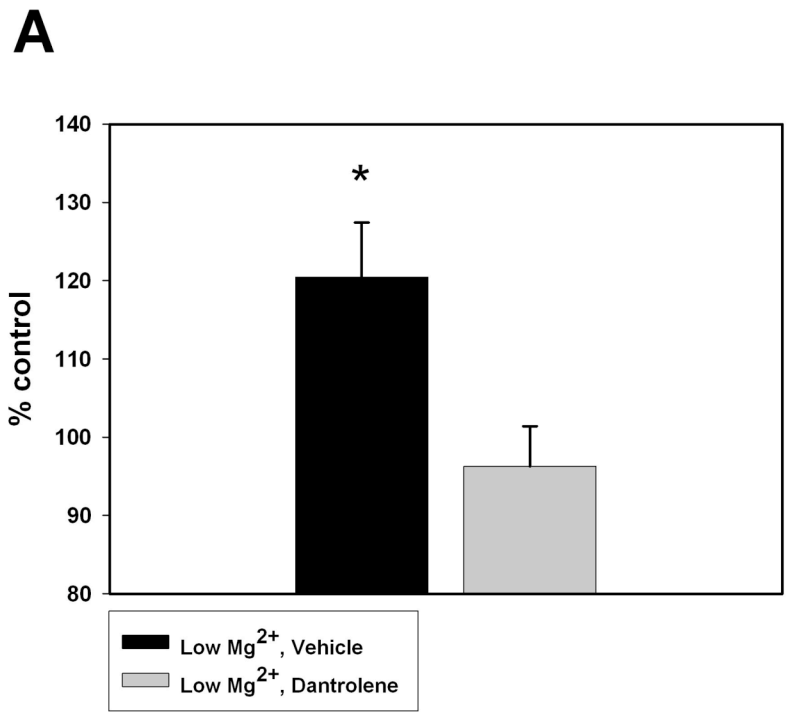

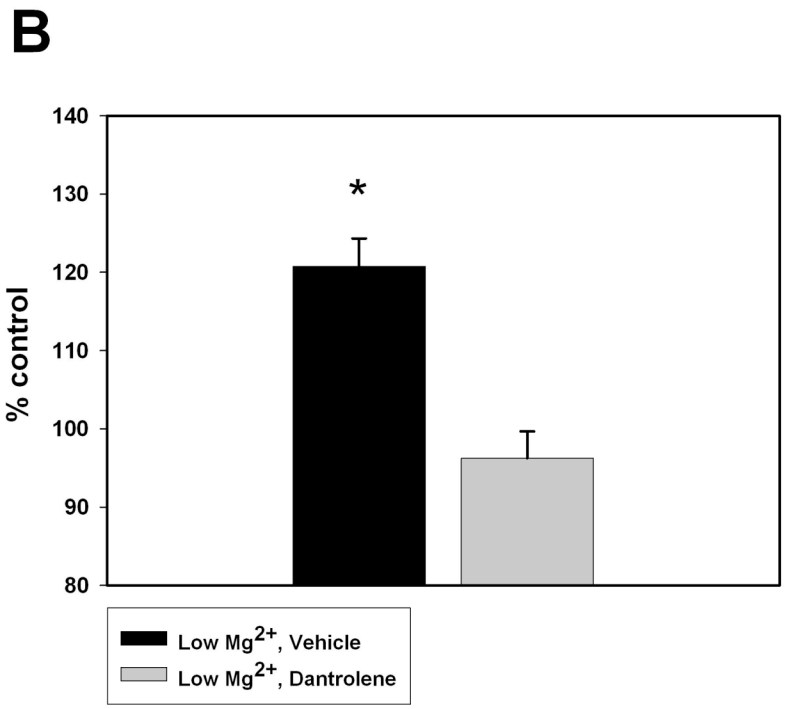

Figure 3-4. Dantrolene maintains baseline Ca^{2+} levels 24 and 48 hrs post-SE. **A**, effect of dantrolene (50μM) (light gray bar) versus vehicle (black bar) on 340/380 ratios 24 hrs post-in vitro SE and **B,** 48 hrs post-in vitro SE. Data represented as average percent of naïve control ± SEM. *$p<0.05$, n=10 or more plates with ~100 cells imaged per treatment group for 24 hr time point; n=5 plates with ~60 cells imaged per treatment group at 48 hr time point.

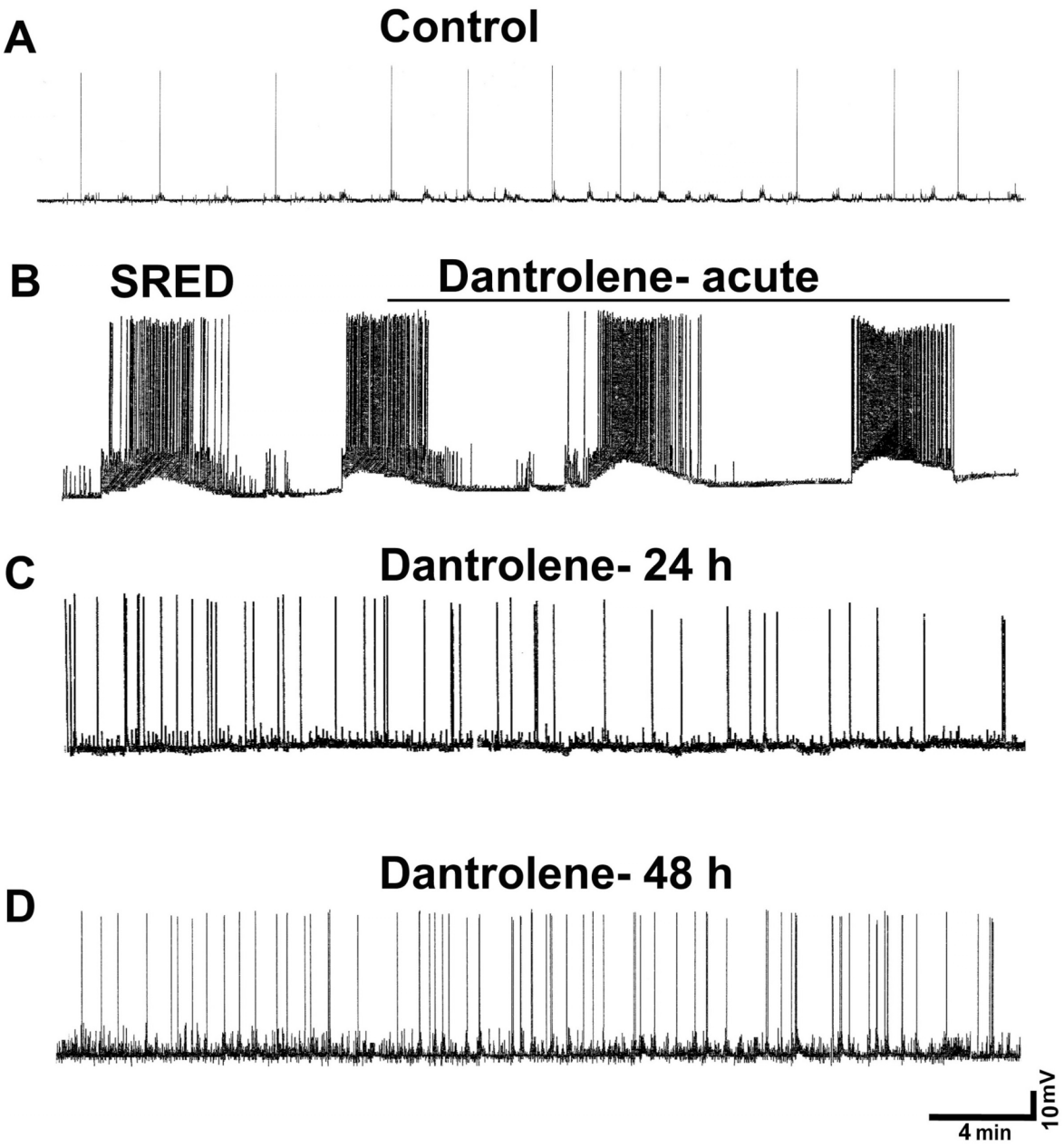

Figure 3-5. Dantrolene prevents the development of SREDs 24 and 48 hours post-SE but does not inhibit SREDs acutely. A, representative current-clamp trace from control neuron, **B,** low Mg^{2+}-treated neuron displaying characteristic SREDs, and **C,** neurons treated with low Mg^{2+} then dantrolene at both 24 hrs and D, 48 hrs post-treatment. Dantrolene did not inhibit SRED activity when added acutely to neurons displaying SREDs (line over **B**).

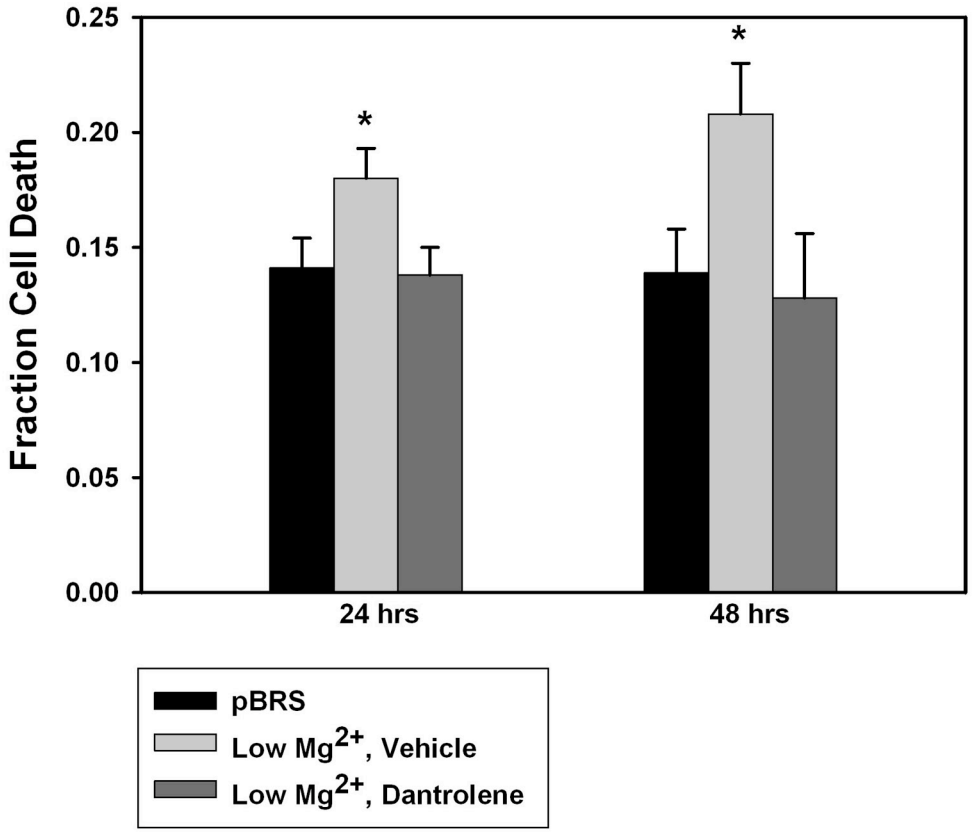

Figure 3-6. Dantrolene is neuroprotective. **A**, Cell death was assessed at 24 hrs and **B**, 48 hrs post-treatment with pBRS (sham, black bars), low Mg^{2+} then vehicle (light gray bars), and low Mg^{2+} then dantrolene (50μM) (dark gray bars). No significant difference observed between sham and drug-treated group at either of the time points. Low Mg^{2+} neurons demonstrated significantly more cell death than the other two groups at both 24 and 48 hrs post-treatment. Data represented as mean fraction cell death ± SEM. *$p<0.05$, n=7 or more plates per treatment and time point.

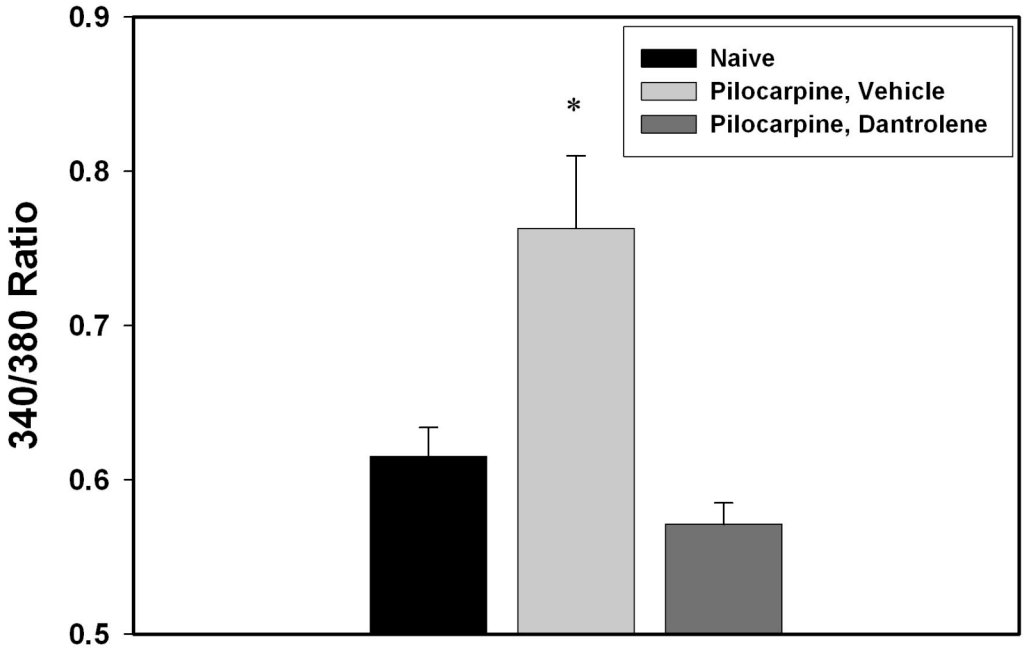

Figure 3-7. In the rat pilocarpine model of SE-induced AE, dantrolene is able to lower hippocampal neuronal Ca^{2+} post-SE. Animals were treated with vehicle (DMSO) or dantrolene (10 mg/kg) following pilocarpine-induced SE. 24 hrs later hippocampal neurons were isolated and imaged for Ca^{2+} levels. Bar graph compares naïve control animals (black bar), SE-vehicle animals (light gray bar), and SE-dantrolene animals (dark gray bar). Data is represented as mean 340/380 ratio ± SEM. *$p<0.05$, n=2 or more animals in each group with approximately 30 cells imaged per animal.

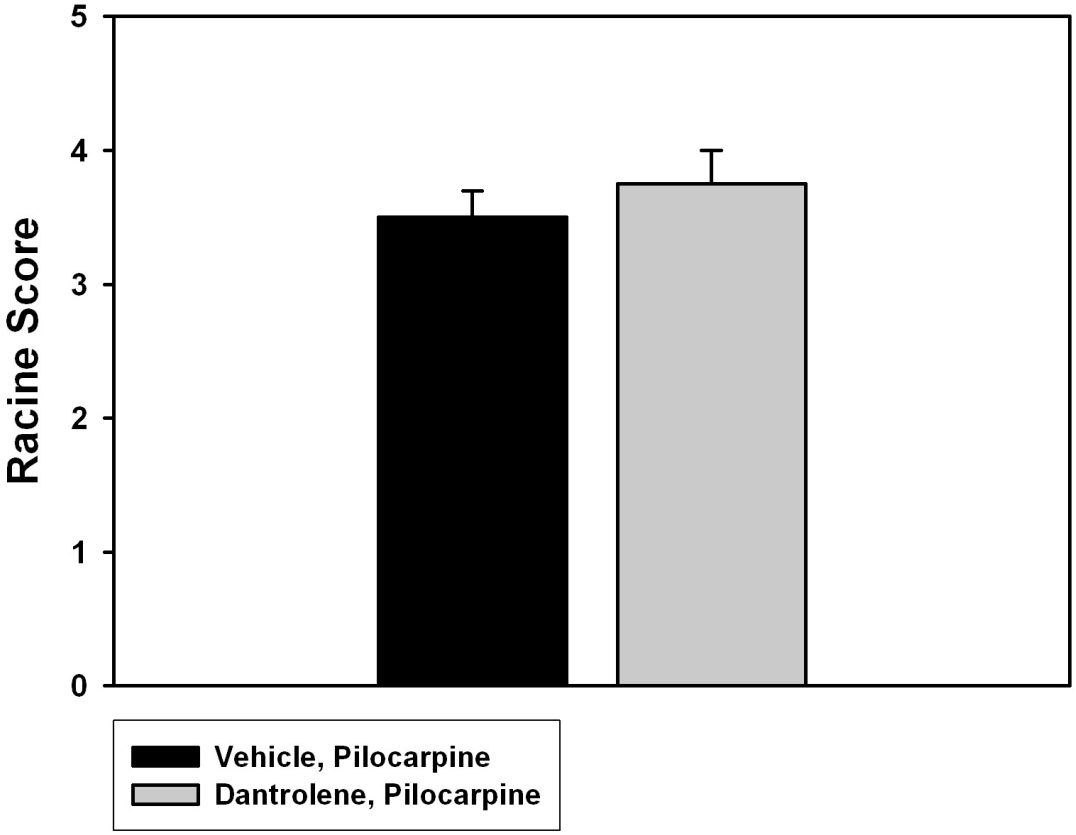

Figure 3-8. Dantrolene does not affect the severity of pilocarpine-induced SE. The severity of pilocarpine-induced seizures was quantified using a modified Racine scale (0-6, with 0= no response to 6= death) by averaging scores from 2 independent observers. Data is represented as mean ± SEM. n=4 animals per group

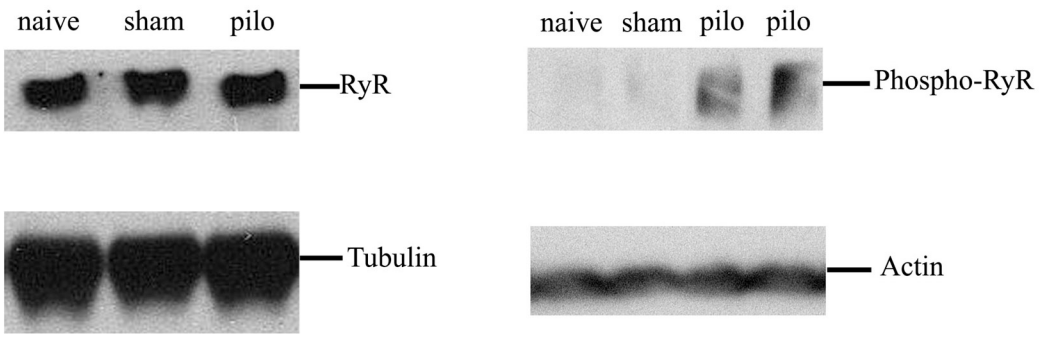

Figure 3-9. The Ca^{2+} plateau may be maintained in vivo by "leaky" RyR2. **A**, western blot analysis of hippocampal RyR2 and **B**, phospho-RyR2 expression 1wk after pilocarpine-induced SE. The data demonstrated no change in the expression of the $5x10^2$ kD RyR between the naïve, sham, and pilocarpine groups. However, the expression of the $5x10^2$ kD phospho-RyR is significantly increased in the pilocarpine-treated group.

Chapter 4: Levetiracetam Inhibits Both Ryanodine and IP3 Receptor Activated Calcium Induced Calcium Release in Hippocampal Neurons in Culture

Introduction

Epilepsy is a major neurological condition that affects approximately 1-2% of the population worldwide and over 40% of all epilepsy cases arise following a previous brain insult [106], [107]. Progress has been made in the treatment of epilepsy during the past decade with the discovery of newer antiepileptic drugs (AEDs) and surgical treatments. Understanding the mechanisms of action of AEDs has helped in better characterizing neuronal excitability and may also aid in the development of more effective strategies to treat epilepsy. Levetiracetam (LEV) is a new AED that is currently in widespread clinical use. However, LEV appears to have different anticonvulsant properties from other AEDs [108] and little is known of its mechanism of action except that it acts in a manner and at sites distinct from other commonly used AEDs [109]. Understanding how this drug works as an AED and an examination of its ability to block certain cellular changes could provide insights into its powerful anticonvulsant effect and into the development of more effective AEDs that act in a similar manner.

LEV, the *S*-enantiomer of α-ethyl-2-oxo-1-pyrrolidine acetamide, is used to treat a variety of forms of epilepsy [110]. Unlike many AEDs, LEV does not appear to exhibit direct effects on GABAergic neurotransmission, fails to interact with the benzodiazepine binding site, and lacks a significant affinity for GABAergic or glutamatergic receptors [111],[112],[113]. In addition, compared to other AEDs, LEV is not effective in a use dependent fashion on sodium channel inhibition, maximal electric shock or pentylenetetrazole tests for anticonvulsant agents [114]. Most recently, it has been demonstrated that LEV inhibits GABA-A current run-down [115] and that it binds to the synaptic vesicle protein 2A (SV2A) [109]. While studies have demonstrated that SV2A modulates exocytosis of neurotransmitter-containing vesicles [116],[117], the specific mechanistic relationship between LEV and SV2A remains to be elucidated. Thus, LEV represents a distinct class of AEDs.

Both changes in Ca^{2+} homeostatic mechanisms and persistent elevations in baseline intracellular calcium ($[Ca^{2+}]_i$) have been implicated in playing a key role in the induction and maintenance of post-injury spontaneous recurrent seizures, or acquired epilepsy (AE) [4]. Studies have demonstrated that inositol 1,4,5-triphosphate (IP3) and ryanodine receptor (RyR) mediated calcium-induced calcium release (CICR) play key roles in the changes in $[Ca^{2+}]_i$ observed in epileptic conditions [48],[97]. The effect of LEV on Ca^{2+} remains to be fully elucidated. However, it is known that LEV does not affect T-type voltage-gated Ca^{2+} and exhibits only a mild inhibition of high voltage activated Ca^{2+} channels [118]. LEV has been shown to inhibit caffeine-induced calcium transients in

studies in rat pheochromocytoma PC12 cells [51], and bradykinin-induced calcium transients in hippocampal slices [119]. Since it has been shown that $[Ca^{2+}]_i$ regulation in hippocampal neurons plays an important role in modulating anticonvulsant and epileptogenic effects and in mediating injury during seizures [32],[120],[121] it is important to evaluate the effects of LEV on $[Ca^{2+}]_i$ in hippocampal neurons by regulating IP3R or RyR induced CICR.

This study was initiated to evaluate whether LEV was able to inhibit both IP3R- and RyR-induced CICR in primary hippocampal neurons in culture. The results demonstrate that LEV affects CICR from IP3 and Ry-sensitive stores, employing the use of single-cell Fura-2 imaging to record the response to caffeine and bradykinin, two agents that induce prototypic IP3 and Ry-mediated calcium release respectively [122],[123]. The exploration of whether LEV modulates CICR could prove a valuable addition to what is currently understood on the effects of LEV on hippocampal neurons. Moreover, the ability of a drug to reduce $[Ca^{2+}]_i$ may make it an ideal therapeutic candidate in neuroprotection following injury and the prevention of long-term plasticity changes leading to epilepsy.

Materials and Methods

Reagents

UCB Pharma supplied Levetiracetam. Caffeine and bradykinin were obtained from Sigma-Aldrich (St. Louis, MO). All agents were solubilized in physiologic bath-recording solution.

Hippocampal neuronal culture preparation

Preparation of primary mixed hippocampal neuronal culture was performed as previously described [23]. In summary, hippocampal cells were isolated from 2-day post-natal Sprague-Dawley rats (Harlan, Frederick, MD). Cells ($7.5x10^4$) were plated onto a glial support layer that was previously plated onto poly-L-lysine (0.05 mg/ml) coated Lab-Tex glass chambers (Nalge-Nunc International, Naperville, IL). Cultures were maintained at 37°C in 5% CO_2/95% O_2 incubator and fed twice weekly with Neurobasal A medium (Invitrogen, Carlsbad, CA) with B-27 serum-free supplement (Invitrogen) and 0.5mM L-glutamine. All experiments were performed on neurons maintained for 14-17 days *in vitro* to ensure proper development. All procedures adhered strictly to the National Institutes of Health Guide for the Care and Use of Laboratory Animals and were approved by Virginia Commonwealth University's Institutional Animal Care and Use Committee.

Ca^{2+} Microfluorometry

Primary hippocampal cultures were loaded with Fura-2 acetoxymethyl ester and then placed on the 37°C stage of an Olympus IX-70 inverted microscope (Olympus, Center Valley, PA) coupled to an ultra-high-speed fluorescence imaging system (Perkin-Elmer Life and Analytical Sciences, Boston, MA) as described previously [94]. Data were collected using the UltraVIEW Imaging System. Ratio images were acquired every 5 s using alternating excitation wavelengths (340/380 nm) with a filter wheel (Sutter Instruments, Novato, CA) and fura filter cube at 510/540 nm emissions with a dichroic

mirror at 400 nm [94]. Image pairs were captured for 50 s before and 100 s post-addition of bradykinin or caffeine, and were corrected for background fluorescence by imaging a non-indicator loaded field [94].

Data Analysis

Data were statistically analyzed using StatView (Version 5.0.1). Experiments were repeated at least three times from different culture batches. The significance of the data was tested by one-way analysis of variance (ANOVA), or one-way repeated measures (RM) ANOVA followed by Fisher's post-hoc test when appropriate. $P < 0.05$ was considered significant for all data analysis.

Results

LEV does not affect baseline $[Ca^{2+}]_i$ in cultured hippocampal neurons

To determine the effect of LEV on basal $[Ca^{2+}]_j$, Fura-2 340/380 ratios were measured in the presence and absence of clinically relevant concentrations [119] of LEV (1, 10, 33, and 100 μM). Cells were pre-treated for 20 minutes with either vehicle (control) or LEV and Fura-2 ratios were recorded. As shown in Figure 4-1, no significant changes in 340/380 ratios were observed between control and LEV-treated cells during the 20-minute period following the addition of LEV to the hippocampal culture. These results demonstrate that at all concentrations tested, LEV does not affect baseline $[Ca^{2+}]_i$.

LEV inhibits caffeine induced CICR in hippocampal neurons

Caffeine-induced Ca^{2+} transients are mediated by stimulation of RyR [119],[124]. Thus, in order to investigate the effects of LEV on ryanodine induced Ca^{2+} release, caffeine-induced Ca^{2+} transients were studied following pre-treatment with 33 μM LEV in accordance with other studies [119]. Before the addition of caffeine, both control and LEV pre-treated cells exhibited similar baseline ratios of 0.294±0.018 and 0.319±0.120 respectively, consistent with ratios observed in Figure 4-1. Stimulation with caffeine elicited a marked increase in $[Ca^{2+}]_i$ in control neurons as evidenced by increased 340/380 Fura-2 ratios from the baseline value of 0.294±0.018 to 0.653±0.026, as shown in representative trace (Figure 4-2 A). Pseudocolor ratio images prior and subsequent to caffeine stimulation demonstrate this change in calcium following caffeine challenge (Figure 4-2 B). Thus, the overall change from baseline 340/380 ratio following treatment with 10mM caffeine was 0.328±0.018 (Figure 4-2 C).

In contrast, cells pre-treated with LEV displayed a significantly diminished response to caffeine-induced stimulation. In LEV-treated cells, the baseline 340/380 ratio of 0.319±0.120 increased to a maximum value of 0.445±0.045 following the caffeine challenge (Figure 4-2 A). Pseudocolor ratio images demonstrate the contrast in the ability of caffeine to mediate changes in calcium in LEV pre-treated cells when compared to control (Figure 4-2 B). Thus, as shown in Figure 4-2 C, following treatment with 10mM caffeine, the overall change from baseline 340/380 ratio was 0.126±0.022 in cells pre-

treated with 33μM LEV. Therefore, LEV pre-treatment inhibits the height of caffeine-induced Ca^{2+} transients by 61.50%.

LEV inhibits bradykinin induced Ca^{2+} transients in hippocampal neurons

To investigate how LEV affects IP3R activated Ca^{2+} release, the effect of LEV (100μM) pre-treatment on the inhibition of bradykinin-induced Ca^{2+} release was evaluated. Bradykinin-induced Ca^{2+} transients are mediated by activation of IP3R [125]. Before the addition of bradykinin, similar baseline ratio values of 0.304±0.020 in control and 0.263±0.015 in LEV (100μM) pre-treated cells were observed, as shown in Figure 4-1. Control neurons demonstrated a marked increase in $[Ca^{2+}]_i$ when stimulated with bradykinin (1μM) from baseline to 0.574±0.055 (Figure 4-3 A). This change in Fura-2 ratio in control neurons is shown in the pseudocolor ratio image (Figure 4-3 B). Thus, treatment with 1 μM bradykinin caused a change in 340/380 ratio of 0.269±0.063 from the baseline.

LEV-treated neurons showed a markedly diminished response to bradykinin when compared to control neurons. Stimulation with bradykinin caused a small increase from baseline to 0.332±0.037 (Figure 4-3 A), as shown also in the pseudocolor ratio image (Figure 4-3 B). Therefore, neurons pre-treated with 100 μM LEV, bradykinin elicited a change from baseline of only 0.069±0.032 (Figure 4-3 C). Thus, LEV pre-treatment inhibited the height of bradykinin-induced Ca^{2+} transients by 74.35%. We found at

concentrations lower than 100μM LEV, there was no significant inhibition in bradykinin-induced Ca^{2+} transients.

Discussion

The results from this study provide direct evidence that LEV inhibits RyR and IP3R induced CICR in hippocampal neurons in culture. LEV was effective in decreasing both caffeine-mediated activation of RyR induced CICR and bradykinin activation of IP3R stimulated CICR. These results indicate that LEV is an effective inhibitor of $[Ca^{2+}]_i$ release mediated by two of the major CICR receptor activated systems. While the effect of LEV on Ca^{2+} dynamics in an in vitro model of acquired epilepsy remains to be determined, Ca^{2+} is a major second messenger and has been implicated in neurotoxicity, neuronal plasticity and the maintenance of epilepsy [34], [32]; thus, the ability of LEV to inhibit CICR may prove to be an important property of this drug.

The experiments performed in this study were designed to test whether LEV was able to inhibit CICR and to evaluate the mechanisms mediating its effects on these systems, as dysregulation of RyR and IP3R has been associated with neurotoxicity, neuronal plasticity and epilepsy [34]. To study the ryanodine system, caffeine was employed because it has been demonstrated that it functions similarly on RyR as nanomolar concentrations of ryanodine with the added benefit of faster kinetics and the ability to quickly reverse its effects by washing [124]. Non-physiologic concentrations of caffeine (in the millimolar range) are utilized in studies evaluating RyR-mediated Ca^{2+} release and the Ca^{2+} response

elicited has been well-characterized [126],[127],[119]. At sub-millimolar doses, the actions of caffeine are dependent on cytosolic concentrations of Ca^{2+}, whereas, at concentrations greater than 5 mM, caffeine causes a Ca^{2+} independent activation of the ryanodine receptor [128]. Thus, using caffeine is an established method to activate RyR-mediated Ca^{2+} release [126],[127],[119]. One study employed caffeine in a hippocampal slice model to suggest that LEV reduces caffeine-mediated Ca^{2+} transients [119]. In studying IP3R-mediated CICR, lack of commercially available membrane-permeable IP3 makes bradykinin an ideal choice to study this system because it has been demonstrated that it stimulates Ca^{2+} release through IP3 stores [125]. One study in PC12 cells demonstrated that LEV was able to reduce bradykinin-induced Ca^{2+} transients [51]. However, no studies have investigated the effect of LEV on both IP3 and RyR in the highly relevant hippocampal culture model. Conducting these studies in hippocampal cultures is of utility because networks of hippocampal neurons have been used as models to study AE [23],[4].

Our results supplement the current literature aimed at elucidating the mechanism of action of LEV [115],[118],[129]. Currently, little is known regarding the mechanism behind the anti-epileptic properties of LEV. Studies have demonstrated that while LEV does not exhibit any direct action on GABAergic transmission and does not show affinity for GABAergic or glutamatergic receptors, it does induce a change in GABA turnover in the striatum [111],[112],[113],[108]. Other studies have focused on biochemical alterations induced by LEV and have found that it decreases levels of the amino acid taurine, a low

affinity agonist for $GABA_A$ receptors, in the hippocampus but does not elicit changes in other amino acids [129].

The most promising mechanistic hypothesis explaining the actions of LEV has come from experiments that suggest that the action of LEV is presynaptic, as it binds to the presynaptic membrane protein, SV2A [130],[109]. SV2A is ubiquitously expressed in the brain [131], yet little is known regarding the effects of the interaction between SV2A and LEV. It appears that SV2A is involved in controlling exocytosis of neurotransmitter-containing vesicles [116],[132]. More recently, it has been demonstrated that LEV prevents GABA-A current run-down [115]; thus, increasing inhibitory tone. Interestingly, it has been observed that increases in cytoplasmic Ca^{2+} triggered by caffeine-induced Ca^{2+} release from intracellular pools depress the GABA-A response [133]. In light of our studies, it will be interesting to study whether the ability of LEV to inhibit RyR-mediated CICR contributes to the inhibition of GABA-A current run-down following treatment with LEV.

Studying the effect of LEV on CICR mechanisms is also important, since alterations in $[Ca^{2+}]_i$ have been associated with many of the second messenger effects of Ca^{2+} [134] and have been shown to play an important role in underlying neurotoxicity, neuronal plasticity, and the development of AE [34], [32]. Moreover, the neuroprotective properties of LEV have been observed in several different models [135],[136],[137]. Following neuronal injury, excitotoxic glutamate release has been associated with increased stimulation of

NMDA receptors and the massive influx of Ca^{2+} into the cell [138],[4],[139]. This influx of Ca^{2+} triggers CICR and this irreversible Ca^{2+} overload has been linked to cell death [140],[97],[134]. Agents that can reduce these elevations in $[Ca^{2+}]_i$ have the potential to be neuroprotective [34] and thus, the findings in this study may shed light on a new application for LEV.

This study demonstrates that LEV is able to significantly inhibit Ca^{2+} release through both the RyR and IP3R systems. The ability of LEV to modulate the two major CICR systems demonstrates an important molecular effect of this agent on a major second messenger system in neurons. Further studies on the effects of LEV may offer insight into novel therapeutic uses for this agent and may offer further opportunities to study Ca^{2+}-mediated epileptogenesis, neuronal plasticity and neurotoxicity.

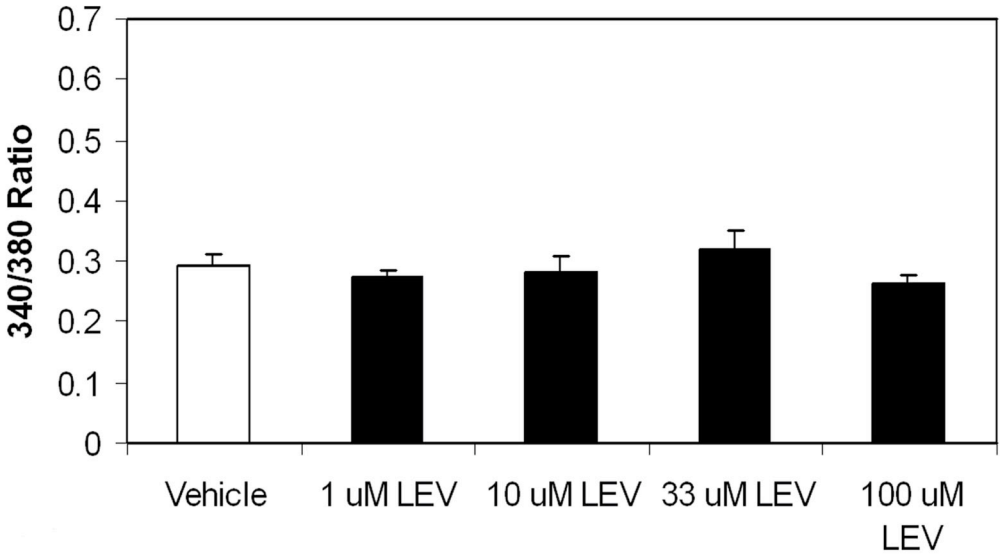

Figure 4-1. LEV has no effect on baseline $[Ca^{2+}]_i$ in cultured hippocampal neurons. Hippocampal neurons loaded with Ca^{2+} indicator, Fura-2, were treated for 20 minutes with vehicle (control) or LEV (1, 10, 33, and 100 μM). No significant difference in 340/380 ratio was observed between vehicle and drug treated cells at all concentrations tested. n=9, 3, 3, 7, 5 (Vehicle, 1, 10, 33, 100 μM LEV, respectively) plates with ~15-20 cells imaged per plate.

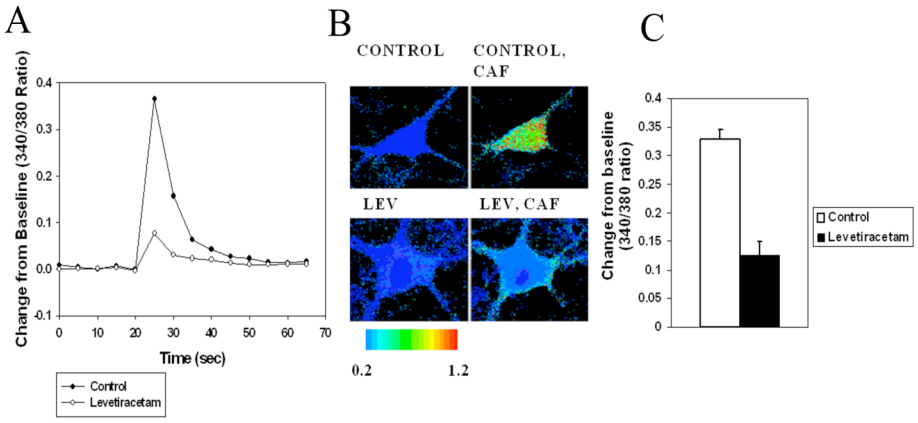

Figure 4-2. LEV inhibits caffeine induced CICR in cultured hippocampal neurons. **A**, representative time course of Ca^{2+} 340/380 ratios with baseline normalized to zero before and after 10 mM caffeine challenge in control (n=74) and LEV pre-treated (n=88) cells. 5 s intervals showing ratios 25 s before and 55 s following the addition of caffeine are displayed. Caffeine elicits an increase in basal Ca^{2+}, this increase is diminished in cells pre-treated with LEV (33 μM). **B**, 340/380 ratio images of representative cell before and after caffeine in both control and LEV-treated group. **C**, LEV inhibits height of caffeine-induced Ca^{2+} transients by 61.50%. An increase of 0.328±0.0183 from the baseline was observed in control neurons post-caffeine; whereas, upon caffeine stimulation cells pre-treated with LEV showed a change from baseline of 0.126±0.0229. n=5, control and n=6, LEV group, with ~15 cells imaged per plate (p=0.0002).

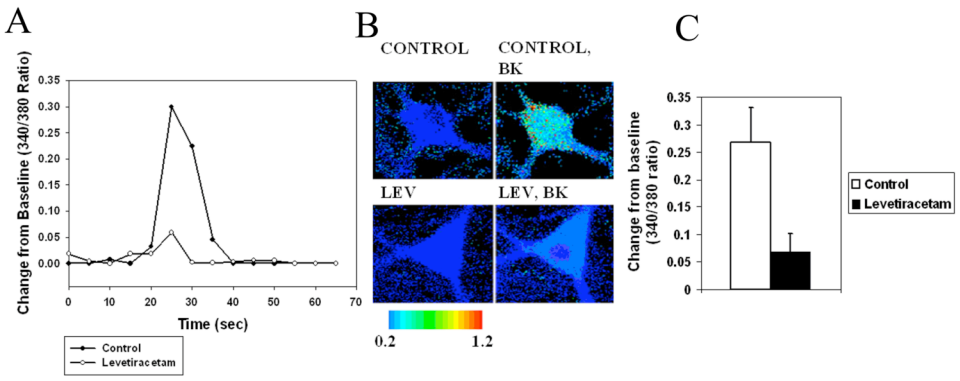

Figure 4-3. LEV inhibits bradykinin induced Ca^{2+} transients in hippocampal neuronal cultures. **A**, representative time course of Ca^{2+} 340/380 ratios with baseline normalized to zero before and after 1μM bradykinin challenge in control (n=119) and LEV-treated (n=82) cells. 5 s intervals showing ratios 20 s before and 50 s following the addition of bradykinin are displayed. Bradykinin elicits an increase in basal Ca^{2+}, this increase is diminished in cells pre-treated with LEV (100 μM). **B**, 340/380 ratio images of representative cell before and after bradykinin in both control and LEV-treated group. **C**, LEV inhibits height of bradykinin-induced Ca^{2+} transients by 74.35%. An increase of 0.269±0.063 from the baseline was observed in control neurons post-bradykinin; whereas, upon bradykinin stimulation cells pre-treated with LEV showed a change from baseline of 0.069±0.032. n=7 (control), n=5 (LEV group) with ~15 cells imaged per plate ($p<0.05$).

Chapter 5: The Novel Antiepileptic Drug Carisbamate (RWJ 333369) Is Effective in Inhibiting Spontaneous Recurrent Seizure Discharges and Blocking Sustained Repetitive Firing in Cultured Hippocampal Neuron

Introduction

Epilepsy is one of the most common neurological disorders affecting approximately 1-2% of population worldwide [141,142]. It is characterized by the occurrence of spontaneous, recurrent unprovoked seizure discharges [143]. A seizure is the symptomatic, behavioral manifestation of abnormal, disordered, spontaneous, and synchronized high frequency firing of populations of neurons in the CNS [4,142,143]. Epilepsy also has severe socio-economic implications [144]. Although great advances have been made in the development of newer antiepileptic drugs (AEDs) and surgical interventions for the treatment of epilepsy, approximately 40% of the patients are still refractory to treatment with conventional AED's [141,145]. A sizeable population of epileptic patients deals with the issue of daily management of epilepsy that ultimately affects their quality of life [146]. Thus, there is a growing demand for developing newer medications to treat epilepsy.

Carisbamate, or RWJ-333369 (*S*-2-*O*-carbamoyl-1-*o*-chlorophenyl-ethanol), is a novel neuromodulator initially developed by SK-Biopharmaceuticals and now under development by Johnson & Johnson, Pharmaceutical Research & Development L.L.C. It has completed phase 2 clinical trials for the treatment of epilepsy [147]. Carisbamate is a monocarbamate derivate of the broad spectrum AED felbamate, that is no longer used clinically due to its hematological and hepatic toxicities [148]. Unlike felbamate, carisbamate has only two carbons in its side chain and only one carbamate group that prevents the formation of the toxic aldehyde causing the toxicity of felbamate [147]. Because of its potential safety, carisbamate has been evaluated as a novel AED and has been demonstrated to possess anticonvulsant activity in a variety of in vivo seizure models including hippocampal and corneal kindling [147,149] and the GAERS model of absence epilepsy [150]. It also inhibits spontaneous recurrent seizures after kainite [151] or Li-Pilocarpine [152] induced epilepsy. Carisbamate is also anticonvulsant against bicuculline and picrotoxin induced seizures and in pentylenetetrazole and maximal electroshock induced seizure models [147,149,153]. However, the exact mechanism of action of carisbamate is still unknown. The dicarbamate, felbamate, has been reported to affect a variety of ionic currents including the sodium (Na^{+}) [154], calcium (Ca^{2+}) [155], and N-methyl d-aspartate (NMDA) currents [156]. However, significance of this action for seizure protection is uncertain. Thus, it is important to determine mechanisms underlying the antiepileptic effects of carisbamate.

This study was initiated to investigate mechanisms underlying the antiepileptic effects of carisbamate using the hippocampal neuronal culture model of status epilepticus (SE)-induced acquired epilepsy (AE) [4,23,157]. The low Mg^{2+} model of AE utilizes an episode of continuous seizure activity (in vitro SE) for 3 hrs to induce epileptogenesis. Upon return to solutions containing $MgCl_2$, networks of neurons manifest synchronized spontaneous recurrent epileptiform discharges (SREDs) for the life of the neurons in culture (in vitro AE). The low Mg^{2+} model of SREDs in hippocampal neuronal cultures has been routinely used to characterize biochemical, electrophysiological, and molecular mechanisms underlying epilepsy in an in vitro setting [4,48,157,158]. This in vitro model allows for careful control of the neuronal environment and is thus, ideally suited to evaluate the effects of various investigational compounds on electrographic seizure activity.

Materials and Methods

Reagents

All reagents were purchased from Sigma Chemical Co (St. Louis, MO) unless otherwise noted. Sodium pyruvate, minimum essential media containing Earle's salts, fetal bovine serum and horse serum were obtained from Gibco-BRL (Invitrogen Corp., Carlsbad, CA). Carisbamate was provided by Johnson & Johnson, Pharmaceutical Research & Development L.L.C., Titusville, NJ, USA and was dissolved in sterile water made slightly basic with sodium hydroxide and diluted to a final concentration in buffer.

Hippocampal neuronal culture preparation

All animal use procedures were in strict accordance with the National Institutes of Health Guide for the Care and Use of Laboratory Animals and approved by Virginia Commonwealth University's Institutional Animal Care and Use Committee. Studies were conducted on primary mixed hippocampal neuronal cultures prepared as described previously with slight modifications [23,159,160]. In brief, hippocampal cells were obtained from 2-day postnatal Sprague-Dawley rats (Harlan, Frederick, MD) and plated at a density of 1 x 10^5 cells/cm^2 onto 35-mm Falcon cell culture dishes (Becton Dickinson and Co., Franklin Lakes, NJ) previously coated with poly-L-lysine (0.05 mg/ml). Glial cultures were maintained at 37°C in a 5% CO_2/95% air atmosphere and fed thrice weekly with glial feed (minimal essential media with Earle's Salts, 25 mM HEPES, 2 mM L-Glutamine, 3 mM Glucose, and 10% fetal bovine serum). When confluent, glial beds were treated with 5 μM cytosine arabinoside for 2 days to curtail cell division. On the 13th day in vitro, the media was fully replaced with a 5% horse serum supplemented neuronal feed (composition given below) in preparation for neuronal plating on the following day. At this time, these cultures predominantly consisted of glial cells with few, if any, neurons. On the 14th day in vitro, hippocampal cell suspension was plated on these confluent glial beds at a density of 2 x 10^5 cells/cm^2. 24 hrs after plating, cultures were treated with 5 μM cytosine arabinoside to inhibit non-neuronal growth. Cultures were maintained at 37°C in a 5% CO_2/95% air atmosphere and fed twice weekly with neuronal feed (minimal essential media with Earle's Salts, 25 mM HEPES, 2 mM L-Glutamine, 3 mM Glucose, 100 μg/ml

transferrin, 5 μg/ml insulin, 100 μM putrescine, 3 nM sodium selenite, 200 nM progesterone, 1 mM sodium pyruvate, 0.1% ovalbumin, 0.2 ng/ml triiodothyroxine and 0.4 ng/ml corticosterone supplemented with 20% conditioned media). These mixed cultures were used for experiments from 13 days in vitro following neuronal plating through the life of the cultures.

Whole-cell current clamp recordings

Whole-cell current clamp recordings were performed using previously established procedures [23,159,160]. Briefly, a cell culture dish was mounted on the stage of an inverted microscope (Nikon Diaphot, Tokyo, Japan) continuously perfused with physiological basal recording solution (pBRS) containing (in mM): 145 NaCl, 2.5 KCl, 10 HEPES, 2 $CaCl_2$, 1 $MgCl_2$, 10 glucose, and 0.002 glycine, pH 7.3, and osmolarity adjusted to 325 ± 5 mOsm with sucrose. Patch electrodes with a resistance of 2 to 4 mΩ were pulled on a Brown-Flaming P-80C electrode puller (Sutter Instruments, Novato, CA), fire-polished and filled with a solution containing (in mM): 140 K^+ gluconate, 1.1 EGTA, 1 $MgCl_2$, and 10 Na-HEPES, pH 7.2, osmolarity adjusted to 290 ± 10 mOsm with sucrose. Whole-cell recordings were carried out using an Axopatch 200B amplifier (Molecular Devices, Foster City, CA) in a current-clamp mode. Data were digitized via Digidata 1322A (Molecular Devices, Foster City, CA) and transferred to VHS tape using a PCM device (Neurocorder, New York, NY) and then played back on a DC-500 Hz chart recorder (Astro-Med Dash II, Warwick, RI). Carisbamate was included in the recording solution

and applied to the whole-cell dish by using a multi-channel gravity-feed perfusion system (Warner Instruments, Hamden, CT).

Hippocampal neuronal culture model of SREDs

SREDs were induced into neuronal cultures by exposing them for 3 hrs to a solution containing no added $MgCl_2$ (low Mg^{2+}) using procedures described previously [23,159,160]. Briefly, after the removal of maintenance media, neurons were gently washed with pBRS or low Mg^{2+} and then allowed to incubate in this solution at 37°C under 5% CO_2/95% air atmosphere. At the end of the 3-h period, cultures were restored to the physiological concentration (1 mM) of $MgCl_2$, returned to maintenance media, and incubated at 37°C under 5% CO_2/95% air atmosphere.

Sustained repetitive firing in cultured hippocampal neurons

Sustained repetitive firing (SRF) was induced by S-90 Tri-level Stimulator (Medical Systems Corp., Greenvale, NY) by depolarizing pulses of 500 ms duration, 0.3 Hz and increasing current strength from 0.1 to 0.5 nA through the micropipette. The duration and frequency of depolarizing pulses were kept constant for all experiments. Current strength was increased until the cell under study exhibited a suitable number of action potentials throughout the duration of the depolarizing pulse.

Hippocampal neuronal culture model of SE

After 2 weeks in cultures, neurons were utilized for experimentation. SE-like activity was induced in vitro as described previously [23]. Maintenance media was replaced with pBRS

with or without $MgCl_2$. Continuous high frequency epileptiform bursts (in vitro SE) were induced by exposing neuronal cultures to pBRS without added $MgCl_2$ (low Mg^{2+}). The high frequency spiking continued until pBRS containing 1 mM $MgCl_2$ was added back to the cultures. Unless indicated as low Mg^{2+} treatment, experimental protocols utilized pBRS containing 1 mM $MgCl_2$.

Data analyses

Data are reported as mean ± SEM. For concentration-response analysis, suppression of SE or SREDs was determined as a percentage decrease in frequency over increasing concentrations of carisbamate. Status epilepticus frequency was determined by counting individual epileptiform bursts over a recording duration of 5 min for each neuron analyzed before and after application of the drug. SRED frequency was determined by counting individual SREDs over a recording duration of 30 min for each neuron analyzed before and after application of the drug. Frequency analysis was carried out on multiple neurons at each concentration of carisbamate. SRF data were examined using one-way analysis of variance (ANOVA) followed by a post-hoc Tukey test. Data were analyzed using SigmaStat 2.0 and graphs were generated using SigmaPlot analysis software 8.02 (SPSS Inc., Chicago, IL).

Results

Effects of carisbamate on SREDs

Whole-cell current clamp recordings from neurons in cultures 1 day after a 3 hr low-Mg^{2+} treatment demonstrated SREDs or in vitro seizure events. Figure 5-1 B shows recording from a neuron that exhibited 3 SREDs that lasted between 1-2 min in duration. These SREDs occurred for the life of the neurons in culture and manifested paroxysmal depolarization shifts, pathophysiological characteristic of AE. SREDs started in an unprovoked manner and stopped spontaneously. Multiple recordings from adjacent neurons demonstrate that these SREDs were synchronous events occurring throughout the neuronal network in populations of neurons (data not shown, [23]). Thus, SREDs are the in vitro equivalent of spontaneous electographic seizure discharges. Age-matched control neurons revealed "normal" baseline activity consisting of intermittent action potentials (Figure 5-1 A). There were no significant differences in membrane potential and input resistance between control and epileptic neurons.

To evaluate the antiepileptic effects of carisbamate we used the in vitro hippocampal neuronal culture model of SREDs. As shown in Figure 5-1 C, application of carisbamate (100 μM) fully inhibited the expression and reoccurrence of SREDs. The effects of carisbamate were dose dependent and concentrations of 10-100 μM caused a progressive decrease in the occurrence of SREDs. The graph in Figure 5-2 demonstrates the effects of increasing carisbamate concentration on the frequency of SREDs. Carisbamate displayed a steep dose-response curve. The lower doses were less effective in stopping SREDs while

higher doses produced almost complete inhibition of SREDs. The ED_{50} value was computed to be 58.75 ± 2.43 μM. Carisbamate was applied to neurons during SREDs and it took approximately 10-15 min for its antiepileptic effect to be fully manifested. Upon washout of carisbamate, SREDs returned and seizures recurred after approximately 15-20 min (Figure 5-1 C).

Carisbamate produced identical effects to well-known anticonvulsants in this in vitro model of AE (Sombati and DeLorenzo, 1995). Phenytoin, a clinically used AED, is a use-dependent Na^+ channel blocker that is utilized for the treatment of generalized tonic-clonic and partial complex seizures [161,162]. As shown in Figure 5-1 D, Phenytoin (10 μM) at therapeutically relevant concentrations reversibly blocked SREDs. Phenobarbital, a GABAergic agonist, is another anticonvulsant that effectively blocked SREDs in our model (data not shown). Ethosuximide, a T-type Ca^{2+} channel blocker used to treat absence seizures, failed to block SREDs at concentrations up to 1 mM in this model (Figure 5-1 E). These results are consistent with clinical effects of these drugs for the treatment of temporal lobe epilepsy.

Effect of carisbamate on SRF

Several AEDs including phenytoin, carbamazepine, phenobarbital, and lamotrigine are known to block SRF in neurons [161,162]. This effect of AEDs is believed to be due to their ability to block voltage-gated Na^+ channels. We investigated if carisbamate shares this property with other AEDs. Cultured hippocampal neurons respond to a sustained

depolarizing current by generating a series of action potentials. Under control conditions, a depolarizing current (0.5 nA, 0.3 Hz) elicited between 4-10 action potentials (spikes) (Figure 5-3 A). Carisbamate (100 μM) caused a significant ($p < 0.001$) decrease in the frequency of spikes elicited by the depolarizing current and abolished the late sustained phase of firing without blocking the initial spike (Figure 5-3 B,D). These results suggest that carisbamate blocks Na^+ channels in a state- or use-dependent manner. While the effects of carisbamate were reversible, it took between 10-15 min for the restoration of SRF following washout (Figure 5-3 C). Spike frequency following carisbamate washout was not significantly different from pre-carisbamate spike frequency (Figure 5-3 D).

Effects of carisbamate on low Mg^{2+} induced high frequency spiking

In normal conditioned media, cultured hippocampal neurons exhibited spontaneous action potentials that were comparatively infrequent and irregular (Figure 5-4 A). However, upon removal of Mg^{2+} from extracellular environment, neurons generated bursts of action potentials resulting in the development of continuous high frequency epileptiform discharges (Figure 5-4 B). This epileptiform activity consisted of repetitive burst discharges with each burst comprised of multiple spikes overlaying a depolarization shift. Spike frequency upon removal of Mg^{2+} was greater than 3 Hz, meeting the criteria of clinical electrographic in vitro SE [23]. This technique has been widely used to model the electrographic SE-like condition in vitro.

As shown in Figure 5-4, clinically used AEDs including phenytoin (50 μM) and ethosuximide (1 mM) at therapeutic concentrations or higher failed to stop low Mg^{2+} induced in vitro SE activity in this model [23]. This type of in vitro continuous seizure discharge has been extremely refractory to anticonvulsant treatment [23,159,160]. We investigated if carisbamate could act differently and block this high frequency spike activity. Treatment with carisbamate (100 μM) appeared to marginally slow down the low Mg^{2+}-induced high frequency spiking (Figure 5-4 E). However, this effect was not significantly different from low Mg^{2+} treated neurons alone. The graph in Figure 5-5 shows the effects of increasing concentrations of carisbamate on the inhibition of low Mg^{2+}-induced high frequency spike activity. Even at concentrations of up to 200 μM, carisbamate inhibited spike frequency only by 10-15%. The ED_{50} value for effects of carisbamate on inhibition of SE-like activity could not be calculated since the effects never reached 50% inhibition. High frequency firing was restored within 10-15 min following washout of carisbamate with low Mg^{2+} solution.

Discussion

This study demonstrates that carisbamate blocks the expression of SREDs in the hippocampal neuronal culture model of in vitro AE. In addition, carisbamate reduced the frequency of action potentials generated during depolarization-induced SRF. Our results are consistent with other studies that have demonstrated antiepileptic properties of carisbamate in various in vivo models of seizures [147,149-153]. While the exact mechanism of action of carisbamate is actively pursued, the ability of carisbamate to

inhibit depolarization-induced SRF suggests that it may block Na^+ channels in a state- or use-dependent manner and that this effect may account in part for some of the anticonvulsant effects of carisbamate.

The majority of patients with epilepsy have their seizures well controlled with conventional AEDs; however, approximately 40% of patients manifest refractory epilepsy [163,164]. Thus, there is a significant need to develop new AEDs to attempt to treat refractory patients. Novel AEDs are being designed to treat drug resistant epilepsy [147,149]. In fact, out of the currently available 20 AEDs, 8 were introduced in past decade [165]. However, despite the introduction of newer AEDs, the prognosis still remains poor [163,166]. Thus, there are continual efforts to develop more efficacious drugs that have fewer side effects and a wider margin of safety [147,149].

The novel neuromodulator, carisbamate, displays high potency in a variety of in vivo and in vitro seizure models at doses well below those that produce CNS toxicity [167]. However, its mechanism of action remains to be elucidated. Chemically, carisbamate is a monocarbamate that is a derivative of the dicarbamate, felbamate. Felbamate has been shown to affect Na^+, Ca^{2+}, and NMDA currents [154] [155,156]. All of these effects could contribute to the antiepileptic properties of dicarbamates. While the effects of carisbamate on various ionic currents and the contribution of these effects towards its antiepileptic profile remain to be investigated, our studies indicate that a use- or state-dependent block of Na^+ channels could account for such properties. Alterations in intracellular Ca^{2+}

dynamics have been shown to affect the expression of SREDs in this in vitro model of acquired epilepsy. The ability of carisbamate to inhibit SREDs could also be due to its ability to restore altered Ca^{2+} homeostasic mechanisms in epileptic neurons. It will be interesting to investigate this possibility in future studies

The model of recurrent epileptiform discharges after low Mg^{2+}-induced in vitro SE is a commonly used system to study the mechanisms underlying seizures, seizure-induced plasticity, and the development of pharmacoresistant seizures [4,168-170]. The hippocampal neuronal culture model of SREDs mimics the electrophysiological and molecular changes observed during the induction, maintenance, and expression phases of epilepsy [4]. Moreover the SREDs exhibited in cultured neurons manifest identical electrographic properties, neuronal population synchronicity, and anticonvulsant sensitivity as observed in epileptic seizures recorded in in vivo models [4,23,83]. While the neuronal cultures do not have true anatomical connections and do not display clinical seizures, the hippocampal neuronal culture models offer the ability to utilize various in vitro techniques to study molecular mechanisms underlying epilepsy and mechanisms of actions of investigational drugs in a more controlled environment.

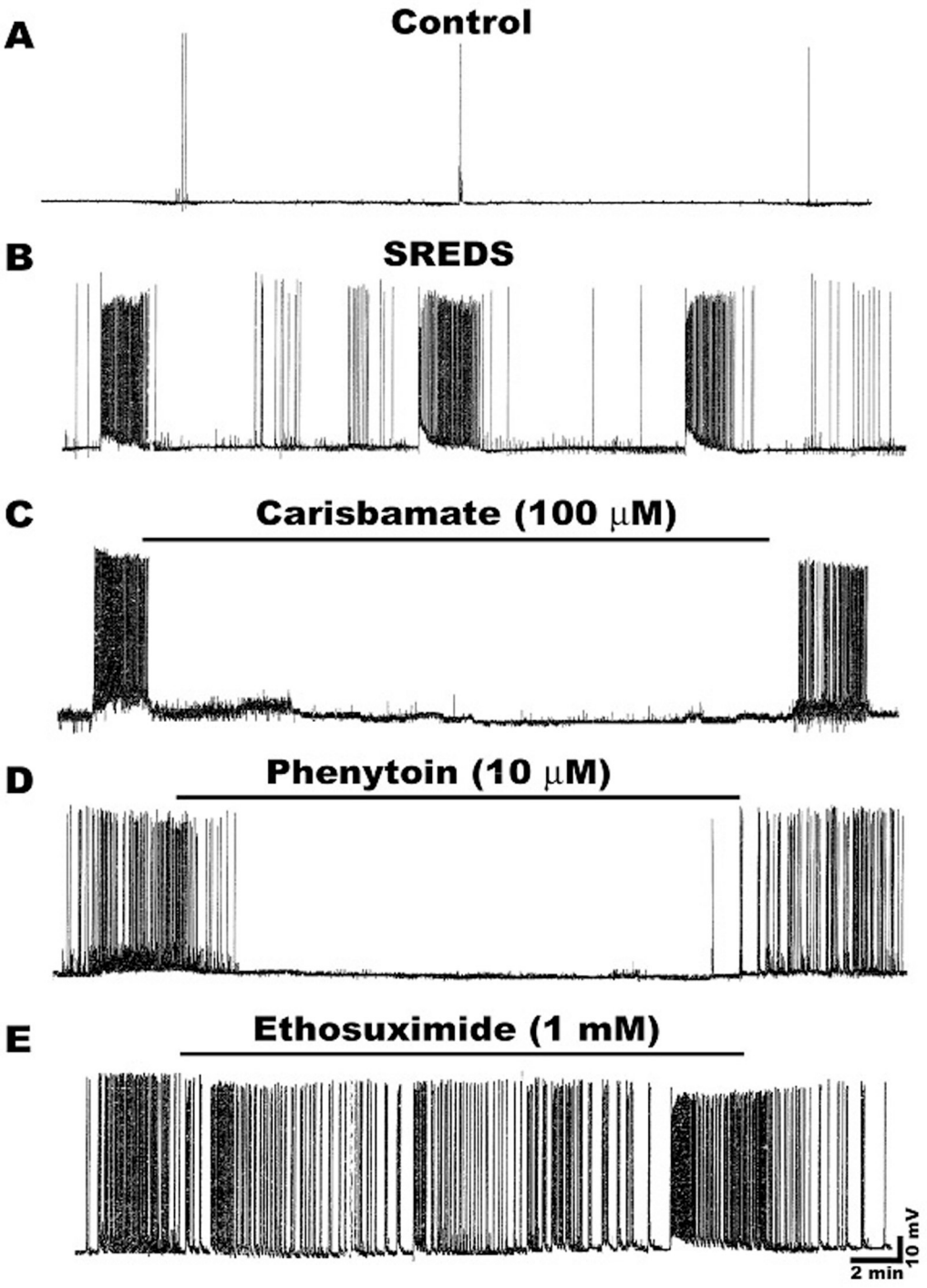

Figure 5-1. Effects of carisbamate on SREDs in cultured hippocampal neurons. **A,** Current-clamp recording from a representative control neuron displaying baseline activity consisting of intermittent action potentials. **B,** Recording from an "epileptic" neuron 1-day following a 3-h exposure to low Mg^{2+} solution demonstrates occurrence of characteristic SREDs. Three SREDs or spontaneous seizure episodes lasting ~60-90s can be seen in this recording frame. These SREDs occurred throughout the life of the cultures and are indicative of the pathophysiological "epileptic" phenotype. Effects of various AEDs on SREDs in cultured hippocampal neurons. Application of **C,** carisbamate (100 μM) or **D,** phenytoin (10 μM) to the epileptic neurons abolished the expression of SRED activity. However application of **E,** ethosuximide (1 mM) failed to stop SRED activity. The effects of AEDs on SREDs were reversible and seizures reappeared following drug washout.

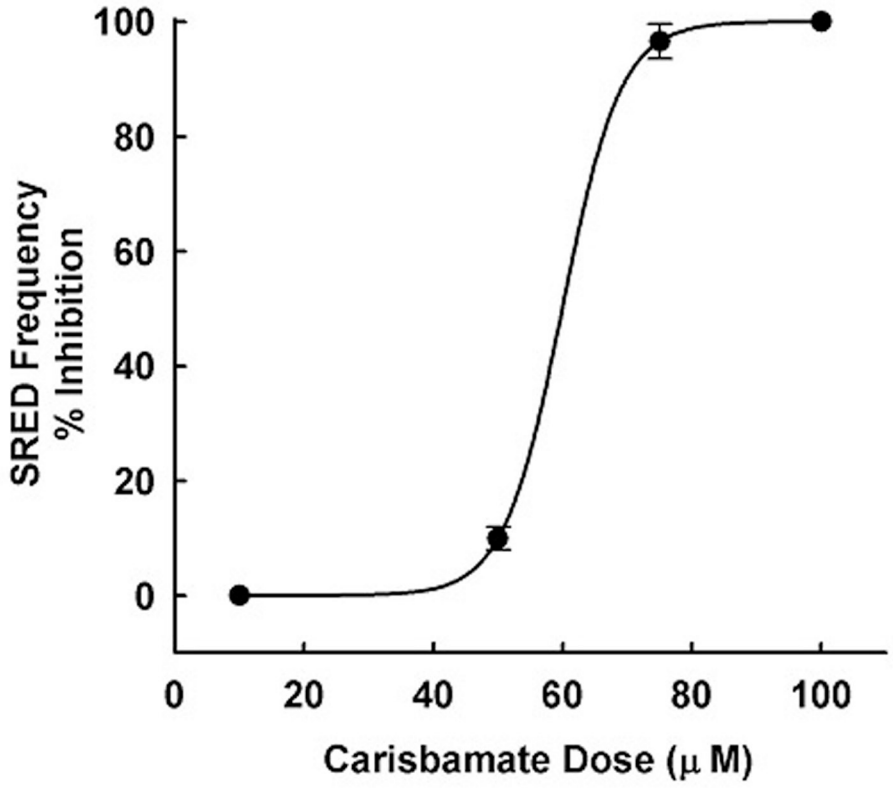

Figure 5-2. Carisbamate inhibits low Mg^{2+}-induced SRED activity in a concentration dependent manner. Frequency of SREDs in the presence of varying concentrations of carisbamate was measured over a 30-min period and then plotted as a percentage change (inhibition) from control (absence of carisbamate) SRED frequencies. Carisbamate blocked low Mg^{2+}-induced SREDs with an EC_{50} = 58.75 ± 2.43 μM. Each data point represents percentage change from control ± S.E.M. (n = 5-7 neurons/ concentration).

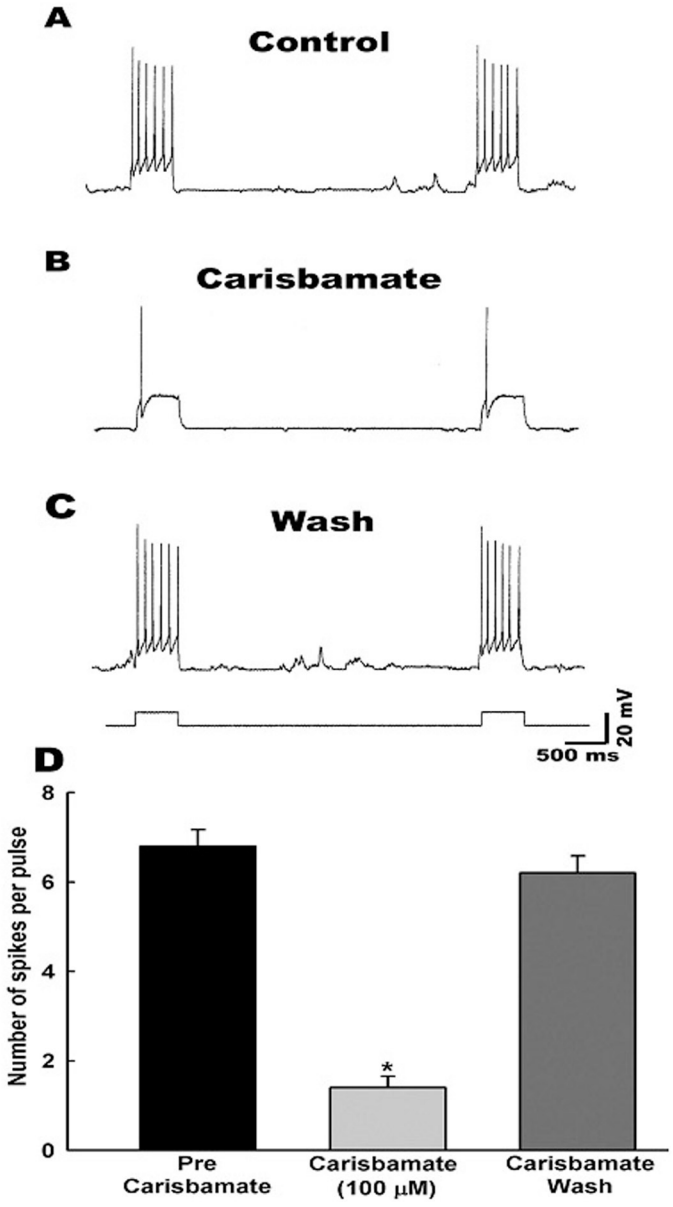

Figure 5-3. Carisbamate inhibition of sustained repetitive firing (SRF) in cultured hippocampal neurons. Depolarizing pulses (0.5 nA, 1 s) were applied during each set of recordings obtained as follows: **A,** control period before application of carisbamate, **B,** during the application of carisbamate (100 μM) and **C,** following carisbamate washout. **D,** A bar graph representation of average inhibitory effect of carisbamate on SRF in hippocampal neurons. Data represented as mean spike frequency ± S.E.M. (n = 6, * $p < 0.001$).

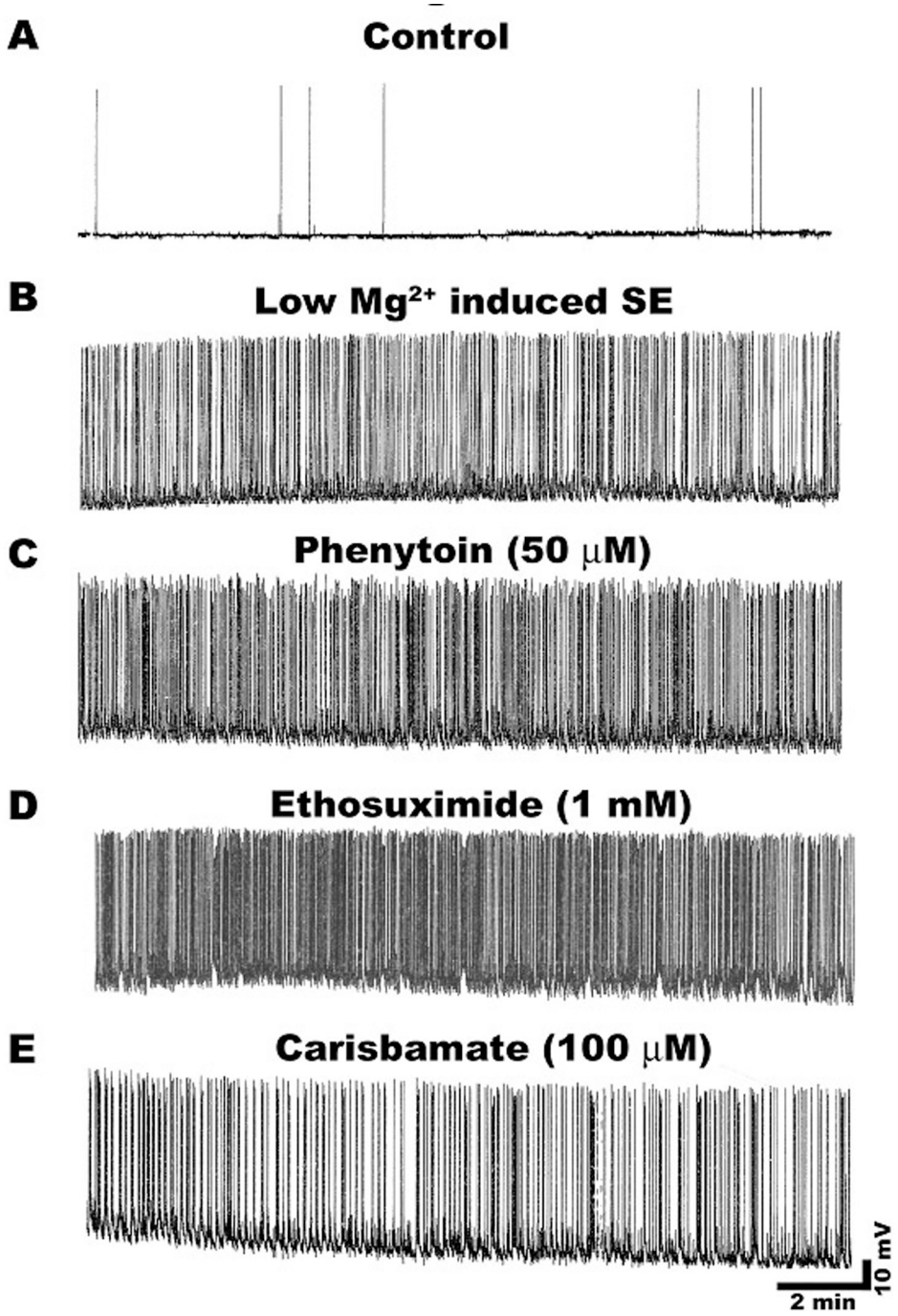

Figure 5-4. Effect of carisbamate and other AEDs on low Mg^{2+}-induced SE in cultured hippocampal neurons. A, Representative control neuron displaying intrinsic baseline activity consisting of spontaneous action potentials. **B,** Induction of continuous epileptiform status epilepticus activity in a neuron upon low Mg^{2+} treatment. Effects of clinically used AEDs on low Mg^{2+} induced high frequency spiking. **C,** phenytoin (50 μM) or **D,** ethosuximide (1 mM) failed to block high frequency spiking. **E,** carisbamate (100 μM) appeared to slow down spike frequency compared to phenytoin or ethosuximide but this effect was not different from neurons exposed to low Mg^{2+} alone.

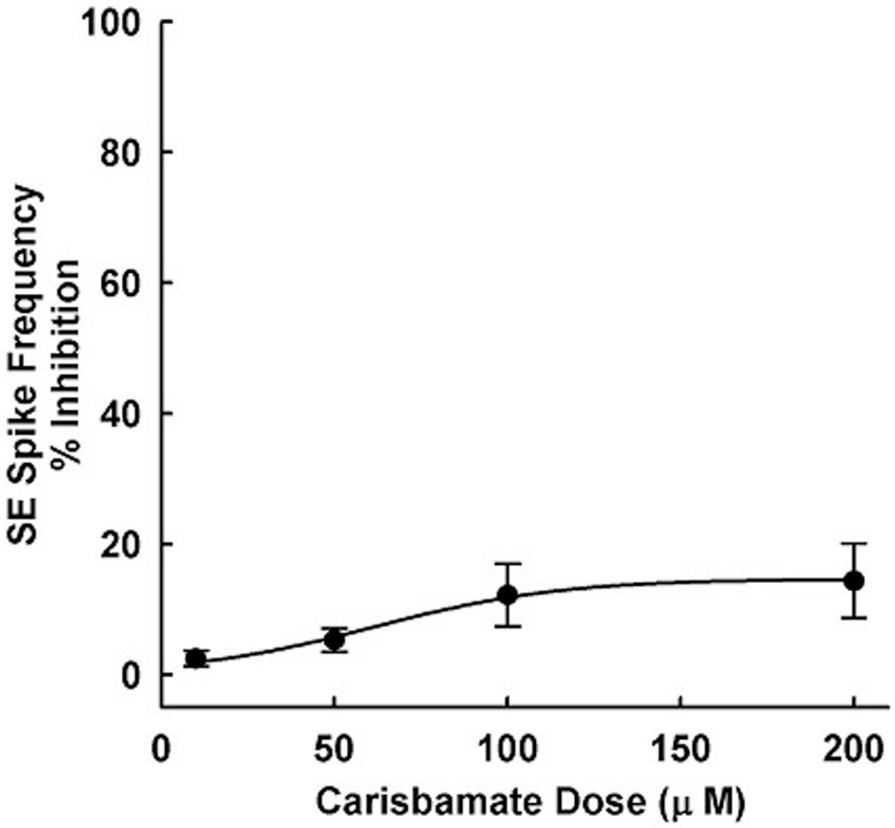

Figure 5-5. Concentration-response analysis of effects of carisbamate on low Mg^{2+} induced high frequency spiking in cultured hippocampal neurons. Increasing concentrations of carisbamate had little effect on low Mg^{2+} induced high frequency spiking. Even at concentrations of up to 200 μM only a 10-12% inhibition was achieved. Spike frequencies in the presence of varying concentrations of carisbamate were measured over a 15-min period and then plotted as a percentage change (inhibition) from control (absence of carisbamate) spike frequencies. An EC_{50} value could not computed since 50% inhibition was not achieved. Each data point represents percentage change from control ± S.E.M. (n = 5-7 neurons/ concentration).

Chapter 6: Carisbamate Prevents the Development and Expression of Spontaneous Recurrent Epileptiform Discharges and is Neuroprotective in Cultured Hippocampal Neurons

Introduction

Epilepsy is a common neurological disorder affecting approximately 1–2% of the population worldwide and is characterized by the occurrence of recurrent, unprovoked seizures[81,171]. It is estimated that 50% of epilepsy cases are of idiopathic (genetic) etiology, but the other 50% develop after a presumed brain injury, such as status epilepticus (SE), stroke, traumatic brain injury, or CNS infections, and are classified as acquired epilepsy (AE), resulting in permanent plasticity changes in the brain that cause the development of spontaneous recurrent seizures [4,81]. This process of transformation of healthy CNS tissue with a functional balance between excitation and inhibition to a brain manifesting hyperexcitable neuronal epileptiform discharges is called epileptogenesis [4,18,172]. Despite important advances in our understanding of the regulation of neuronal excitability and antiepileptic drug (AED) action [173,174], approximately 40% of patients remain refractory to treatment with conventional AEDs [81,175]. Thus, it is important to develop novel AEDs [176]. Compounds that prevent the process of epileptogenesis have

important clinical ramifications, because administering such agents following a brain injury could potentially prevent acquired epilepsy [4,172,177].

Carisbamate (RWJ 333369) is a novel AED with a wide margin of safety in humans based on a completed phase 2 clinical trial for the treatment of epilepsy [178,179]. Carisbamate has been reported to possess anticonvulsant effects in a variety of seizure models [180]. Although there are no peer-reviewed studies demonstrating that carisbamate can prevent epileptogenesis, a recent abstract presented at the American Epilepsy Society's annual meeting did show that carisbamate might delay or prevent the occurrence of spontaneous seizures in the lithium-pilocarpine model of epilepsy [181]. The mechanism of action of carisbamate is still unknown and is being investigated by several research groups including our own. However, there are no studies evaluating the ability of carisbamate to inhibit the development and expression of epileptiform discharges in vitro and comparing it to other conventional AEDs.

This study was initiated to investigate the ability of carisbamate to inhibit the development and expression of spontaneous recurrent epileptiform discharges (SREDs) in cultured hippocampal neurons injured following SE-like activity in vitro. While the neuronal cultures do not have true anatomical connections and do not display clinical seizures, this in vitro model has been routinely used to characterize biochemical, electrophysiological, and molecular mechanisms underlying acquired epilepsy [4,24,48,67]. Moreover, the SREDs demonstrate electrographic properties, neuronal population synchronicity, and

anticonvulsant sensitivity identical to those of epileptic seizures recorded in vivo [4,23]. This system also allows for control of the extracellular milieu and is ideally suited to evaluate the effects of investigational compounds on in vitro seizure-like activity.

Materials and Methods

Reagents

All the reagents were purchased from Sigma Chemical Co. (St Louis, MO, U.S.A.) unless otherwise noted. Carisbamate was provided by Johnson & Johnson (Pharmaceutical Research & Development L.L.C., Titusville, NJ, U.S.A.). Carisbamate and phenytoin were dissolved in sterile water made slightly basic with sodium hydroxide. Phenobarbital was dissolved in sterile water. All stocks were made fresh daily.

Hippocampal neuronal culture preparation

All animal use procedures were in strict accordance with the National Institutes of Health Guide for the Care and Use of Laboratory Animals and approved by Virginia Commonwealth University's Institutional Animal Care and Use Committee. Studies were conducted on primary mixed hippocampal neuronal cultures prepared as described previously with slight modifications [23,24]. In brief, hippocampal cells were obtained from 2-day postnatal Sprague–Dawley rats (Harlan, Frederick, MD, U.S.A.) and plated at a density of 2×10^5 cells/cm^2 onto glial beds grown on 35-mm Falcon cell culture dishes (Becton Dickinson and Co., Franklin Lakes, NJ, U.S.A.) previously coated with poly-L-lysine (0.05 mg/mL). Cultures were maintained at 37°C in a 5% CO_2/95% air

atmosphere and fed twice weekly with neuronal feed (minimal essential media with Earle's Salts, 25 mM HEPES, 2 mM l-Glutamine, 3 mM Glucose, 100 µg/mL transferrin, 5 µg/mL insulin, 100 µM putrescine, 3 nM sodium selenite, 200 nM progesterone, 1 mM sodium pyruvate, 0.1% ovalbumin, 0.2 ng/mL triiodothyroxine, and 0.4 ng/mL corticosterone supplemented with 20% conditioned media). These mixed cultures were used for experiments from 13 days in vitro following neuronal plating through the life of the cultures.

Whole-cell current clamp recordings

Whole-cell current clamp recordings were performed using previously established procedures [23,24]. Briefly, a cell culture dish was mounted on the stage of an inverted microscope (Nikon Diaphot, Tokyo, Japan) continuously perfused with physiological basal recording solution (pBRS) containing (in mM): 145 NaCl, 2.5 KCl, 10 HEPES, 2 $CaCl_2$, 10 glucose, and 0.002 glycine, pH 7.3, and osmolarity adjusted to 325 ± 5 mOsm with sucrose. Patch electrodes with a resistance of 2–4 mΩ were pulled on a Brown-Flaming P-80C electrode puller (Sutter Instruments, Novato, CA, U.S.A.), fire-polished and filled with a solution containing (in mM): 140 K^+ gluconate, 1.1 EGTA, 1 $MgCl_2$, and 10 Na-HEPES, pH 7.2, osmolarity adjusted to 290 ± 10 mOsm with sucrose. Whole-cell recordings were carried out using an Axopatch 200B amplifier (Molecular Devices, Foster City, CA, U.S.A.) in a current-clamp mode. Data were digitized via Digidata 1322A (Molecular Devices) and transferred to VHS tape using a PCM device (Neurocorder, New York, NY, U.S.A.) and then played back on a DC-500 Hz chart recorder (Astro-Med Dash

II, Warwick, RI). All the recordings were performed in the current-clamp mode at I = 0 setting. No current was injected at any stage of recording in the presence or absence of drugs.

Hippocampal neuronal culture model of SREDs

SREDs were induced in neuronal cultures by exposing them for 3 hrs to a solution containing no added $MgCl_2$ (low Mg^{2+}) using procedures described previously [23,24]. Briefly, after the removal of maintenance media, neurons were gently washed with 3 × 1.5 ml of pBRS (with or without 1 mm $MgCl_2$) and then allowed to incubate in this solution at 37°C under 5% CO_2/95% air atmosphere. At the end of the 3 hr period, cultures were restored to the physiological concentration (1 mm) of $MgCl_2$ by gently washing with minimum essential medium, returned to the maintenance medium, and incubated at 37°C under 5% CO_2/95% air atmosphere. Thus, low Mg^{2+} treatment was carried out with pBRS without added $MgCl_2$, whereas sham controls were treated with pBRS containing 1 mm $MgCl_2$.

Analysis of the effects of carisbamate on the in vitro development and expression of epileptiform discharges

To investigate the effects of carisbamate on the generation and expression of SREDs, neuronal cultures were first subjected to 3 hrs of low Mg^{2+}-induced continuous high-frequency epileptiform activity to mimic in vivo SE. At the end of the 3 hr period, cultures were washed with a solution containing physiological concentrations of Mg^{2+} so as to

immediately terminate the SE-like activity [23], and the cultures were returned to maintenance media (neuronal feed) containing carisbamate (200 μM), phenytoin (50 μM), phenobarbital (50 μM), or control solution. After a 12 hr treatment period, the media containing drug or control solution was removed by washing the cultures with neuronal feed and the cultures were maintained at 37°C in a 5% CO_2/95% air atmosphere. Neurons were patch-clamped 24 hrs following this 12 hr treatment with carisbamate, phenytoin, phenobarbital, or control solutions for the presence or absence of SREDs. Control neurons were treated with the same number of washes and media changes as the treatment cultures. Sham controls were also subjected to the same number of washes with respective drugs in a solution containing normal Mg^{2+} concentrations. Experiments were performed on multiple neurons from multiple culture plates, spread across several weeks. Concentrations of all the drugs chosen to study their effect on the development and expression of SREDs were at least twice the concentration at which they produced maximal anti-SRED effects based on the dose-response curves generated in our laboratory (data not shown). A higher concentration was chosen to maximize the effects of the agents studied and to determine if this agent could produce a significant reduction in epileptiform discharges.

Cell death assay

Neuronal death was assessed at the same time point as patch clamp experiments using fluorescein diacetate (FDA)-propidium iodide (PI) microfluorometry [24]. Three randomly selected fields were marked and photographed. Both fluorescent and phase bright images were captured. Neurons labeled with FDA or PI were quantified by means of

the Ultraview image analysis software package (Perkin Elmer Life Sciences, Waltham, MA, U.S.A.) and the fraction of neuronal death was calculated as the number of neurons labeled by PI divided by the sum of the number of neurons labeled by PI and those labeled by FDA. Fluorescent images were compared with phase bright images to confirm that only pyramid-shaped neurons were counted. To quantify neuronal death with this technique, cells in three randomly selected fields were counted manually and averaged per culture (approximately 18–25 neurons per field).

Data analyses

Data are reported as mean ± SEM. Differences in percentage of neurons displaying SREDs, frequency and duration of SREDs, and neuronal death were examined using one-way analysis of variance (ANOVA) followed by a post hoc Tukey test. Data were analyzed using SigmaStat 2.0 and graphs were generated using SigmaPlot 8.02 (SPSS, Inc., Chicago, IL, U.S.A.). All or no effect of a given drug on SREDs was taken as the criterion for its antiepileptic effect. In a given culture plate we patch-clamped three neurons before moving on to another plate. All experiments were performed over a period of 3 weeks. Depending on the number of culture plates available, we analyzed three to five culture plates for every condition each week. Thus, the results reported are representative of multiple culture plates belonging to different batches.

Results

In vitro antiepileptic effects of carisbamate

Whole cell current clamp recordings obtained from neurons in cultures 2 days after a treatment with low-Mg^{2+} for 3 hrs demonstrated characteristic SREDs, or in vitro seizure events. Three SREDs lasting between 1–2 min (Figure 6-1 B) were observed in a continuous 30 min recording. SREDs occurred spontaneously in the network of neurons, had durations between 1 and 3 min, occurred at frequencies of up to 3-4 episodes/hr and were observed for the life of the neurons in culture. Expansion of SREDs revealed characteristic paroxysmal depolarization shifts, a pathophysiological characteristic observed in epilepsy (data not shown, [23]). Age-matched control neurons never demonstrated SREDs and had "normal" baseline activity consisting of intermittent action potentials (Figure 6-1 A).

In contrast, bath application of carisbamate (200 μM) acutely inhibited SREDs compared to the non-treated epileptic cultures (Figure 6-1 C). The effect of carisbamate was fully reversible and SREDs returned upon washout of the drug from the culture medium (data not shown). Thus, carisbamate prevented SREDs in this in vitro model of seizures. Similar to carisbamate, bath application of clinically used AEDs, such as phenytoin (50 μM) and phenobarbital (50 μM), also acutely inhibited SREDs (Figures 6-1 D,E). Greater than 95% of the neurons exhibited evidence of an in vitro antiepileptic effect following application of carisbamate/phenytoin/phenobarbital. It took approximately 10–15 min for the anti-SRED effect to be fully manifested. In addition, there were no significant differences in membrane potential and input resistance between age-matched control neurons, neurons

exhibiting SREDs [23,157], and neurons treated with carisbamate acutely. Thus, neurons displaying SREDs and carisbamate-treated neurons had mean membrane potential of −64.1 ± 1.4 mV and −62.9 ± 1.1 mV and a mean input resistance of 138.5 ± 6.03 mΩ and 136.2 ± 6.7 mΩ, respectively. These values were not significantly different from each other (n = 9, p = 0.5 and 0.8, respectively).

Effects of carisbamate on the development and expression of SREDs

As shown in Figure 6-2 A, in comparison to control neurons that did not manifest SREDs, neurons exposed to 3 hrs of low Mg^{2+} treatment (n = 15 neurons, 5 culture plates) displayed characteristic SREDs when patch clamped 36 hrs following the cessation of the 3 hrs of SE-like treatment. To investigate the effects of carisbamate on the development and expression of SREDs, hippocampal neuronal cultures were treated with carisbamate (200 μM) for 12 hrs after the 3 hr SE-like injury. Thus, carisbamate was not present during low Mg^{2+} treatment but was present only after the SE-like injury (Materials and Methods). Whole cell current clamp recordings from neurons (n = 18, 6 culture plates) 24 hrs following carisbamate (200 μM) treatment were devoid of any SRED activity (Figure 6-2 B). The electrographic recordings did not display any SREDs, and only manifested occasional action potentials, resembling the recordings from sham-control neurons. Further, neurons displaying SREDs and neurons treated with carisbamate for 12 hrs had a mean membrane potential of −65.4 ± 1.2 mV and −64.6 ± 1.1 mV and a mean input resistance of 133.36 ± 6.6 mΩ and 131.69 ± 8.43 mΩ, respectively. These values were not different from each other (n = 8, p = 0.6 and 0.8, respectively). These results provide

direct evidence that cells evaluated the day after treatment with carisbamate were still free of in vitro seizure activity and did not develop SREDs. Thus, carisbamate had long-lasting effects on the hippocampal neurons that were independent from its in vitro antiepileptic effects.

Quantitation of the effects of carisbamate on the development and expression of SREDs

Although the whole cell current clamp recordings from 18 neurons 24 hrs following carisbamate (200 μM) treatment were devoid of any SRED activity (Figure 6-2 B), we wanted to evaluate a larger population of neurons to carefully quantitate the effects of carisbamate on the development and expression of SREDs. A total of 98 neurons from different treatment groups were analyzed. For the studies in this paper, we only evaluated recordings that were maintained for over 1 hr and some recordings were held for up to 2.5 hrs. Recordings were made from 53 neurons in carisbamate treated groups (n = 15 culture plates), 30 neurons from low Mg^{2+} alone groups (n = 10 culture plates), and 15 neurons from sham treated (drug control) groups (n = 5 culture plates). Greater than 97% of the low Mg^{2+} alone-treated neurons displayed SREDs. In contrast, in the 53 neurons treated with carisbamate for 12 hrs after SE-like injury, 80% of the neurons (n = 42) were completely devoid of SREDs, and only 20% of the neurons displayed occasional epileptiform activity (n = 11). No SREDs or hyperexcitability were observed in the control neurons.

We then calculated the seizure frequency by averaging total number of SREDs over 3 min recording periods. The SRED frequency in neurons treated with low Mg^{2+} alone was 8.2 ± 3.6 episodes/30 min. In carisbamate treated cells, the SRED frequency was reduced to 0.58 ± 0.14 episodes/30 min (Figure 6-3 B). This represented a 93% reduction in SRED frequency in carisbamate treated neurons. We also compared the duration of SREDs between the low Mg^{2+} alone and carisbamate-treated groups. The average SRED duration in the low Mg^{2+}-treated group was 152.4 ± 14.13 s. In the small percentage of neurons that displayed an occasional SRED in the carisbamate treated group, the average SRED duration was 77.6 ± 9.45 s (Figure 6-3 C). This represented an approximately 50% reduction in the duration of SREDs in neurons from the carisbamate treated group. Thus, carisbamate not only inhibited the development and expression of SREDs in the majority of neurons, but it also decreased seizure frequency and duration in the few neurons that still had an occasional epileptiform event.

Comparison of the effects of carisbamate on the development and expression of SREDs with other AEDs

As there are currently no known agents that offer an antiepileptogenic effect in vivo, there were no positive control drugs for comparing the ability of carisbamate to prevent the development and expression of SREDs. However, we utilized clinically employed AEDs that displayed anti-SREDs properties in our in vitro model as control conditions. Phenytoin (50 μM) or phenobarbital (50 μM) was included in the neuronal feed following the 3 hr low Mg^{2+} treatment (SE, Materials and Methods) for 12 hrs in an identical manner to the

carisbamate treatment. Both phenytoin and phenobarbital at this concentration blocked SREDs, producing the same in vitro antiepileptic effects observed following treatment with carisbamate (Figure 6-1). 24 hrs following drug washout, neurons were patch-clamped and observed for the presence of SREDs. As observed earlier, low Mg^{2+} alone-treated neurons displayed characteristic SREDs (Figures 6-1 B, 6-2 A, 6-4 A), whereas control and carisbamate treated cells were devoid of any SRED activity (Figures 6-1 A, 6-2 B, 6-4 B). In contrast, neurons treated with either phenytoin or phenobarbital after the SE-like injury (n = 10 neurons, 5 culture plates) (Figure 6-1 D,E) clearly demonstrated SREDs similar to low Mg^{2+} alone-treated cells (Figure 6-4 C,D). SRED frequency in the low Mg^{2+} alone-treated group was 8.2 ± 3.6 episodes/30 min, while SRED frequency in the phenytoin or phenobarbital treated groups were 8.0 ± 4.0 and 7.8 ± 4.6 episodes/30 min, respectively. The average SRED duration in the low Mg^{2+} alone-treated group was 152.4 ± 14.13 s, while the average SRED duration in the phenytoin- or phenobarbital-treated groups were 162.4 ± 10.03 s and 149.4 ± 12.44 s, respectively. There were no significant differences between low Mg^{2+} alone-treated and phenytoin- or phenobarbital-treated group for these two criteria of SREDs (n = 10, p = 0.79, 0.85 and 0.43, 0.79). Thus, phenytoin and phenobarbital did not prevent the development and expression of SREDs after SE-like injury at concentrations that were acutely antiepileptic in vitro.

Carisbamate is neuroprotective

The neuronal injury caused by the removal of extracellular Mg^{2+} (in vitro SE-like injury) in this model has been well characterized [24]. The removal of the Mg^{2+} block produces

repetitive depolarizations, resulting in prolonged activation of NMDA receptors. This persistent activation of NMDA receptors allows for excessive entry of extracellular calcium (Ca^{2+}), resulting in excitotoxic activation of cell-death pathways and culminating in neuronal demise [16]. In order to investigate if carisbamate was neuroprotective, we evaluated the effects of carisbamate exposure after the 3 hr SE-like treatment on the viability of neurons. The fraction of neuronal death was evaluated using FDA-PI staining 24 hrs following the termination of the drug or sham control treatment employing our previously established procedures [24]. Sham control cultures that were not exposed to SE-like activity had a fraction of cell death of 0.117 ± 0.006. Low Mg^{2+} cultures exposed to 3 hrs of SE-like injury showed fraction of cell death of 0.323 ± 0.006, which was significantly different from sham control ($n = 5$; $p < 0.001$, one-way ANOVA, post hoc Tukey test, Figure 6-5). In contrast, carisbamate (200 μM) treated cultures had fraction of cell death of 0.106 ± 0.005 after 3 h of SE-like injury, which was not significantly different from sham controls. These results provide direct evidence that carisbamate can provide neuroprotection when administered after the SE-like activity is completed.

Discussion

This study provides direct evidence that the novel neuromodulator carisbamate not only inhibits the development and expression of SREDs but is also neuroprotective when administered following SE-like injury in cultured hippocampal neurons. The process of epileptogenesis refers to the development of spontaneous recurrent seizures in a previously normal brain [4,18,172]. Our model employs low Mg^{2+}-induced continuous electrographic

epileptiform discharges for 3 hrs to mimic SE-like injury in vitro. Restoration of physiological Mg^{2+} concentrations terminates the high frequency epileptiform discharges but produces a permanent plasticity change in neuronal excitability, such that the surviving neurons manifest synchronized SREDs for their life in culture. Presence of carisbamate following SE-like injury prevented the chronic development and expression of SREDs. This property was unique to carisbamate, because conventional AEDs such as phenytoin and phenobarbital failed to prevent the development and expression of SREDs following neuronal injury. We studied phenytoin and phenobarbital because they represent two diverse mechanisms of antiepileptic action. However, it will be important to investigate if other AEDs prevent the development of epileptiform discharges in our model. The ability of carisbamate to prevent the development and expression of SREDs when administered after 3 hrs of continuous SE-like activity offers major implications in the use of this antiepileptic agent in treating SE, because this drug is not only antiepileptic, but may also delay the development and expression of epileptiform discharges, at least in vitro.

Our results also demonstrate that control of seizures with carisbamate may also have an added benefit of providing a neuroprotective effect on the hippocampus. Preventing neuronal damage after prolonged seizures is an important therapeutic goal. Several studies have demonstrated that SE causes neuronal damage, memory loss, and several long-term plasticity changes that can result in significant mortality and morbidity [14,74,76]. This was an important test, because it evaluated the effects of carisbamate on neuronal death when the drug is administered after the injury phase of SE. To our knowledge, this is the

first demonstration of neuroprotection following SE-like activity in vitro. We also evaluated the effects of ongoing SREDs in epileptic cultures on neuronal death by comparing cell death using FDA-PI staining on cultures that were undergoing SREDs versus carisbamate-treated or control sham cultures. The results of these experiments (data not shown) demonstrated that the ongoing activity of SREDs did not increase cell death in comparison to sham control cultures when evaluated starting 2 days after induction of SREDs [24]. Thus, SE but not SREDs caused neuronal death in this model, and carisbamate was able to block the cell death caused by SE-like activity. Carisbamate was neuroprotective when given after SE-like injury and thus offers considerable therapeutic potential in preventing brain injury following SE. However, it has been recently shown that carisbamate reduced posttraumatic hippocampal edema without affecting neurobehavioral or histological outcome [182]. Future studies are needed to determine the mechanism of the neuroprotective action of carisbamate.

A long-standing question in neuroscience has been how the initial CNS injury produces long-term plasticity changes that result in the development, expression, and maintenance of epilepsy. Emerging research has indicated that the alterations in the levels and handling of the ubiquitous intracellular second messenger, Ca^{2+}, could underlie these injury-induced long-term plasticity changes in neuronal excitability, thus leading to the proposal of the Ca^{2+} hypothesis of epileptogenesis [4]. In concordance with this hypothesis, our laboratory and many others have observed alterations in Ca^{2+} dynamics in all three phases of development of acquired epilepsy [4]. Results from our laboratory have provided evidence

that the epileptogenic and neurotoxic effects of SE are mediated both by alterations in intraneuronal Ca^{2+} levels during and after SE and by altered Ca^{2+} homeostatic mechanisms in the injured neurons that survive SE [32,85]. It will be insightful to investigate the effects of carisbamate on neuronal Ca^{2+} dynamics and determine if this mechanism contributes to the ability of this drug to not only prevent the development and expression of SREDs but also afford neuroprotection following neuronal injury.

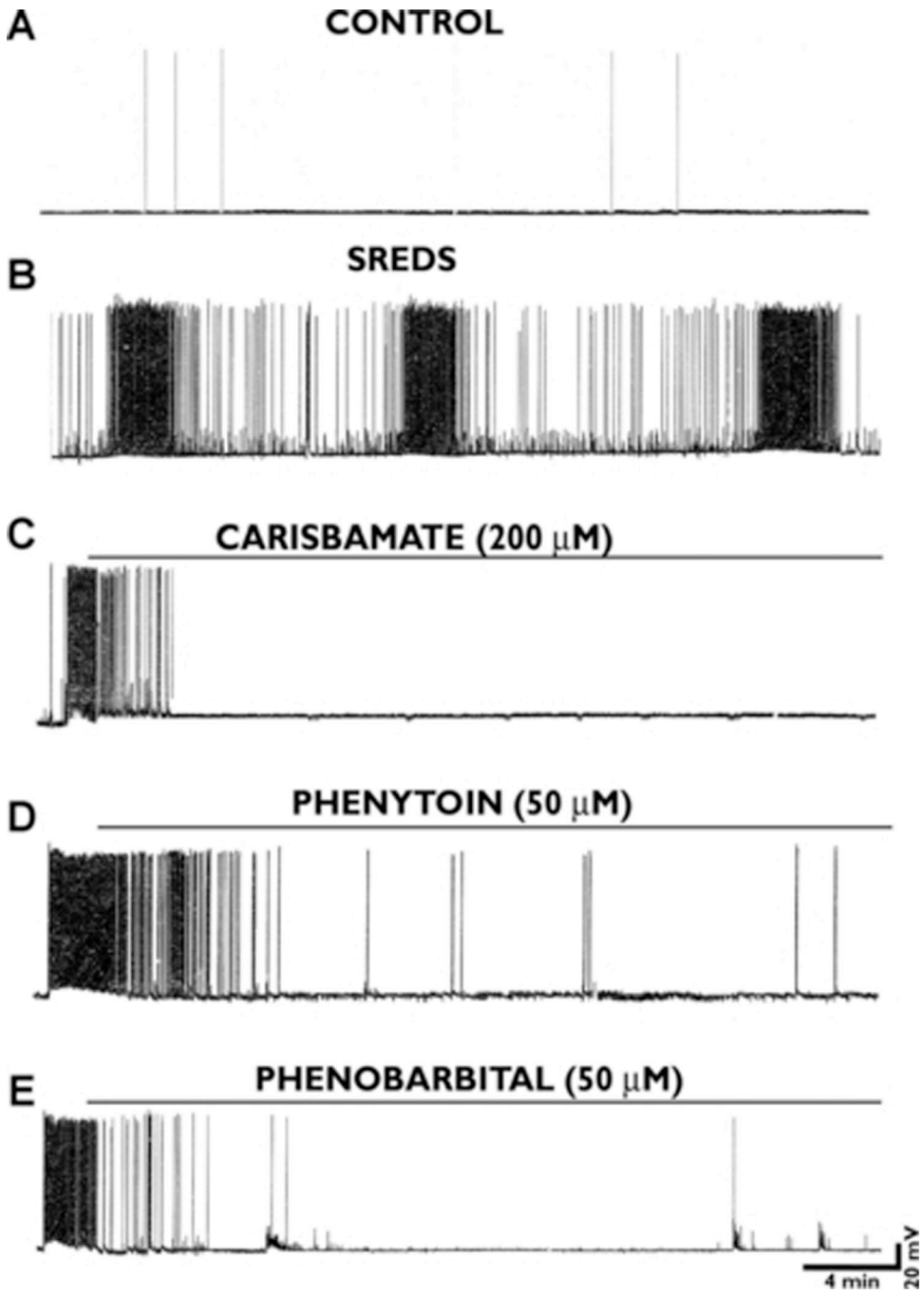

Figure 6-1. Effects of carisbamate and other clinically used AEDs on SREDs in cultured hippocampal neurons. **A,** current-clamp recording from a representative control neuron displaying baseline activity consisting of intermittent action potentials. **B**, recording from an "epileptic" neuron 3 days following a 3 hr exposure to low Mg^{2+} solution demonstrates occurrence of characteristic SREDs. Three SREDs or spontaneous seizure episodes lasting ~1–1.5 min can be seen in this recording time frame. These SREDs occurred throughout the life of the cultures and are indicative of the pathophysiological "epileptic" phenotype. Effects of various AEDs on SREDs in cultured hippocampal neurons. Application of **C**, carisbamate (200 μM) or **D**, phenytoin (50 μM) or **E**, phenobarbital (50 μM) to the epileptic neurons abolished the expression of SRED activity. The solid bar above each trace represents the duration for drug exposure. Thus, the beginning of the bar is the point of addition of drug.

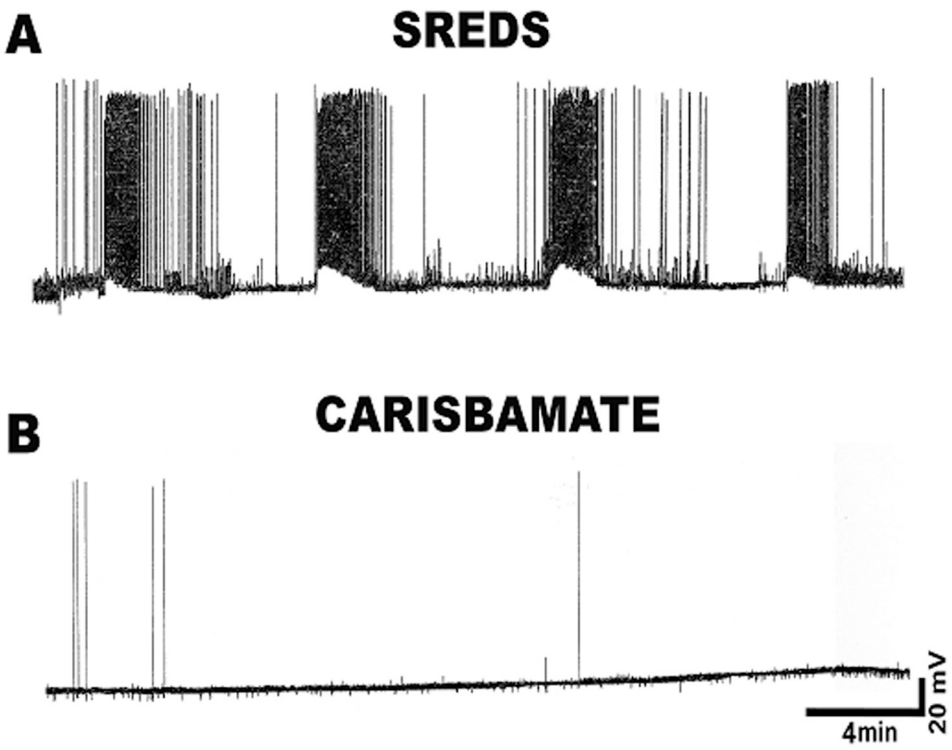

Figure 6-2. Effects of carisbamate on the development and expression of SREDs. Hippocampal neuronal cultures were treated with or without carisbamate (200 μM) immediately following the low Mg^{2+} treatment. Drug was washed off the next day and 24 hrs later neurons were patch clamped. **A,** representative control neuron displaying characteristic SREDs 24 hrs following the sham washout. The recording is representative of 30 different neurons. **B,** current clamp recordings from a representative neuron 24 hrs following carisbamate (200 μM) washout. The neuron was devoid of any SRED activity and manifested occasional action potentials resembling the recordings from sham-control neurons. The recording is representative of 53 different neurons.

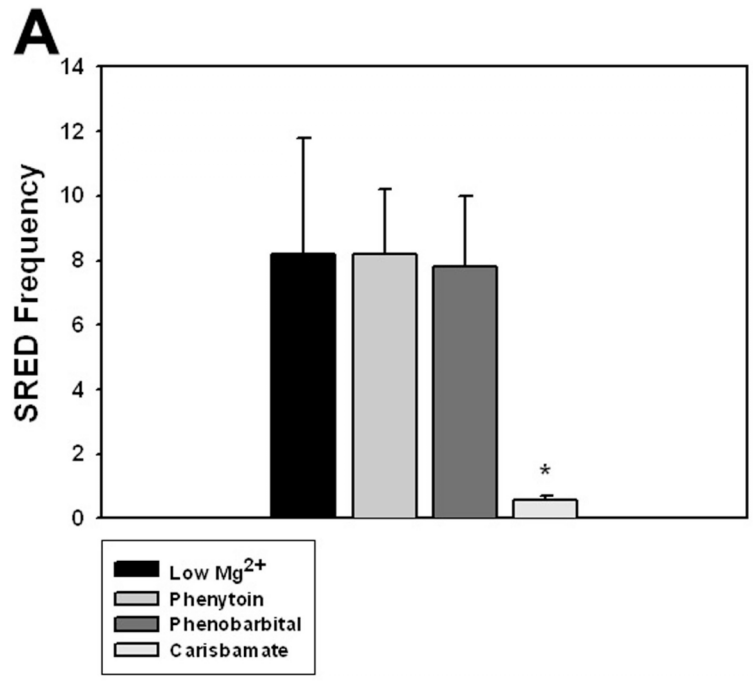

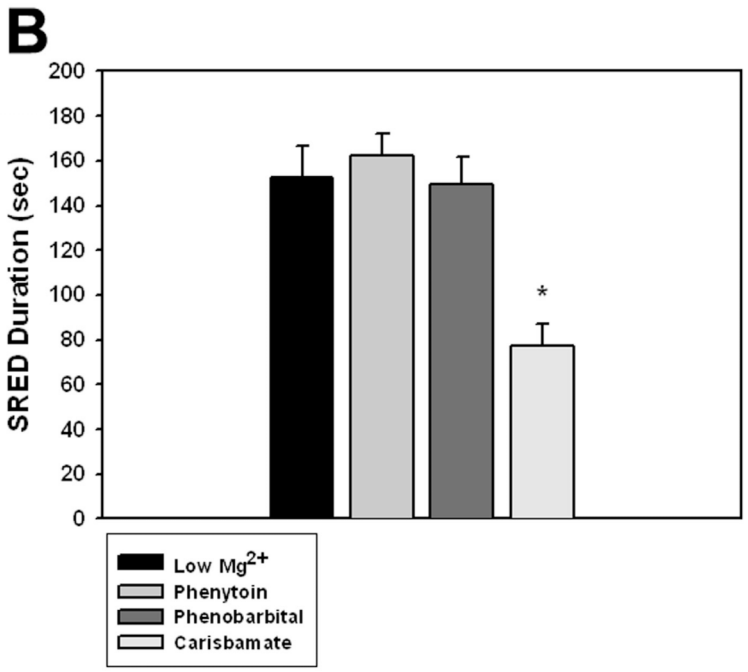

Figure 6-3. Analyses of the effects of carisbamate on the development and expression of SREDs. A, SRED frequency in low Mg^{2+} alone-treated group was 8.2 ± 3.6 episodes/30 min. Phenytoin- and phenobarbital-treated groups had SRED frequencies of 8 ± 2 and 7.8 ± 2.2 episodes/30 min, respectively, while the carisbamate treated group displayed a SRED frequency of 0.58 ± 0.14 episodes/30 min. **B,** average SRED duration in the low Mg^{2+} alone treated group was 152.4 ± 14.13 s. Phenytoin and phenobarbital groups had average SRED durations of 162.4 ± 10.03 s and 149.4 ± 12.44 s, respectively, while the average SRED duration of the carisbamate-treated group was 77.6 ± 9.45 s (*$p < 0.001$, one-way ANOVA, post hoc Tukey test).

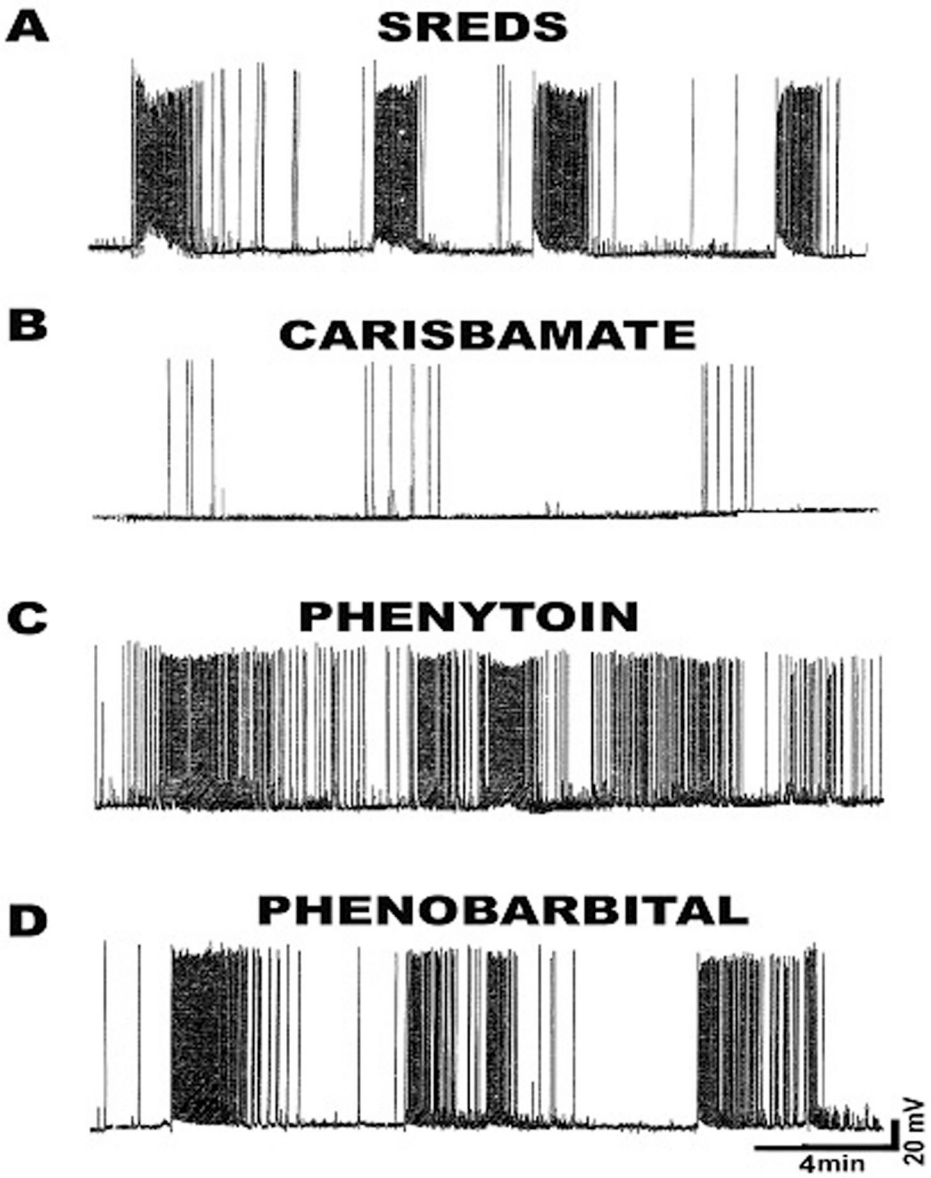

Figure 6-4. Comparison of the effects of carisbamate on the development and expression of SREDs with other AEDs. A, recordings from a low Mg^{2+}-treated neuron displaying characteristic SREDs. **B,** treatment with carisbamate (200 μM) following SE-like injury prevents the development and recurrence of SREDs. No SREDs are observed in this neuron even after removal of carisbamate. **C** and **D**, other clinically used AEDs such as phenytoin (50 μM) and phenobarbital (50 μM) did not prevent the development and expression of SREDs. All the patch clamp recordings were performed 24 h following the drug washout.

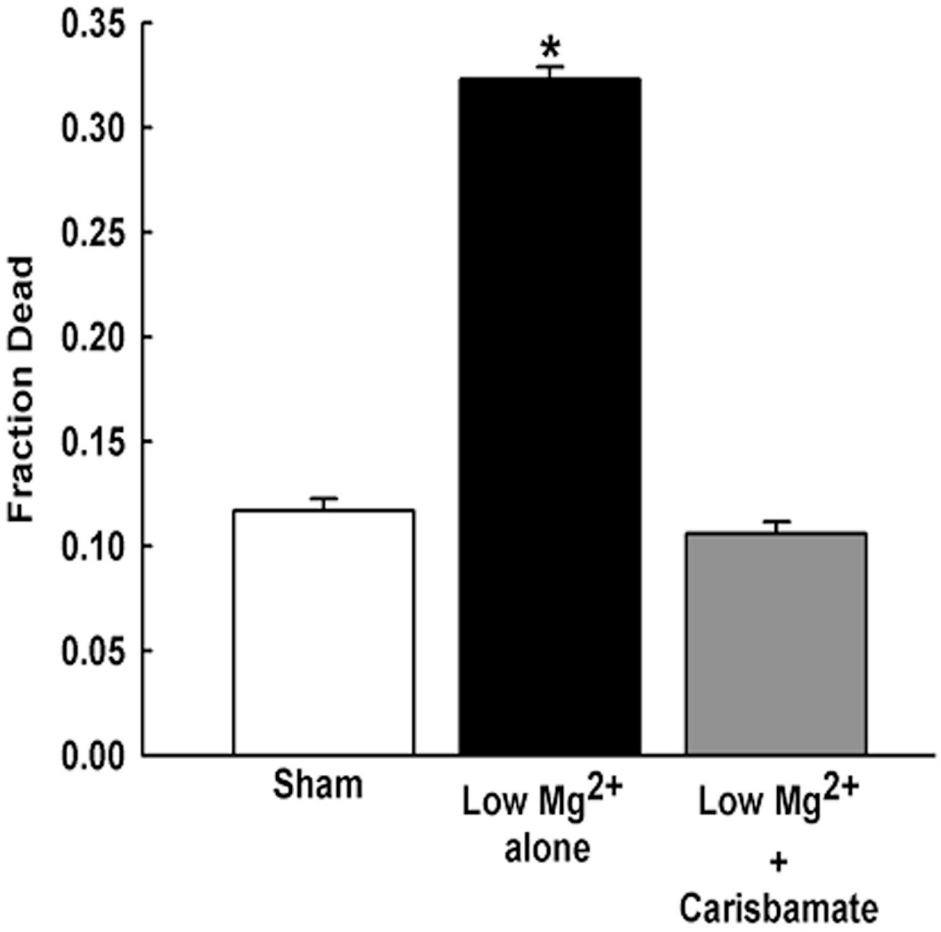

Figure 6-5. Neuroprotective effects of carisbamate. Fraction of cell death was analyzed using FDA-PI staining after the removal of the drug. Sham control cultures were not exposed to SE, but were handled similar to other cultures. They displayed a fraction of cell death of 0.117 ± 0.006. Cultures exposed to 3 hrs of low Mg^{2+} SE showed a fraction of cell death of 0.323 ± 0.006 (n = 5; *p < 0.001, one-way ANOVA, post hoc Tukey test). Carisbamate (200 μM) treated cultures had a fraction of cell death of 0.106 ± 0.005 when administered after 3 hrs of SE-like injury. This fraction of cell death was not significantly different from sham controls

Chapter 7: The Novel Anti-Epileptic Drug Carisbamate (RWJ333369) Modulates Calcium and Restores Calcium Homeostatic Mechanisms in Hippocampal Neuronal Cultures

Introduction

Approximately 2% of the world's population is affected by epilepsy, a common neurological condition characterized by spontaneous, recurrent seizures [81]. 40% of all cases of epilepsy develop following some neuronal injury, such as status epilepticus (SE), stroke, or traumatic brain injury (TBI) and are, thus, classified as acquired epilepsy (AE) [81,183]. This transformation can be characterized as a progression through three stages: injury, epileptogenesis, and the maintenance of chronic epilepsy. During the epileptogenesis phase, recurrent seizures may not be present; however, neurons are undergoing plasticity changes that will ultimately lead to the expression of epilepsy. Understanding the pathophysiological changes that occur during this process is important in the development of anti-epileptogenic agents to prevent the ultimate development of epilepsy. While much progress has been made in the development of new anti-epileptic drugs (AEDs), or anti-convulsants, currently there are no therapeutics that can prevent epileptogenesis following neuronal injury. Such compounds that can be administered after

brain injury and halt epileptogenesis are clinically very important, and the development of these agents represents an important area of research.

Carisbamate (RWJ333369) is a novel neuromodulator that is currently in phase II clinical trials for the treatment of epilepsy [178,179]. It has been shown that this drug, a carbamate closely related to felbamate, not only demonstrates anti-convulsant properties but also displays a wide margin of safety in humans [178,179,181]. More recently, we have demonstrated that carisbamate is able to inhibit spontaneous recurrent epileptiform discharges (SREDs), the in vitro correlate to epilepsy, in hippocampal neuronal cultures [184]. In the same low Mg^{2+} model, we were also able to demonstrate that when given following low Mg^{2+}-induced in vitro SE, carisbamate prevented the development of SREDs even following the removal of the drug from the system [185]. This is the first time a drug has been shown to be anti-epileptogenic in this in vitro model; thus, elucidating the mechanism of action is critical to understanding how anti-epileptogenic agents work. Currently the mechanism of action behind this drug is not known so many groups are actively investigating potential mechanisms responsible for both its anti-convulsive and its anti-epileptogenic properties.

This study was initiated to elucidate a potential mechanism of action behind the ability of carisbamate to inhibit epileptogenesis in the low Mg^{2+}, in vitro hippocampal neuronal

culture model of SE-induced AE. This model is well-characterized and used widely. Moreover, due to several similarities between the model and both in vivo models and the human condition, it provides a useful tool in preliminary studies investigating pathophysiological mechanisms and potential therapeutics. The changes in Ca^{2+} dynamics observed in the rat pilocarpine model of SE-induced AE are also observed in the in vitro model. Essentially, it has been demonstrated that during in vitro SE, $[Ca^{2+}]_i$ increases significantly. These elevations are maintained well past the duration of the injury, and while they decrease over time, they remain significantly elevated for at least 48 hrs post-in vitro SE. Similar changes in Ca^{2+} also exist in the rat pilocarpine model, wherein hippocampal neuronal $[Ca^{2+}]_i$ remains elevated only in those animals that later develop epilepsy [32]. As an important second messenger, such long-lasting increases in $[Ca^{2+}]_i$ have the potential to affect neurotransmission, gene transcription, and neuronal plasticity leading to the development of chronic epilepsy. Moreover, studies that have blocked the elevations in $[Ca^{2+}]_i$ by administering NMDA antagonists before SE have prevented the development of epilepsy; therefore, this suggests that these alterations in Ca^{2+} are responsible for epileptogenesis and the maintenance of the epileptic phenotype. Thus, examining how carisbamate affects these changes in Ca^{2+} is important in understanding epileptogenesis and potentially, how this drug affects neuronal plasticity.

Materials and Methods

Reagents

Carisbamate was provided by Johnson & Johnson (Pharmaceutical Research & Development L.L.C., Titusville, NJ, U.S.A.). Carisbamate was dissolved in sterile water made slightly basic with sodium hydroxide and diluted to final concentration in physiologic basal recording solution (pBRS).

Hippocampal neuronal culture preparation

Preparation of primary mixed hippocampal neuronal culture was performed as previously described [23]. In summary, hippocampal cells were isolated from 2-day post-natal Sprague-Dawley rats (Harlan, Frederick, MD). Hippocampal neurons ($8.75x10^4$) were plated onto a glial support layer that was previously plated onto poly-L-lysine (0.05 mg/ml) coated Lab-Tex glass chambers (Nalge-Nunc International, Naperville, IL). Cultures were maintained at 37°C in a 5% CO2/95% O_2 incubator and fed twice weekly with neuronal feed containing 20% conditioned media, as described previously [23,50]. All experiments were performed on neurons maintained for 14-17 days in vitro to ensure proper development. All procedures adhered strictly to the National Institutes of Health Guide for the Care and Use of Laboratory Animals and were approved by Virginia Commonwealth University's Institutional Animal Care and Use Committee.

Ca^{2+} microfluorometry

Primary hippocampal cultures were loaded with Fura-2 acetoxymethyl ester (Fura-2AM) and then placed on the 37°C stage of an Olympus IX-70 inverted microscope (Olympus,

Center Valley, PA) coupled to an ultra-high-speed fluorescence imaging system. Ratio images were acquired using alternating excitation wavelengths (340/380 nm) with a filter wheel (Sutter Instruments, Novato, CA) and fura filter cube at 510/540 nm emissions with a dichroic mirror at 400 nm [94]. MetaFluor (Olympus, Center Valley, PA) was used for image acquisition and analysis. Images were acquired from any given field at various time intervals depending on the specific experiment and background fluorescence was subtracted from all acquired data by imaging hippocampal neuronal cultures that were not loaded with Fura-2AM [94].

Glutamate challenge: assessing Ca^{2+} homeostatic mechanisms

In order to assess Ca^{2+} homeostatic mechanisms, neurons were loaded with Fura-2AM according to previously described protocols [50] and challenged with 50 μM glutamate for 2 minutes. After 2 min, the cultures were washed with pBRS to remove the glutamate. 340/380 ratio images were captured every 30 seconds to record both the response to and recovery from glutamate exposure, as described previously [4].

Data analysis

Data were statistically analyzed using StatView (Version 5.0.1). Experiments were repeated over a period of a few weeks so as to sample from different culture batches. The significance of the data was tested by one-way analysis of variance (ANOVA), or one-way

repeated measures (RM) ANOVA followed by Fisher's post-hoc test when appropriate. $P < 0.05$ was considered significant for all data analysis.

Results

It has been demonstrated that in vitro SE causes long-lasting elevations in intracellular Ca^{2+} ($[Ca^{2+}]_i$). The ability to lower $[Ca^{2+}]_i$ post-SE to normal, baseline concentrations may help prevent the second messenger effects that lead to plasticity changes and the development of epilepsy.

Carisbamate restores Fura-2 Ca^{2+} ratios following low Mg^{2+}-induced in vitro SE

During treatment with low Mg^{2+}(in vitro SE), cells exhibited increased $[Ca^{2+}]_i$ as indicated by an elevation in 340/380 ratios to approximately 0.78 (Figure 7-1). Following the low Mg^{2+} treatment, neurons were returned to Mg^{2+}-containing solution containing either carisbamate (200 μM) or vehicle at time point 0 on the x-axis. In cells treated with the drug following low Mg^{2+}, the 340/380 ratios are lowered rapidly to ratios observed in naïve neurons, unlike the vehicle-treated neurons, which continue to exhibit 340/380 ratios that are significantly elevated. Thus, it appears that when given acutely following in vitro SE, carisbamate is able to significantly lower $[Ca^{2+}]_i$.

Basal Ca^{2+} levels are maintained 24 hours post-carisbamate washout

Carisbamate, when used following in vitro SE, was able to maintain baseline $[Ca^{2+}]_i$ for at least 24 hrs after drug washout. After neurons were returned to normal, Mg^{2+}-containing solution following treatment with low Mg^{2+}, the cells displayed SREDs. SREDs are the in vitro correlate to epilepsy and these 'epileptic' cells exhibit paroxysmal depolarization shifts. Similarly to the experimental protocols used in the study that demonstrated that carisbamate was anti-epileptogenic (prevented the development of SREDs when administered immediately post-SE) [185], following 3 hrs of low Mg^{2+} treatment cells were returned to maintenance media containing vehicle or 200μM carisbamate. 12 hrs later the drug was washed out of the hippocampal neuronal cultures, and 24 hrs following the removal of the drug the neurons were imaged to determine $[Ca^{2+}]_i$. At this time point, drug-treated neurons fail to display SREDs, in contrast to the vehicle-treated, or 'epileptic' neurons [185]. Moreover, as shown in Figure 7-2, the carisbamate-treated neurons showed Fura-2 ratios significantly lower than the vehicle-treated neurons that displayed SREDs, 0.328 ± 0.025 and 0.424 ± 0.019 respectively (n=5; $P<0.001$, one-way ANOVA, post-hoc Fisher test). Moreover, the Fura-2 ratio observed in the drug-treated cells is consistent with that of the sham controls, 0.314 ± 0.018. This demonstrates that caribamate, as far out as 24 hrs post-drug washout, was able to maintain $[Ca^{2+}]_i$ at baseline values.

Carisbamate-treated neurons exhibit enhanced recovery following glutamate challenge

It has been demonstrated that following treatment with low Mg^{2+}, 'epileptic' neurons that display SREDs also show altered homeostatic mechanisms [4]. Therefore, if these neurons are briefly stimulated with glutamate, they are unable to restore normal $[Ca^{2+}]_i$ in the cell [4]. In contrast, naïve or sham-control neurons have intact homeostatic mechanisms and are thus, able to recover from such challenges [4].

Following 3 hrs of treatment with low Mg^{2+} (in vitro SE), cells were returned to maintenance media containing vehicle or carisbamate (200μM). 12h later the drug was washed out of the cultures and 24h post-washout the carisbamate-treated neurons were loaded with the Ca^{2+} indicator Fura-2AM. These neurons were then subjected to glutamate stimulation (50μM, 2 min). The neurons that were treated with carisbamate showed an increased ability to recover from this challenge when compared to vehicle-treated (epileptic) neurons (Figure 7-3). Glutamate elicited an increase in $[Ca^{2+}]_i$ in both treatment groups. Neurons treated previously with carisbamate were able to restore $[Ca^{2+}]_i$ to basal levels in 25 min (consistent with that observed in sham controls, data not shown but as observed previously [4]). Vehicle-treated, 'epileptic' neurons showed a diminished ability to recover from this challenge and in 25 min, $[Ca^{2+}]_i$ is still elevated at 150% of baseline. Thus, SE induces long-lasting alterations in Ca^{2+} homeostatic mechanisms that treatment with carisbamate is able to restore.

Discussion

The results of this study demonstrate that the novel AED, carisbamate, when administered immediately following in vitro SE, is able to lower $[Ca^{2+}]_i$ to baseline concentrations observed in control neurons in the hippocampal neuronal culture model of SE-induced AE. Moreover, in order to test whether immediate treatment post-SE was able to cause more long-lasting changes in these neurons, the drug was washed out of the system 12 hrs post-treatment. Interestingly, 24 hrs after the wash-out of drug, the carisbamate-treated neurons appear to have normal $[Ca^{2+}]_i$ and unaltered homeostatic mechanisms, unlike the low Mg^{2+} neurons that were not treated with the drug. At this same time point (24 hrs following wash-out of drug), the neurons that were treated with carisbamate also fail to display SREDs. Thus, it appears that lowering $[Ca^{2+}]_i$ and the restoration of homeostatic mechanisms correlates with a positive outcome, the prevention of SRED development. In the model of SE-induced AE that was used in these studies, hippocampal neuronal cultures were treated for 3 hrs with low Mg^{2+} to trigger high frequency, SE-like activity. The ability to treat these neurons after an insult such as SE and prevent the process of epileptogenesis- wherein cells begin to express SREDs- is important in addressing the significant clinical challenge of developing anti-epileptogenic agents.

Carisbamate was initially developed to be an effective AED that did not produce the unwanted side effects observed in earlier generations of carbamates such as felbamate. Several studies have started utilizing this drug in various models of epilepsy, and have

found that it displays potent neuroprotective, as well as anti-convulsant properties [178-181]. However, despite these positive results, the mechanisms of action behind these properties are currently unknown. Many groups have initiated studies aimed at better understanding how this drug works. Some groups have proposed that the anti-convulsant effects are mediated by voltage-gated sodium channels [186] and another study has affirmed these results by showing that caribsmate is able to inhibit sustained repetitive firing (SRF), an effect thought to be dependent on voltage-gated sodium channels [184]. However, the effect that carisbamate has on other channels has not been as thoroughly examined. Moreover, no studies besides the current one have examined potential mechanisms of action behind its anti-epileptogenic properties in the in vitro model. The ability to modulate Ca^{2+}, while perhaps not important in contributing to the anti-convulsant properties of carisbamate, may prove to be an important feature in terms of preventing epileptogenesis.

Ca^{2+} plays an important role as an ubiquitous second messenger; thus, alterations in $[Ca^{2+}]_i$ have been shown to significantly affect cellular functions. While it has been repeatedly demonstrated that injuries such as SE can cause profound injury to neuronal cells and trigger the activation of cell death pathways [187,188], no studies have been successful in preventing epileptogenesis following neuronal injury. Studies in our lab have implicated Ca^{2+}, and Ca^{2+} regulatory systems, as playing a key role in the development of epilepsy after an initial insult [32,63,85]. During neuronal injury, glutamate is released which

stimulates a variety of receptors, one of which is the Ca^{2+}-permeable NMDA receptor [4]. This event causes an acute elevation in $[Ca^{2+}]_i$, which is then maintained or perpetuated by Ca^{2+}-induced Ca^{2+} release systems and inhibition of Ca^{2+} uptake by sarco-endoplasmic reticulum Ca^{2+}-ATPase (SERCA). Increased $[Ca^{2+}]_i$ leads to an elevation in nuclear Ca^{2+} levels, and consequently signals the transcription of several epileptogenic/pro-apoptotic genes. These events cause alterations in neuronal functions such as excitability, transmitter release, receptor expression, and synaptic plasticity [79]. Thus, a drug that can affect $[Ca^{2+}]_i$ and Ca^{2+} homeostatic mechanisms, and in doing so prevent the plasticity changes that lead to epilepsy, may prove to be an important step in the search for anti-epileptogenic agents.

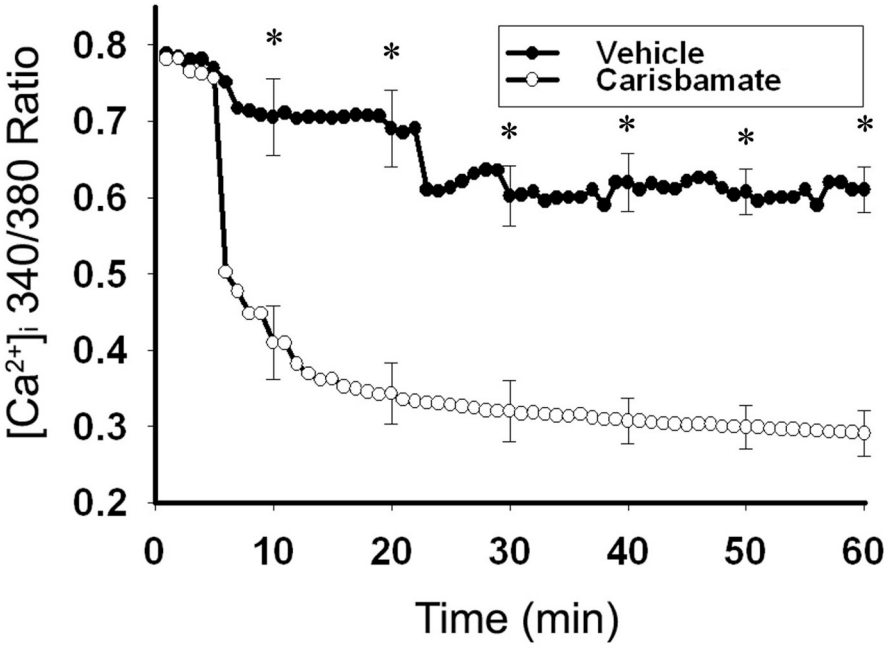

Figure 7-1. Carisbamate restores Fura-2 Ca^{2+} ratios following low Mg^{2+}-induced in vitro SE. Following 3 hrs of in vitro SE (time=0), cells were treated with either carisbamate (200μM, clear white circles) or vehicle (solid black circles). 340/380 ratios were recorded every 30 sec for 60 mins. Carisbamate is able to significantly lower $[Ca^{2+}]_i$ to levels in naïve, control neurons, whereas the vehicle-treated neurons, maintain persistent elevations. *$p<0.01$.

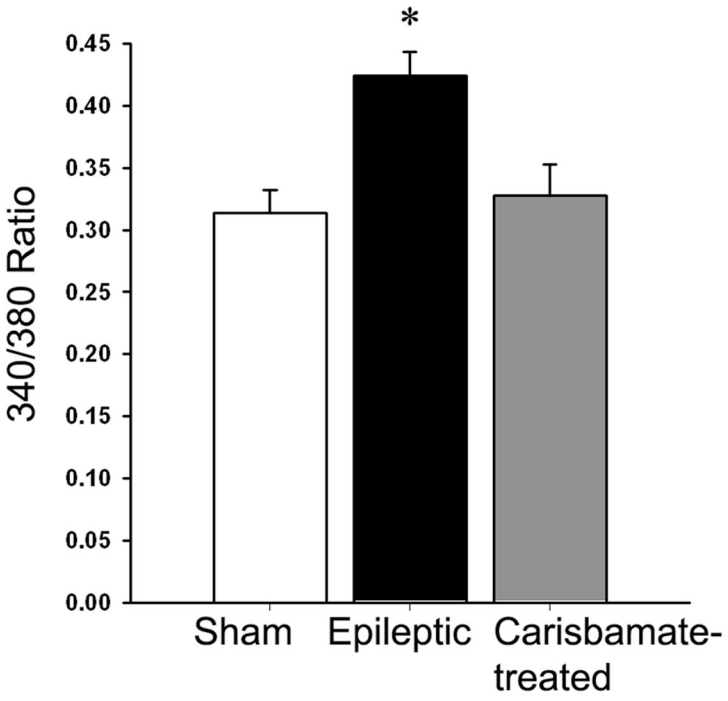

Figure 7-2. Basal Ca^{2+} levels are maintained 24 hours post-carisbamate washout. Carisbamate (200μM), when used following in vitro SE, was able to maintain baseline $[Ca^{2+}]_i$ for at least 24 hrs after drug washout. At this time point, Fura-2 ratios in the drug-treated group were significantly lower than the vehicle-treated (epileptic) neurons, 0.328 ± 0.025 and 0.424 ± 0.019, respectively. The Fura-2 ratio observed in the drug-treated cells was consistent with that of the sham controls, 0.314 ± 0.018. *$p<0.001$, n=5 plates per group.

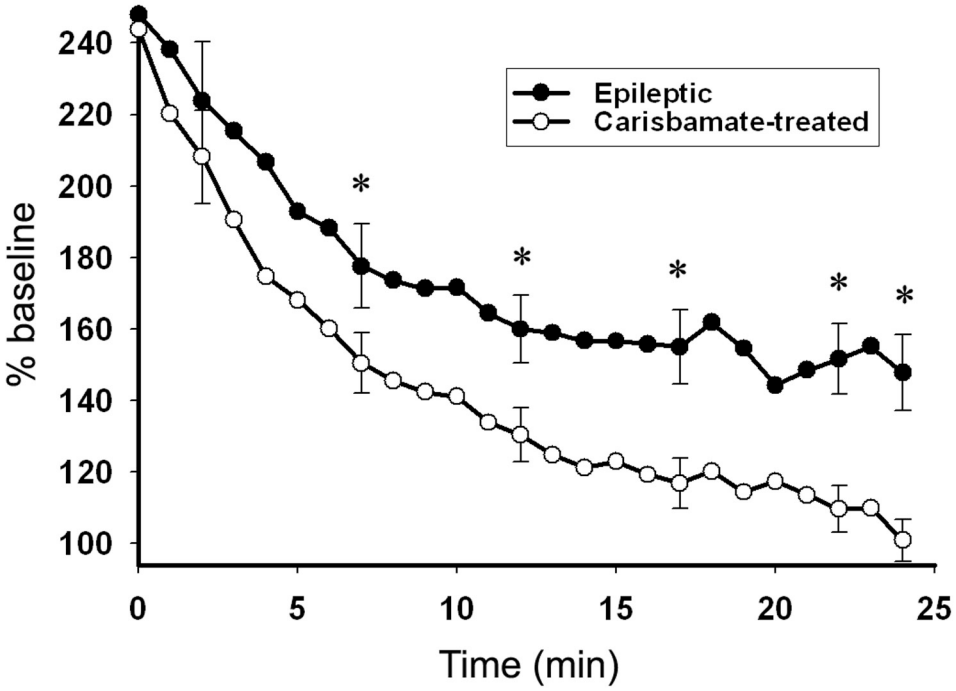

Figure 7-3. Carisbamate-treated neurons exhibit enhanced recovery following glutamate challenge. Treatment with carisbamate (200μM) following in vitro SE restores Ca^{2+} homeostatic mechanisms for at least 24 hrs post-washout of the drug. Carisbamate-treated neurons (clear white dots) show enhanced recovery from glutamate stimulation (50μM, 2min) when compared to vehicle-treated, 'epileptic' neurons (solid black dots). Neurons treated with carisbamate are able to restore $[Ca^{2+}]_i$ to basal levels in 25min. Vehicle-treated (epileptic) neurons show a diminished ability to recover from this challenge and in 25min $[Ca^{2+}]_i$ is elevated, 150% of baseline. *$p<0.05$, n=5 plates per group.

Chapter 8: Discussion

The results from these studies suggest that the Ca^{2+} plateau that exists in the in vivo pilocarpine model of SE-induced AE is also observed in the in vitro, low Mg^{2+} model. It appears that SE causes a tremendous increase in $[Ca^{2+}]_i$ which decreases slowly over time, but overall is maintained for at least 48 hrs post-SE. These sustained elevations in $[Ca^{2+}]_i$ may be responsible for long-term plasticity changes, ultimately leading to the development of SREDs, or in vitro epilepsy. Understanding the physiology behind this elevation in Ca^{2+} may offer new therapeutic targets to provide neuroprotection and, potentially, prevent epileptogenesis following neuronal injuries such as SE.

It has been demonstrated that NMDA receptors are largely responsible for the Ca^{2+} influx into the cell during excitatory events such as SE. Studies have demonstrated that pre-treatment with an NMDA antagonist prior to SE inhibited the long-lasting elevations in $[Ca^{2+}]_i$ observed post-SE, improved the outcome of SE, and prevented the development of epilepsy [41,43]. However, from a clinical standpoint, treating a patient prior to neuronal injury in the hopes of preventing epileptogenesis is not a feasible approach. Thus, the downstream consequences of NMDA receptor-mediated increases in $[Ca^{2+}]_i$ remain an important area of research in the development of potential agents to halt the development

of AE. The period between the neuronal injury and the actual development of chronic epilepsy represents a potential therapeutic window of opportunity wherein the plasticity changes that lead to epilepsy may be inhibited.

Thus, our approach was to examine the period between SE and chronic epilepsy to determine which systems contribute to the alterations in $[Ca^{2+}]_i$ and to test whether manipulating these systems pharmacologically could halt epileptogenesis. The in vitro hippocampal neuronal culture model provides an excellent tool for this endeavor in that, unlike in vivo systems, high-throughput screenings of various drugs could be performed under the strict environmental control to prevent confounders. Moreover, multiple assays could be performed to determine how each drug affected Ca^{2+} regulatory systems, cell viability, $[Ca^{2+}]_i$, and the development of SREDs. Therefore, the observation that the in vitro model mimics the in vivo model in terms of Ca^{2+} changes is an important finding that will aid in the testing of new therapeutic approaches before commencing such studies in a more complex in vivo model.

Several studies have examined various regulators of intracellular Ca^{2+} at myriad time points before, during, and after SE. These regulators include CICR systems (IP3 and RyR), Ca^{2+} binding proteins, Ca^{2+}-regulated enzymes, and Ca^{2+} channels on the cell membrane. In these studies, we focused on the RyR, a tetrameric Ca^{2+} channel present on the endoplasmic reticulum. This channel is able to gauge $[Ca^{2+}]_i$ and then release Ca^{2+} from intracellular stores based on the cytoplasmic concentration. Studies on the RyR have

utilized dantrolene, a pharmacological inhibitor of the receptor, as a tool to investigate the role of the channel in several pathologies. In the field of epilepsy, several groups have used dantrolene prior to the inciting injury to demonstrate that treatment with this drug decreases neuronal cell death [97]. Two studies have demonstrated in both animal and slice models that dantrolene protects neurons from kainic acid-induced apoptosis, thus suggesting that RyRs may play a role in mediating cell death triggered by kainic acid [189,190]. In addition, Pelletier et al. demonstrated that RyRs are involved in cell death produced in a tetanic stimulation in vitro model of seizures [191]. Other labs have shown that dantrolene can prevent the acquisition of amygdaloid kindling, another model of acquired epilepsy [105]. While these studies have made novel findings regarding the role of RyR in seizure-induced cell death, no study has examined whether dantrolene could be neuroprotective when given post-neuronal injury and if so, whether this neuroprotection could also contribute to anti-epileptogenic properties.

One group has performed several interesting studies in a model of ventricular arrhythmias in the heart and has demonstrated that increased phosphorylation of the RyR can cause them to be "leaky" and release more calcium into the cytoplasmic space [99,100]. This leak leads to the arrhythmia and can be controlled by treatment with a benzothiazepine, which stops the leak by increasing the affinity of a protein, calstabin with the receptor [100]. We demonstrated in the in vivo pilocarpine model that the expression of RyR does not change during SE, or at 1 hr, 1 day, 1 wk, or 7 wks post-SE. Thus, we hypothesized that SE triggered an increase in phosphorylation of the receptor, thereby leading to

increased Ca^{2+}. This hypothesis was confirmed with western blot using an antibody for the phosphorylated form of the receptor. We demonstrated that in the pilocarpine model of SE-induced AE, during the period of epileptogenesis hippocampal neurons show a marked increase in the phosphorylated form of the receptor. This may potentially explain how dantrolene, a RyR inhibitor, was effective in lowering Ca^{2+} to baseline levels and preventing epileptogenesis. The similarities between the ventricular arrhythmia model and epilepsy are striking: both are disorders of cellular hyperactivity triggered by ionic imbalances, RyR are important components of both cardiac cells and neurons, and benzothiazepines effectively treat the arrhythmias and benzodiazepines are the most prevalent treatment for epilepsy. Thus, these studies in cardiac tissue support our hypothesis and also suggest that Ca^{2+} dysregulation could be a result of alterations to the RyR. This represents an interesting and novel area of future research, with clinically relevant implications in both the fields of neurology and cardiology.

These studies demonstrating the role of RyR in ventricular arrhythmias and in seizure-induced cell death served to bolster our own studies. The in vitro, low Mg^{2+} model was utilized to determine if treatment with dantrolene following SE could lower $[Ca^{2+}]_i$ and prevent the development of SREDs. In this model, we observed that dantrolene is able to lower $[Ca^{2+}]_i$ to concentrations observed in control neurons, maintain these baseline levels, offer neuroprotection, and inhibit the development of SREDs. These results, in combination with the results from other studies, make dantrolene a potential therapeutic candidate to be tested in an in vivo model.

Our studies have also shown that the novel AED, carisbamate, appears to block SREDs when used on "epileptic" neurons and prevents the development of SREDs when employed immediately post-SE. We found that the drug had to be present in the cultures to inhibit SREDs; the episodes returned following wash-out of the drug. Interestingly, however, when cultures were treated with the drug for 12 hrs after low Mg^{2+} and examined 24 hrs after wash-out of the drug, the neurons failed to display SREDs. We also demonstrated that this drug not only lowered $[Ca^{2+}]_i$ post-SE but was also able to restore Ca^{2+} homeostatic mechanisms. This is the first account of this drug exhibiting anti-epileptogenic properties and further studies are being conducted to determine if similar properties exist when used in vivo. We are interested in more thoroughly examining how this drug affects regulators of intracellular Ca^{2+} release such as the RyR and IP3R.

We have also utilized another commonly used AED, levetiracetam. No mechanism of action is known for this drug, even though it is used frequently in clinical settings [110]. It is known that levetiracetam does not directly affect GABAergic neurotransmission or interact with the benzodiazepine binding site [111-113,192]. Thus, the effect of levetiracetam on Ca^{2+} and Ca^{2+} regulatory systems proved to be an interesting, unexplored potential mechanism of action. We demonstrated in hippocampal neuronal cultures that this drug did not affect baseline $[Ca^{2+}]_i$ in naïve neurons; however, when RyR and IP3R were over-stimulated, the drug inhibited CICR mediated through both of these systems. The ability to modulate Ca^{2+} levels inside hippocampal neurons is an important

characteristic, and may make the drug an ideal candidate in neuroprotection following neuronal injury.

All of these studies have aimed at modulating $[Ca^{2+}]_i$, and in doing so, determining the role that various calcium regulatory systems have in epileptogenesis and, to some extent, neuronal plasticity. The question of how Ca^{2+} affects plasticity is of utmost importance in understanding basic neuronal functions such as learning and memory, as well as long-term neuronal adaptations. Moreover, the observation that elevations in $[Ca^{2+}]_i$ are maintained post-SE in animals that develop epilepsy is not limited to models of SE-induced AE. Other conditions such as stroke and TBI can also lead to the development of chronic epilepsy and alterations in $[Ca^{2+}]_i$ have been observed in these models. Finding common pathophysiologic mechanisms that lead to the development of a single phenotype—epilepsy—following distinct injuries is important in understanding neuronal plasticity and in creating new treatments to prevent epileptogenesis. Each of these injuries, while resulting from different etiologies, is excitotoxic and has been shown to trigger the massive release of glutamate, activation of NMDA receptors, and finally, influx of Ca^{2+} into the cell [4]. As a ubiquitous second messenger, this increase is enough to trigger significant downstream effects that can affect neurotransmission, transcription, cell death pathways, and ultimately, the fate of the neuron. Therefore, the examination of Ca^{2+} dynamics in various models of injury-induced epilepsy may be of great clinical importance and may aid in our understanding of the precise role between Ca^{2+} and epileptogenesis.

Currently, approximately 30% of epileptic patients are resistant to conventionally used AEDs [72,84]; therefore, new treatment modalities are needed. In the development of new AEDs, many research groups screened large numbers of drugs in in vivo models in the hopes that they would find potential therapeutic agents. Once drugs were found that displayed these properties, the cellular and molecular mechanisms behind the anti-convulsant action were studied. We are only now starting to understand the specific effect that these agents have on individual channels, receptor expression, and myriad cellular processes. While these studies contributed greatly to the current body of knowledge on epilepsy, such massive screening efforts are not necessarily the most appropriate or efficient in the search for anti-epileptogenic agents. Research groups studying anti-epileptogenic drugs are focusing on pathophysiological mechanisms as a means of better understanding the process of epileptogenesis and as targets for therapeutics [193]. This approach has led to a significantly more thorough understanding of mechanisms of excitability and plasticity and the clinical implications of utilizing these studies to affect patient care are tremendous. Thus, observations such as changes in Ca^{2+} and Ca^{2+} homeostatic mechanisms represent a clinically interesting area of future study with therapeutic implications.

It should be noted that while many Ca^{2+} channel antagonists have been shown to exhibit anticonvulsive properties or potentiate the effects of AEDs both in experimental models and in clinical trials [90,91], there are also several reports that other Ca^{2+} channel inhibitors are completely ineffective [91]. Even less work has been done examining the effect of

Ca^{2+}-modifying agents in models of epileptogenesis, and the data demonstrating the anti-convulsive properties of these drugs suggests that numerous types of inhibitors will have to be tested. One study has shown that the NMDA antagonist, MK-801, was effective in decreasing the number of animals that developed chronic epilepsy following electrically-induced SE [43]. However, in the kainic acid-induced SE model, MK-801 did not prevent the development of epilepsy [92]. Conflicting results between different models of epileptogenesis have made the search for new therapeutics challenging [93] and have underscored the importance of utilizing several different models of epileptogenesis.

Studies aimed at discerning whether lowering Ca^{2+} to basal levels can diminish or halt the process of epileptogenesis may be of importance. The long-lasting Ca^{2+} plateau observed post-injury appears to be controlled by a multitude of channels, Ca^{2+} binding proteins, and other regulators. Currently, Ca^{2+} modifying agents have been employed for other pathologies of the CNS. For example, the NMDA antagonist, memantine, has been utilized in patients with Alzheimer's disease [89]. Interestingly, one Phase II clinical trial administered the Ca^{2+}-chelating agent, DP-BAPTA, to patients following stroke and found that this drug improved the National Institutes of Health stroke scores with no major cardiovascular or neurological side effects even at the highest dose tested [88]. The ability to modulate Ca^{2+} without causing long-lasting, severe side effects is important. Since Ca^{2+} is found ubiquitously in the body and is necessary for many cellular processes, the potential side effects of altering Ca^{2+} pharmacologically could be tremendous and thus, represent a major hurdle in the utilization of Ca^{2+} modifying drugs. The ability to

synthesize these observations on altered Ca^{2+} dynamics with those from molecular-genetic studies identifying potential genes involved in epilepsy could provide novel insight in the generation of new anti-epileptogenic targets.

Literature Cited

Literature Cited

1. Kwan P, Brodie MJ. Early identification of refractory epilepsy. *N Engl J Med*, 342(5), 314-319 (2000).
2. Duncan JS, Sander JW, Sisodiya SM, Walker MC. Adult epilepsy. *Lancet*, 367(9516), 1087-1100 (2006).
3. CDC. online <http://www.cdc.gov/epilepsy/>.
4. Delorenzo RJ, Sun DA, Deshpande LS. Cellular mechanisms underlying acquired epilepsy: the calcium hypothesis of the induction and maintainance of epilepsy. *Pharmacol Ther*, 105(3), 229-266 (2005).
5. Willmore LJ. Post-traumatic epilepsy: cellular mechanisms and implications for treatment. *Epilepsia*, 31 Suppl 3, S67-73 (1990).
6. Cavalheiro EA, Leite JP, Bortolotto ZA *et al.* Long-term effects of pilocarpine in rats: structural damage of the brain triggers kindling and spontaneous recurrent seizures. *Epilepsia*, 32(6), 778-782 (1991).
7. Lothman EW, Bertram EH, 3rd. Epileptogenic effects of status epilepticus. *Epilepsia*, 34 Suppl 1, S59-70 (1993).
8. Hesdorffer DC, Logroscino G, Cascino G, Annegers JF, Hauser WA. Risk of unprovoked seizure after acute symptomatic seizure: effect of status epilepticus. *Ann Neurol*, 44(6), 908-912 (1998).
9. DeLorenzo RJ, Hauser WA, Towne AR *et al.* A prospective, population-based epidemiologic study of status epilepticus in Richmond, Virginia. *Neurology*, 46(4), 1029-1035 (1996).
10. Hauser WA. Status epilepticus: epidemiologic considerations. *Neurology*, 40(5 Suppl 2), 9-13 (1990).
11. Wasterlain CG, Chen JW. Mechanistic and pharmacologic aspects of status epilepticus and its treatment with new antiepileptic drugs. *Epilepsia*, 49 Suppl 9, 63-73 (2008).
12. DeLorenzo RJ, Pellock JM, Towne AR, Boggs JG. Epidemiology of status epilepticus. *J Clin Neurophysiol*, 12(4), 316-325 (1995).
13. Li JM, Chen L, Zhou B, Zhu Y, Zhou D. Convulsive status epilepticus in adults and adolescents of southwest China: Mortality, etiology, and predictors of death. *Epilepsy Behav*, (2008).
14. Drislane FW. Presentation, Evaluation, and Treatment of Nonconvulsive Status Epilepticus. *Epilepsy Behav*, 1(5), 301-314 (2000).
15. Fountain NB, Lothman EW. Pathophysiology of status epilepticus. *J Clin Neurophysiol*, 12(4), 326-342 (1995).

16. Deshpande LS, Lou JK, Mian A *et al.* Time course and mechanism of hippocampal neuronal death in an in vitro model of status epilepticus: role of NMDA receptor activation and NMDA dependent calcium entry. *Eur J Pharmacol*, 583(1), 73-83 (2008).
17. Fisher RS. Animal models of the epilepsies. *Brain Res Brain Res Rev*, 14(3), 245-278 (1989).
18. McNamara JO, Huang YZ, Leonard AS. Molecular signaling mechanisms underlying epileptogenesis. *Sci STKE*, 2006(356), re12 (2006).
19. Klitgaard H, Matagne A, Vanneste-Goemaere J, Margineanu DG. Pilocarpine-induced epileptogenesis in the rat: impact of initial duration of status epilepticus on electrophysiological and neuropathological alterations. *Epilepsy Res*, 51(1-2), 93-107 (2002).
20. Pitkanen A, Kharatishvili I, Karhunen H *et al.* Epileptogenesis in experimental models. *Epilepsia*, 48 Suppl 2, 13-20 (2007).
21. Nagarkatti N, Deshpande, L.S., DeLorenzo, R.J. The role of calcium in mediating neuronal plasticity in epileptogenesis. In: *Encyclopedia of Basic Epilepsy Research.* Schwartzkroin, PA (Ed. (Elsevier, 2009) 2496.
22. Cavalheiro EA. The pilocarpine model of epilepsy. *Ital J Neurol Sci*, 16(1-2), 33-37 (1995).
23. Sombati S, Delorenzo RJ. Recurrent spontaneous seizure activity in hippocampal neuronal networks in culture. *J Neurophysiol*, 73(4), 1706-1711 (1995).
24. Deshpande LS, Lou JK, Mian A *et al.* In vitro status epilepticus but not spontaneous recurrent seizures cause cell death in cultured hippocampal neurons. *Epilepsy Res*, 75(2-3), 171-179 (2007).
25. DeGiorgio CM, Tomiyasu U, Gott PS, Treiman DM. Hippocampal pyramidal cell loss in human status epilepticus. *Epilepsia*, 33(1), 23-27 (1992).
26. Sloviter RS. Status epilepticus-induced neuronal injury and network reorganization. *Epilepsia*, 40 Suppl 1, S34-39; discussion S40-31 (1999).
27. Tsuchida TN, Barkovich AJ, Bollen AW, Hart AP, Ferriero DM. Childhood status epilepticus and excitotoxic neuronal injury. *Pediatr Neurol*, 36(4), 253-257 (2007).
28. Pitkanen A. On the way to cure epilepsy. *Expert Rev Neurother*, 4(6), 917-920 (2004).
29. Deshpande LS, Sun DA, Sombati S *et al.* Alterations in neuronal calcium levels are associated with cognitive deficits after traumatic brain injury. *Neurosci Lett*, 441(1), 115-119 (2008).
30. Sun DA, Deshpande LS, Sombati S *et al.* Traumatic brain injury causes a long-lasting calcium (Ca2+)-plateau of elevated intracellular Ca levels and altered Ca2+ homeostatic mechanisms in hippocampal neurons surviving brain injury. *Eur J Neurosci*, 27(7), 1659-1672 (2008).
31. Sun DA, Sombati S, Blair RE, DeLorenzo RJ. Long-lasting alterations in neuronal calcium homeostasis in an in vitro model of stroke-induced epilepsy. *Cell Calcium*, 35(2), 155-163 (2004).

32. Raza M, Blair RE, Sombati S *et al.* Evidence that injury-induced changes in hippocampal neuronal calcium dynamics during epileptogenesis cause acquired epilepsy. *Proc Natl Acad Sci U S A*, 101(50), 17522-17527 (2004).
33. West AE, Chen WG, Dalva MB *et al.* Calcium regulation of neuronal gene expression. *Proc Natl Acad Sci U S A*, 98(20), 11024-11031 (2001).
34. Mody I, MacDonald JF. NMDA receptor-dependent excitotoxicity: the role of intracellular Ca2+ release. *Trends Pharmacol Sci*, 16(10), 356-359 (1995).
35. Malenka RC, Nicoll RA. Long-term potentiation--a decade of progress? *Science*, 285(5435), 1870-1874 (1999).
36. Choi DW, Maulucci-Gedde M, Kriegstein AR. Glutamate neurotoxicity in cortical cell culture. *J Neurosci*, 7(2), 357-368 (1987).
37. Sherwin AL. Neuroactive amino acids in focally epileptic human brain: a review. *Neurochem Res*, 24(11), 1387-1395 (1999).
38. Liu Z, Stafstrom CE, Sarkisian MR *et al.* Seizure-induced glutamate release in mature and immature animals: an in vivo microdialysis study. *Neuroreport*, 8(8), 2019-2023 (1997).
39. Smolders I, Khan GM, Manil J, Ebinger G, Michotte Y. NMDA receptor-mediated pilocarpine-induced seizures: characterization in freely moving rats by microdialysis. *Br J Pharmacol*, 121(6), 1171-1179 (1997).
40. Meldrum BS. First Alfred Meyer Memorial Lecture. Epileptic brain damage: a consequence and a cause of seizures. *Neuropathol Appl Neurobiol*, 23(3), 185-201; discussion 201-182 (1997).
41. Rice AC, DeLorenzo RJ. NMDA receptor activation during status epilepticus is required for the development of epilepsy. *Brain Res*, 782(1-2), 240-247 (1998).
42. Hort J, Brozek G, Mares P, Langmeier M, Komarek V. Cognitive functions after pilocarpine-induced status epilepticus: changes during silent period precede appearance of spontaneous recurrent seizures. *Epilepsia*, 40(9), 1177-1183 (1999).
43. Prasad A, Williamson JM, Bertram EH. Phenobarbital and MK-801, but not phenytoin, improve the long-term outcome of status epilepticus. *Ann Neurol*, 51(2), 175-181 (2002).
44. DeLorenzo RJ, Pal S, Sombati S. Prolonged activation of the N-methyl-D-aspartate receptor-Ca2+ transduction pathway causes spontaneous recurrent epileptiform discharges in hippocampal neurons in culture. *Proc Natl Acad Sci U S A*, 95(24), 14482-14487 (1998).
45. Bardo S, Cavazzini MG, Emptage N. The role of the endoplasmic reticulum Ca2+ store in the plasticity of central neurons. *Trends Pharmacol Sci*, 27(2), 78-84 (2006).
46. Friel D. Interplay between ER Ca2+ uptake and release fluxes in neurons and its impact on [Ca2+] dynamics. *Biol Res*, 37(4), 665-674 (2004).
47. Lazarewicz JW, Rybkowski W, Sadowski M *et al.* N-methyl-D-aspartate receptor-mediated, calcium-induced calcium release in rat dentate gyrus/CA4 in vivo. *J Neurosci Res*, 51(1), 76-84 (1998).

48. Pal S, Sun D, Limbrick D, Rafiq A, DeLorenzo RJ. Epileptogenesis induces long-term alterations in intracellular calcium release and sequestration mechanisms in the hippocampal neuronal culture model of epilepsy. *Cell Calcium*, 30(4), 285-296 (2001).
49. Jin W, Sugaya A, Tsuda T, Ohguchi H, Sugaya E. Relationship between large conductance calcium-activated potassium channel and bursting activity. *Brain Res*, 860(1-2), 21-28 (2000).
50. Nagarkatti N, Deshpande LS, DeLorenzo RJ. Levetiracetam inhibits both ryanodine and IP3 receptor activated calcium induced calcium release in hippocampal neurons in culture. *Neurosci Lett*, 436(3), 289-293 (2008).
51. Cataldi M, Lariccia V, Secondo A, di Renzo G, Annunziato L. The antiepileptic drug levetiracetam decreases the inositol 1,4,5-trisphosphate-dependent [Ca2+]I increase induced by ATP and bradykinin in PC12 cells. *J Pharmacol Exp Ther*, 313(2), 720-730 (2005).
52. Carter DS, Harrison AJ, Falenski KW, Blair RE, DeLorenzo RJ. Long-term decrease in calbindin-D28K expression in the hippocampus of epileptic rats following pilocarpine-induced status epilepticus. *Epilepsy Res*, 79(2-3), 213-223 (2008).
53. Magloczky Z, Halasz P, Vajda J, Czirjak S, Freund TF. Loss of Calbindin-D28K immunoreactivity from dentate granule cells in human temporal lobe epilepsy. *Neuroscience*, 76(2), 377-385 (1997).
54. Nagerl UV, Mody I, Jeub M *et al.* Surviving granule cells of the sclerotic human hippocampus have reduced Ca(2+) influx because of a loss of calbindin-D(28k) in temporal lobe epilepsy. *J Neurosci*, 20(5), 1831-1836 (2000).
55. Baimbridge KG, Miller JJ. Hippocampal calcium-binding protein during commissural kindling-induced epileptogenesis: progressive decline and effects of anticonvulsants. *Brain Res*, 324(1), 85-90 (1984).
56. Shetty AK, Turner DA. Intracerebroventricular kainic acid administration in adult rat alters hippocampal calbindin and non-phosphorylated neurofilament expression. *J Comp Neurol*, 363(4), 581-599 (1995).
57. Lee S, Williamson J, Lothman EW *et al.* Early induction of mRNA for calbindin-D28k and BDNF but not NT-3 in rat hippocampus after kainic acid treatment. *Brain Res Mol Brain Res*, 47(1-2), 183-194 (1997).
58. Sonnenberg JL, Frantz GD, Lee S *et al.* Calcium binding protein (calbindin-D28k) and glutamate decarboxylase gene expression after kindling induced seizures. *Brain Res Mol Brain Res*, 9(3), 179-190 (1991).
59. Lowenstein DH, Gwinn RP, Seren MS, Simon RP, McIntosh TK. Increased expression of mRNA encoding calbindin-D28K, the glucose-regulated proteins, or the 72 kDa heat-shock protein in three models of acute CNS injury. *Brain Res Mol Brain Res*, 22(1-4), 299-308 (1994).
60. DeLorenzo RJ. The calmodulin hypothesis of neurotransmission. *Cell Calcium*, 2(4), 365-385 (1981).

61. Blair RE, Sombati S, Churn SB, Delorenzo RJ. Epileptogenesis causes an N-methyl-d-aspartate receptor/Ca(2+)-dependent decrease in Ca(2+)/calmodulin-dependent protein kinase II activity in a hippocampal neuronal culture model of spontaneous recurrent epileptiform discharges. *Eur J Pharmacol*, 588(1), 64-71 (2008).
62. Erondu NE, Kennedy MB. Regional distribution of type II Ca2+/calmodulin-dependent protein kinase in rat brain. *J Neurosci*, 5(12), 3270-3277 (1985).
63. Carter DS, Haider SN, Blair RE *et al.* Altered calcium/calmodulin kinase II activity changes calcium homeostasis that underlies epileptiform activity in hippocampal neurons in culture. *J Pharmacol Exp Ther*, 319(3), 1021-1031 (2006).
64. Wasterlain CG, Farber DB. Kindling alters the calcium/calmodulin-dependent phosphorylation of synaptic plasma membrane proteins in rat hippocampus. *Proc Natl Acad Sci U S A*, 81(4), 1253-1257 (1984).
65. Yamagata Y, Imoto K, Obata K. A mechanism for the inactivation of Ca2+/calmodulin-dependent protein kinase II during prolonged seizure activity and its consequence after the recovery from seizure activity in rats in vivo. *Neuroscience*, 140(3), 981-992 (2006).
66. Singleton MW, Holbert WH, 2nd, Ryan ML *et al.* Age dependence of pilocarpine-induced status epilepticus and inhibition of CaM kinase II activity in the rat. *Brain Res Dev Brain Res*, 156(1), 67-77 (2005).
67. Churn SB, Sombati S, Jakoi ER, Severt L, DeLorenzo RJ. Inhibition of calcium/calmodulin kinase II alpha subunit expression results in epileptiform activity in cultured hippocampal neurons. *Proc Natl Acad Sci U S A*, 97(10), 5604-5609 (2000).
68. Merrill MA, Chen Y, Strack S, Hell JW. Activity-driven postsynaptic translocation of CaMKII. *Trends Pharmacol Sci*, 26(12), 645-653 (2005).
69. Dong Y, Rosenberg HC. Prolonged changes in Ca2+/calmodulin-dependent protein kinase II after a brief pentylenetetrazol seizure; potential role in kindling. *Epilepsy Res*, 58(2-3), 107-117 (2004).
70. Friel DD, Chiel HJ. Calcium dynamics: analyzing the Ca2+ regulatory network in intact cells. *Trends Neurosci*, 31(1), 8-19 (2008).
71. Ben-Ari Y. Cell death and synaptic reorganizations produced by seizures. *Epilepsia*, 42 Suppl 3, 5-7 (2001).
72. Morimoto K, Fahnestock M, Racine RJ. Kindling and status epilepticus models of epilepsy: rewiring the brain. *Prog Neurobiol*, 73(1), 1-60 (2004).
73. Orrenius S, McCabe MJ, Jr., Nicotera P. Ca(2+)-dependent mechanisms of cytotoxicity and programmed cell death. *Toxicol Lett*, 64-65 Spec No, 357-364 (1992).
74. Fujikawa DG. Prolonged seizures and cellular injury: understanding the connection. *Epilepsy Behav*, 7 Suppl 3, S3-11 (2005).
75. Holmes GL. Seizure-induced neuronal injury: animal data. *Neurology*, 59(9 Suppl 5), S3-6 (2002).

76. Duncan JS. Seizure-induced neuronal injury: human data. *Neurology*, 59(9 Suppl 5), S15-20 (2002).
77. Liu RS, Lemieux L, Bell GS *et al.* Cerebral damage in epilepsy: a population-based longitudinal quantitative MRI study. *Epilepsia*, 46(9), 1482-1494 (2005).
78. Pitkanen A, Nissinen J, Nairismagi J *et al.* Progression of neuronal damage after status epilepticus and during spontaneous seizures in a rat model of temporal lobe epilepsy. *Prog Brain Res*, 135, 67-83 (2002).
79. Simpson PB, Challiss RA, Nahorski SR. Neuronal Ca2+ stores: activation and function. *Trends Neurosci*, 18(7), 299-306 (1995).
80. Sanchez RM, Dai W, Levada RE, Lippman JJ, Jensen FE. AMPA/kainate receptor-mediated downregulation of GABAergic synaptic transmission by calcineurin after seizures in the developing rat brain. *J Neurosci*, 25(13), 3442-3451 (2005).
81. Hauser WA, Hesdorffer, D.C. *Epilepsy: frequency, causes and consequences* (Demos, New York, 1990).
82. Nakatomi H, Kuriu T, Okabe S *et al.* Regeneration of hippocampal pyramidal neurons after ischemic brain injury by recruitment of endogenous neural progenitors. *Cell*, 110(4), 429-441 (2002).
83. Mangan PS, Kapur J. Factors underlying bursting behavior in a network of cultured hippocampal neurons exposed to zero magnesium. *J Neurophysiol*, 91(2), 946-957 (2004).
84. Deshpande LS, Blair RE, Nagarkatti N *et al.* Development of pharmacoresistance to benzodiazepines but not cannabinoids in the hippocampal neuronal culture model of status epilepticus. *Exp Neurol*, 204(2), 705-713 (2007).
85. Raza M, Pal S, Rafiq A, DeLorenzo RJ. Long-term alteration of calcium homeostatic mechanisms in the pilocarpine model of temporal lobe epilepsy. *Brain Res*, 903(1-2), 1-12 (2001).
86. Pal S, Limbrick DD, Jr., Rafiq A, DeLorenzo RJ. Induction of spontaneous recurrent epileptiform discharges causes long-term changes in intracellular calcium homeostatic mechanisms. *Cell Calcium*, 28(3), 181-193 (2000).
87. Sun DA, Sombati S, Blair RE, DeLorenzo RJ. Calcium-dependent epileptogenesis in an in vitro model of stroke-induced "epilepsy". *Epilepsia*, 43(11), 1296-1305 (2002).
88. The Stroke Trials Registry. (Ed.^(Eds) (The Internet Stroke Center at Washington University in St. Louis)
89. Rogawski MA, Wenk GL. The neuropharmacological basis for the use of memantine in the treatment of Alzheimer's disease. *CNS Drug Rev*, 9(3), 275-308 (2003).
90. Pisani A, Bonsi P, Martella G *et al.* Intracellular calcium increase in epileptiform activity: modulation by levetiracetam and lamotrigine. *Epilepsia*, 45(7), 719-728 (2004).
91. Kulak W, Sobaniec W, Wojtal K, Czuczwar SJ. Calcium modulation in epilepsy. *Pol J Pharmacol*, 56(1), 29-41 (2004).

92. Brandt C, Potschka H, Loscher W, Ebert U. N-methyl-D-aspartate receptor blockade after status epilepticus protects against limbic brain damage but not against epilepsy in the kainate model of temporal lobe epilepsy. *Neuroscience*, 118(3), 727-740 (2003).
93. Loscher W. Animal models of epilepsy for the development of antiepileptogenic and disease-modifying drugs. A comparison of the pharmacology of kindling and post-status epilepticus models of temporal lobe epilepsy. *Epilepsy Res*, 50(1-2), 105-123 (2002).
94. Limbrick DD, Jr., Pal S, DeLorenzo RJ. Hippocampal neurons exhibit both persistent Ca2+ influx and impairment of Ca2+ sequestration/extrusion mechanisms following excitotoxic glutamate exposure. *Brain Res*, 894(1), 56-67 (2001).
95. Racine RJ. Modification of seizure activity by electrical stimulation. II. Motor seizure. *Electroencephalogr Clin Neurophysiol*, 32(3), 281-294 (1972).
96. Hernandez-Fonseca K, Massieu L. Disruption of endoplasmic reticulum calcium stores is involved in neuronal death induced by glycolysis inhibition in cultured hippocampal neurons. *J Neurosci Res*, 82(2), 196-205 (2005).
97. Mori F, Okada M, Tomiyama M, Kaneko S, Wakabayashi K. Effects of ryanodine receptor activation on neurotransmitter release and neuronal cell death following kainic acid-induced status epilepticus. *Epilepsy Res*, 65(1-2), 59-70 (2005).
98. Niebauer M, Gruenthal M. Neuroprotective effects of early vs. late administration of dantrolene in experimental status epilepticus. *Neuropharmacology*, 38(9), 1343-1348 (1999).
99. Marks AR, Marx SO, Reiken S. Regulation of ryanodine receptors via macromolecular complexes: a novel role for leucine/isoleucine zippers. *Trends Cardiovasc Med*, 12(4), 166-170 (2002).
100. Marks AR. Novel therapy for heart failure and exercise-induced ventricular tachycardia based on 'fixing' the leak in ryanodine receptors. *Novartis Found Symp*, 274, 132-147; discussion 147-155, 272-136 (2006).
101. Dykstra CM, Ratnam M, Gurd JW. Neuroprotection after status epilepticus by targeting protein interactions with postsynaptic density protein 95. *J Neuropathol Exp Neurol*, 68(7), 823-831 (2009).
102. Acharya MM, Hattiangady B, Shetty AK. Progress in neuroprotective strategies for preventing epilepsy. *Prog Neurobiol*, 84(4), 363-404 (2008).
103. Nagarkatti N, Deshpande LS, DeLorenzo RJ. Development of the calcium plateau following status epilepticus: role of calcium in epileptogenesis. *Expert Rev Neurother*, 9(6), 813-824 (2009).
104. Obenaus A, Mody I, Baimbridge KG. Dantrolene-Na (Dantrium) blocks induction of long-term potentiation in hippocampal slices. *Neurosci Lett*, 98(2), 172-178 (1989).
105. Yoshida M, Sakai T. Dantrolene, a calcium-induced calcium release inhibitor, prevents the acquisition of amygdaloid kindling in rats, a model of experimental epilepsy. *Tohoku J Exp Med*, 209(4), 303-310 (2006).

106. Hauser WA, Annegers JF, Rocca WA. Descriptive epidemiology of epilepsy: contributions of population-based studies from Rochester, Minnesota. *Mayo Clin Proc*, 71(6), 576-586 (1996).
107. Annegers JF, Rocca WA, Hauser WA. Causes of epilepsy: contributions of the Rochester epidemiology project. *Mayo Clin Proc*, 71(6), 570-575 (1996).
108. De Smedt T, Raedt R, Vonck K, Boon P. Levetiracetam: the profile of a novel anticonvulsant drug-part I: preclinical data. *CNS Drug Rev*, 13(1), 43-56 (2007).
109. Lynch BA, Lambeng N, Nocka K *et al.* The synaptic vesicle protein SV2A is the binding site for the antiepileptic drug levetiracetam. *Proc Natl Acad Sci U S A*, 101(26), 9861-9866 (2004).
110. Sirsi D, Safdieh JE. The safety of levetiracetam. *Expert Opin Drug Saf*, 6(3), 241-250 (2007).
111. Gower AJ, Noyer M, Verloes R, Gobert J, Wulfert E. ucb L059, a novel anti-convulsant drug: pharmacological profile in animals. *Eur J Pharmacol*, 222(2-3), 193-203 (1992).
112. Noyer M, Gillard M, Matagne A, Henichart JP, Wulfert E. The novel antiepileptic drug levetiracetam (ucb L059) appears to act via a specific binding site in CNS membranes. *Eur J Pharmacol*, 286(2), 137-146 (1995).
113. Margineanu DG, Klitgaard H. Levetiracetam has no significant gamma-aminobutyric acid-related effect on paired-pulse interaction in the dentate gyrus of rats. *Eur J Pharmacol*, 466(3), 255-261 (2003).
114. Klitgaard H. Levetiracetam: the preclinical profile of a new class of antiepileptic drugs? *Epilepsia*, 42 Suppl 4, 13-18 (2001).
115. Palma E, Ragozzino D, Di Angelantonio S *et al.* The antiepileptic drug levetiracetam stabilizes the human epileptic GABAA receptors upon repetitive activation. *Epilepsia*, 48(10), 1842-1849 (2007).
116. Crowder KM, Gunther JM, Jones TA *et al.* Abnormal neurotransmission in mice lacking synaptic vesicle protein 2A (SV2A). *Proc Natl Acad Sci U S A*, 96(26), 15268-15273 (1999).
117. Custer KL, Austin NS, Sullivan JM, Bajjalieh SM. Synaptic vesicle protein 2 enhances release probability at quiescent synapses. *J Neurosci*, 26(4), 1303-1313 (2006).
118. Zona C, Niespodziany I, Marchetti C *et al.* Levetiracetam does not modulate neuronal voltage-gated Na+ and T-type Ca2+ currents. *Seizure*, 10(4), 279-286 (2001).
119. Angehagen M, Margineanu DG, Ben-Menachem E *et al.* Levetiracetam reduces caffeine-induced Ca2+ transients and epileptiform potentials in hippocampal neurons. *Neuroreport*, 14(3), 471-475 (2003).
120. Freund TF, Ylinen A, Miettinen R *et al.* Pattern of neuronal death in the rat hippocampus after status epilepticus. Relationship to calcium binding protein content and ischemic vulnerability. *Brain Res Bull*, 28(1), 27-38 (1992).
121. Lowenstein DH, Thomas MJ, Smith DH, McIntosh TK. Selective vulnerability of dentate hilar neurons following traumatic brain injury: a potential mechanistic link

between head trauma and disorders of the hippocampus. *J Neurosci*, 12(12), 4846-4853 (1992).
122. Usachev Y, Shmigol A, Pronchuk N, Kostyuk P, Verkhratsky A. Caffeine-induced calcium release from internal stores in cultured rat sensory neurons. *Neuroscience*, 57(3), 845-859 (1993).
123. Fatatis A, Caporaso R, Iannotti E *et al.* Relationship between time of activation of phospholipase C-linked plasma membrane receptors and reloading of intracellular Ca2+ stores in LAN-1 human neuroblastoma cells. *J Biol Chem*, 269(27), 18021-18027 (1994).
124. McPherson PS, Kim YK, Valdivia H *et al.* The brain ryanodine receptor: a caffeine-sensitive calcium release channel. *Neuron*, 7(1), 17-25 (1991).
125. Osugi T, Uchida S, Imaizumi T, Yoshida H. Bradykinin-induced intracellular Ca2+ elevation in neuroblastoma X glioma hybrid NG108-15 cells; relationship to the action of inositol phospholipids metabolites. *Brain Res*, 379(1), 84-89 (1986).
126. Uneyama H, Munakata M, Akaike N. Caffeine response in pyramidal neurons freshly dissociated from rat hippocampus. *Brain Res*, 604(1-2), 24-31 (1993).
127. Greene RW, Haas HL, Hermann A. Effects of caffeine on hippocampal pyramidal cells in vitro. *Br J Pharmacol*, 85(1), 163-169 (1985).
128. Koulen P, Thrower EC. Pharmacological modulation of intracellular Ca(2+) channels at the single-channel level. *Mol Neurobiol*, 24(1-3), 65-86 (2001).
129. Tong X, Patsalos PN. A microdialysis study of the novel antiepileptic drug levetiracetam: extracellular pharmacokinetics and effect on taurine in rat brain. *Br J Pharmacol*, 133(6), 867-874 (2001).
130. Yang XF, Weisenfeld A, Rothman SM. Prolonged Exposure to Levetiracetam Reveals a Presynaptic Effect on Neurotransmission. *Epilepsia*, (2007).
131. Kaminski RM, Matagne A, Leclercq K *et al.* SV2A protein is a broad-spectrum anticonvulsant target: Functional correlation between protein binding and seizure protection in models of both partial and generalized epilepsy. *Neuropharmacology*, (2007).
132. Xu T, Bajjalieh SM. SV2 modulates the size of the readily releasable pool of secretory vesicles. *Nat Cell Biol*, 3(8), 691-698 (2001).
133. Desaulles E, Boux O, Feltz P. Caffeine-induced Ca2+ release inhibits GABAA responsiveness in rat identified native primary afferents. *Eur J Pharmacol*, 203(1), 137-140 (1991).
134. Berridge MJ. Neuronal calcium signaling. *Neuron*, 21(1), 13-26 (1998).
135. Wang H, Gao J, Lassiter TF *et al.* Levetiracetam is neuroprotective in murine models of closed head injury and subarachnoid hemorrhage. *Neurocrit Care*, 5(1), 71-78 (2006).
136. Klitgaard H, Pitkanen A. Antiepileptogenesis, neuroprotection, and disease modification in the treatment of epilepsy: focus on levetiracetam. *Epileptic Disord*, 5 Suppl 1, S9-16 (2003).
137. Willmore LJ. Antiepileptic drugs and neuroprotection: current status and future roles. *Epilepsy Behav*, 7 Suppl 3, S25-28 (2005).

138. Choi DW. Glutamate neurotoxicity in cortical cell culture is calcium dependent. *Neurosci Lett*, 58(3), 293-297 (1985).
139. Choi DW. Ionic dependence of glutamate neurotoxicity. *J Neurosci*, 7(2), 369-379 (1987).
140. Limbrick DD, Jr., Churn SB, Sombati S, DeLorenzo RJ. Inability to restore resting intracellular calcium levels as an early indicator of delayed neuronal cell death. *Brain Res*, 690(2), 145-156 (1995).
141. Hauser WA, Hesdorffer DC. *Epilepsy: Frequency, Causes and Consequences* (Demos, New York, 1990).
142. McNamara JO. Emerging insights into the genesis of epilepsy. *Nature*, 399(6738 (suppl 1)), A15-A22 (1999).
143. Lothman EW, Bertram EH, 3rd, Stringer JL. Functional anatomy of hippocampal seizures. *Prog Neurobiol*, 37(1), 1-82 (1991).
144. Murray MI, Halpern MT, Leppik IE. Cost of refractory epilepsy in adults in the USA. *Epilepsy Research*, 23(2), 139-148 (1996).
145. Brodie MJ. Diagnosing and predicting refractory epilepsy. *Acta Neurol Scand Suppl.*, 181, 36-39 (2005).
146. Cramer JA, Westbrook LE, Devinsky O *et al.* Development of the Quality of Life in Epilepsy Inventory for Adolescents: The QOLIE-AD-48. *Epilepsia*, 40(8), 1114-1121 (1999).
147. Bialer M, Johannessen SI, Kupferberg HJ *et al.* Progress report on new antiepileptic drugs: A summary of the Eigth Eilat Conference (EILAT VIII). *Epilepsy Research*, 73(1), 1-52 (2007).
148. Thompson CD, Miller TA, Barthen MT *et al.* The Synthesis, In Vitro Reactivity, and Evidence for Formation in Humans of 5-Phenyl-1,3-oxazinane-2,4-dione, a Metabolite of Felbamate. *Drug Metab Dispos*, 28(4), 434-439 (2000).
149. Rogawski MA. Diverse mechanisms of antiepileptic drugs in the development pipeline. *Epilepsy Research*

New Horizons in the Development of Antiepileptic Drugs III: Innovative Strategies, 69(3), 273-294 (2006).
150. Nehlig A, Rigoulot MA, Boehrer A. A new drug, RWJ 333369 displays potent antiepileptic properties in genetic models of absence and audiogenic epilepsy. *Epilepsia*, 46(suppl 8), 215 (212.368) (2005).
151. Grabenstatter HL, Dudek FE. The use of chronic models in antiepileptic drug discovery: the effect of RWJ-333369 on spontaneous motor seizures in rats with kainate-induced epilepsy. *Epilepsia*, 45(suppl 7), 197 (192.016) (2004).
152. Francois J, Ferrandon A, Koning E, Nehlig A. A New Drug RWJ 333369 Protects Limbic Areas In The Lithium-Pilocarpine Model (li-pilo) Of Epilepsy And Delays Or Prevents The Occurrence Of Spontaneous Seizures. *Epilepsia*, 46(suppl 8), 269 (C.204) (2005).
153. White HS, Srivastava A, Klein B *et al.* The novel investigational neuromodulator RWJ 333369 displays a broad-spectrum anticonvulsant profile in rodent seizure and epilepsy models. *Epilepsia*, 47(S4), 200-201 (2006).

154. White HS, Wolf HH, Swinyard EA, Skeen GA, Sofia RD. A Neuropharmacological Evaluation of Felbamate as a Novel Anticonvulsant. *Epilepsia*, 33(3), 564-572 (1992).
155. Stefani A, Calabresi P, Pisani A *et al.* Felbamate inhibits dihydropyridine-sensitive calcium channels in central neurons. *J Pharmacol Exp Ther*, 277(1), 121-127 (1996).
156. Subramaniam S, Rho J, Penix L *et al.* Felbamate block of the N-methyl-D-aspartate receptor. *J Pharmacol Exp Ther*, 273(2), 878-886 (1995).
157. Deshpande LS, Sombati S, Blair RE *et al.* Cannabinoid CB1 receptor antagonists cause status epilepticus-like activity in the hippocampal neuronal culture model of acquired epilepsy. *Neurosci Lett*, 411(1), 11-16 (2007).
158. Churn SB, Sombati S, Jakoi ER, Sievert L, DeLorenzo RJ. Inhibition of calcium/calmodulin kinase II alpha subunit expression results in epileptiform activity in cultured hippocampal neurons. *Proc Natl Acad Sci U S A*, 97(10), 5604-5609 (2000).
159. Blair RE, Deshpande LS, Sombati S *et al.* Activation of the cannabinoid type-1 receptor mediates the anticonvulsant properties of cannabinoids in the hippocampal neuronal culture models of acquired epilepsy and status epilepticus. *J Pharmacol Exp Ther*, 317(3), 1072-1078 (2006).
160. Deshpande LS, Blair RE, Ziobro JM *et al.* Endocannabinoids block status epilepticus in cultured hippocampal neurons. *Eur J Pharmacol*, 558(1-3), 52-59 (2007).
161. Kwan P, Sills GJ, Brodie MJ. The mechanisms of action of commonly used antiepileptic drugs. *Pharmacology & Therapeutics*, 90(1), 21-34 (2001).
162. Rogawski MA, Loscher W. The neurobiology of antiepileptic drugs. *Nat Rev Neurosci*, 5(7), 553-564 (2004).
163. French JA. Refractory Epilepsy: Clinical Overview. *Epilepsia*, 48(s1), 3-7 (2007).
164. Duncan JS, Sander JW, Sisodiya SM, Walker MC. Adult epilepsy. *The Lancet*, 367(9516), 1087-1100 (2006).
165. LaRoche SM, Helmers SL. The New Antiepileptic Drugs: Scientific Review. *JAMA*, 291(5), 605-614 (2004).
166. Cramer JA, Fisher R, Ben-Menachem E, French J, Mattson RH. New antiepileptic drugs: Comparison of key clinical trials. *Epilepsia*, 40(5), 590-600 (1999).
167. Novak GP, Kelley M, Zannikos P, Klein B. Carisbamate (RWJ-333369). *Neurotherapeutics*
New Antiepileptic Drugs: Discovery, Development, and Update, 4(1), 106-109 (2007).
168. Engel D, Endermann U, Frahm C, Heinemann U, Draguhn A. Acute effects of [gamma]-vinyl-GABA on low-magnesium evoked epileptiform activity in vitro. *Epilepsy Research*, 40(2-3), 99-107 (2000).
169. Goodkin HP, Yeh J-L, Kapur J. Status Epilepticus Increases the Intracellular Accumulation of GABAA Receptors. *J. Neurosci.*, 25(23), 5511-5520 (2005).

170. Deshpande LS, Blair RE, Nagarkatti N *et al.* Development of pharmacoresistance to benzodiazepines but not cannabinoids in the hippocampal neuronal culture model of status epilepticus. *Experimental Neurology*, 204(2), 705-713 (2007).
171. McNamara JO. Emerging insights into the genesis of epilepsy. *Nature*, 399(6738 Suppl), A15-22 (1999).
172. Scharfman HE. The neurobiology of epilepsy. *Curr Neurol Neurosci Rep*, 7(4), 348-354 (2007).
173. Levy RH, Mattson, R.H., Meldrum, B.S. *Antiepileptic drugs* (Raven Press, New York, 1995).
174. Meldrum BS. Current strategies for designing and identifying new anticonvulsant drugs. In: *Epilepsy: a comprehensive textbook.* Engel, J, Pedley, T.A. (Ed. (Raven Press, New York, 1997) 1405–1416.
175. Brodie MJ. Diagnosing and predicting refractory epilepsy. *Acta Neurol Scand Suppl*, 181, 36-39 (2005).
176. Cramer JA, Westbrook LE, Devinsky O *et al.* Development of the Quality of Life in Epilepsy Inventory for Adolescents: the QOLIE-AD-48. *Epilepsia*, 40(8), 1114-1121 (1999).
177. Rogawski MA. Diverse mechanisms of antiepileptic drugs in the development pipeline. *Epilepsy Res*, 69(3), 273-294 (2006).
178. Bialer M, Johannessen SI, Kupferberg HJ *et al.* Progress report on new antiepileptic drugs: a summary of the Eigth Eilat Conference (EILAT VIII). *Epilepsy Res*, 73(1), 1-52 (2007).
179. Novak GP, Kelley M, Zannikos P, Klein B. Carisbamate (RWJ-333369). *Neurotherapeutics*, 4(1), 106-109 (2007).
180. Francois J, Boehrer, A., Nehlig, A. Effects of carisbamate (RWJ-333369) in two models of genetically determined generalized epilepsy, the GAERS and the audiogenic wistar AS. *Epilepsia*, 49, 393–399 (2007).
181. Francois J, Ferrandon, A., Koning, E., Nehlig, A. A new drug RWJ 333369 protects limbic areas in the lithium-pilocarpine model (li-pilo) of epilepsy and delays or prevents the occurrence of spontaneous seizures (abstract). *Epilepsia*, 46(Suppl.8), 269–270 (2005).
182. Keck CA, Thompson HJ, Pitkanen A *et al.* The novel antiepileptic agent RWJ-333369-A, but not its analog RWJ-333369, reduces regional cerebral edema without affecting neurobehavioral outcome or cell death following experimental traumatic brain injury. *Restor Neurol Neurosci*, 25(2), 77-90 (2007).
183. DeLorenzo RJ, Sun DA. Basic mechanisms in status epilepticus: role of calcium in neuronal injury and the induction of epileptogenesis. *Adv Neurol*, 97, 187-197 (2006).
184. Deshpande LS, Nagarkatti N, Sombati S, DeLorenzo RJ. The novel antiepileptic drug carisbamate (RWJ 333369) is effective in inhibiting spontaneous recurrent seizure discharges and blocking sustained repetitive firing in cultured hippocampal neurons. *Epilepsy Res*, 79(2-3), 158-165 (2008).

185. Deshpande LS, Nagarkatti N, Ziobro JM, Sombati S, DeLorenzo RJ. Carisbamate prevents the development and expression of spontaneous recurrent epileptiform discharges and is neuroprotective in cultured hippocampal neurons. *Epilepsia*, 49(10), 1795-1802 (2008).
186. Liu Y, Yohrling GJ, Wang Y *et al.* Carisbamate, a novel neuromodulator, inhibits voltage-gated sodium channels and action potential firing of rat hippocampal neurons. *Epilepsy Res*, 83(1), 66-72 (2009).
187. Wong J, Hoe NW, Zhiwei F, Ng I. Apoptosis and traumatic brain injury. *Neurocrit Care*, 3(2), 177-182 (2005).
188. Kharatishvili I, Nissinen JP, McIntosh TK, Pitkanen A. A model of posttraumatic epilepsy induced by lateral fluid-percussion brain injury in rats. *Neuroscience*, 140(2), 685-697 (2006).
189. Berg M, Bruhn T, Frandsen A, Schousboe A, Diemer NH. Kainic acid-induced seizures and brain damage in the rat: role of calcium homeostasis. *J Neurosci Res*, 40(5), 641-646 (1995).
190. Popescu BO, Oprica M, Sajin M *et al.* Dantrolene protects neurons against kainic acid induced apoptosis in vitro and in vivo. *J Cell Mol Med*, 6(4), 555-569 (2002).
191. Pelletier MR, Wadia JS, Mills LR, Carlen PL. Seizure-induced cell death produced by repeated tetanic stimulation in vitro: possible role of endoplasmic reticulum calcium stores. *J Neurophysiol*, 81(6), 3054-3064 (1999).
192. Gower AJ, Hirsch E, Boehrer A, Noyer M, Marescaux C. Effects of levetiracetam, a novel antiepileptic drug, on convulsant activity in two genetic rat models of epilepsy. *Epilepsy Res*, 22(3), 207-213 (1995).
193. Pitkanen A, Lukasiuk K. Molecular and cellular basis of epileptogenesis in symptomatic epilepsy. *Epilepsy Behav*, (2008).

VITA

Nisha Nagarkatti was born on February 25, 1982 in Hamilton, Ontario, Canada. She graduated from Blacksburg High School in 2000 as valedictorian of her class and attended Harvard University for her undergraduate education. At Harvard, she obtained her Bachelor of Arts in the History of Science and graduated with honors in 2004. During this period she published several papers, and was subsequently accepted in the M.D./Ph.D. program at Virginia Commonwealth University. She completed two years of medical school and then joined the lab of Dr. Robert DeLorenzo where she commenced her doctoral training studying the role of calcium in epileptogenesis. Over this period, she has published in peer-reviewed journals, authored an encyclopedia chapter on epilepsy, was awarded several merit-based scholarships and fellowships, served as a leader in many student organizations, and has presented her work at numerous meetings, as detailed below.

Publications

Nagarkatti, N., Deshpande, L.S., DeLorenzo, R.J. Dantrolene inhibits long-lasting elevations in intracellular calcium following in vitro status epilepticus and prevents the development of spontaneous recurrent epileptiform discharges in cultured hippocampal neurons. *(In preparation)*.

Nagarkatti, N., Deshpande, L.S., DeLorenzo, R.J. The novel anti-epileptic drug carisbamate (RWJ333369) modulates calcium and restores calcium homeostatic mechanisms in hippocampal neuronal cultures. *(In preparation)*.

Nagarkatti, N., Deshpande, L.S., DeLorenzo, R.J. Development of the calcium plateau following status epilepticus: the role of calcium in epileptogenesis. *Review*. Expert Rev Neurother, 9(6):813-24, June, 2009.

Deshpande, L.S., Nagarkatti, N., Ziobro, J.M., Sombati, S., Delorenzo, R.J. Carisbamate prevents the development and expression of spontaneous recurrent epileptiform discharges and is neuroprotective in cultured hippocampal neurons. Epilepsia, 49(10):1795-802, Oct, 2008.

Nagarkatti, N., Deshpande, L.S., DeLorenzo, R.J. Levetiracetam inhibits both ryanodine and IP3 receptor activated calcium induced calcium release in hippocampal neurons in culture. Neurosci Lett, 436(3):289-93, May, 2008.

Deshpande, L.S., Nagarkatti, N., Sombati, S., DeLorenzo, R.J. The novel antiepileptic drug carisbamate (RWJ 333369) is effective in inhibiting spontaneous recurrent seizure discharges and blocking sustained repetitive firing in cultured hippocampal neurons. Epilepsy Res, 79(2-3):158-65, May, 2008.

Deshpande, L.S., Blair, R.E., Nagarkatti, N., Sombati, S., Martin, B.R., DeLorenzo, R.J. Development of pharmacoresistance to benzodiazepines but not cannabinoids in the hippocampal neuronal culture model of status epilepticus. Exp Neurol, 204(2):705-13, Apr, 2007.

Boyson, J.E., Nagarkatti, N, Nizam, L, Exley, M.A., Strominger, J.L. Gestation stage-dependent mechanisms of iNKT cell-mediated pregnancy loss. PNAS, Mar 14, 2006.

Nagarkatti, N, Davis, B.A. Role of Fas and Fas Ligand in the Killing of Tumor Cells by Anti-Cancer Drugs. Cancer Chemother & Pharmacol, 51(4): 284-90, Apr, 2003.

Nagarkatti, N. Tumor-derived Fas ligand induces toxicity in lymphoid organs and plays an important role in successful chemotherapy. Cancer Immunol and Immunother, 49: 46-55, Apr, 2000.

Book Chapters

Nagarkatti, N., Deshpande, L.S., DeLorenzo, R.J. The Role of Calcium in Mediating Neuronal Plasticity in Epileptogenesis. Encyclopedia of Basic Epilepsy Research. Ed. Philip Schwartzkroin. 3 vols. Elsevier Ltd.

International Conferences

Invited to attend National Institute of Neurological Disoders (NINDS)/Association of University Professors of Neurology (AUPN)/American Neurological Association (ANA) course, "Combining Clinical and Research Careers in Neuroscience"- Washington D.C. (May 29-30, 2009)

Invited Speaker at the "Internet Generation Meets the 68 Generation Session" of the Information Society Technologies Meeting - Nice, France (November 6-8, 2000)

Invited Presenter at the 2nd annual Asian Pacific Economic Cooperation (APEC)/Asian Youth Science Festival (AYSF) - Singapore (July 24-August 4, 2000)

Invited Presenter at the Nobel Foundation's Nobel Week - Stockholm, Sweden (December, 1999)

Selected Presenter at the 4th International Conference of the Asian Clinical Oncology Society - Bali, Indonesia. "Fas-Fas ligand interactions play an important role in successful therapy of cancer." (August 3-8, 1999)

Abstracts/Meetings

Nagarkatti, N., Blair, R.E., DeLorenzo, R.J. The role of leaky ryanodine receptors in the rat pilocarpine model of acquired epilepsy. Society for Neurosciences Meeting, Chicago, IL, October 17-21, 2009.

Nagarkatti, N., Deshpande, L.S., DeLorenzo, R.J. The prevention of epileptogenesis through calcium modulation in a hippocampal neuronal culture model of status epilepticus-induced acquired epilepsy. Virginia Academy of Sciences, Richmond, VA, May 28-29, 2009.

Nagarkatti, N., Deshpande, L.S., DeLorenzo, R.J. The generation and maintenance of a long lasting calcium plateau in cultured hippocampal neurons following in vitro status epilepticus. American Epilepsy Society Meeting, Seattle, WA, Dec. 5-9, 2008.

Nagarkatti, N., Deshpande, L.S., Ziobro, J.M., DeLorenzo, R.J. Carisbamate exhibits anti-epileptogenic properties mediated through calcium modulation in cultured hippocampal neurons. Society for Neurosciences Meeting, Washington D.C., Nov. 15-19, 2008.

Nagarkatti, N., Carter, D.S., Deshpande, L.S., Blair, R.E., DeLorenzo, R.J. The inhibition of the injury-induced calcium plateau through modulation of intracellular calcium stores in an in vitro model of acquired epilepsy. Watts Day Symposium, Richmond, VA, Oct. 30, 2008.

Nagarkatti, N. and DeLorenzo, R.J. Levetiracetam inhibits both ryanodine and IP3 mediated calcium induced calcium release in hippocampal neurons in culture. American Epilepsy Society Meeting, Philadelphia, PA, Nov. 30-Dec. 4, 2007.

Nagarkatti, N., Deshpande, L.S., Blair, R.E. and DeLorenzo, R.J. The role of the injury-induced calcium plateau during epileptogenesis in mediating neuronal plasticity changes and the development of acquired epilepsy. Society for Neurosciences Meeting, San Diego, CA, Nov. 3-7, 2007.

Nagarkatti, N. and DeLorenzo, R.J. The effect of levetiracetam on IP3 and ryanodine receptor-mediated calcium induced calcium release in hippocampal neuronal culture. Watts Day Symposium, Richmond, VA, Oct. 16, 2007.

Nagarkatti, N., Deshpande, L.S., Blair, R.E., Sombati, S., Martin, B.R., DeLorenzo, R.J. Treatment of benzodiazepine-resistant status epilepticus (SE) through the use of cannabinoid CB1 agonists in the hippocampal neuronal culture model of SE. American Society of Clinical Investigators Meeting, Chicago, IL, April 13-15, 2007.

Nagarkatti, N. and DeLorenzo, R.J. Development of pharmacoresistance to benzodiazepines but not cannabinoids in the hippocampal neuronal culture model of status epilepticus. Watts Day Symposium, Richmond, VA, Oct. 23, 2006.

Awards and Honors

- Awarded Philanthropic Educational Organization (PEO) Scholar Award, $15,000 (May 2009)
- First place winner (Best Student Paper) at Virginia Academy of Sciences (VAS) Meeting (May 2009)
- Awarded American Heart Association's pre-doctoral fellowship (July 2008)
- Recipient of Sigma Xi Grant in Aid of Research (October 2002)
- Featured in Teen People magazine - "20 teens who will change the world" (February 2000)
- Winner of Pinnacle Award (Grand Award) $40,000 (Intel Young Scientist Scholarship) at the 1999 Intel International Science and Engineering Fair (ISEF) held in Philadelphia, out of 1179 participants from 40 countries.
- Winner at ISEF of Glenn T. Seaborg Award (2^{nd} Grand Award)- Trip to Nobel Prize Ceremonies in Stockholm, Sweden (December 1999)
- Winner at ISEF of the Office of Naval Research Naval Science Award $8000 (1999)

Leadership Positions

- American Physician and Scientist Association (APSA) – Institutional Representative (2007-2009); Annual Meeting Planning Committee (2008-2009).
- Virginia Commonwealth University (VCU) Women in Science (WIS) – Vice-President Community Outreach (2008-2009)
- Virginia Commonwealth University (VCU) Graduate School Mentoring Program (GSMP) – Mentor to Undergraduate (2008-2009)
- Virginia Commonwealth University (VCU) MD/PhD Program – President (2007-2008)
- Virginia Commonwealth University (VCU) Student International Health Organization (SIHO) - Vice-President for Campus Awareness (2005-present)

- VCU Hematology/Oncology Interest Group Cancer Day 2005 - organizer (March 2005)
- VCU Women in Medicine group - active member (2004-present)
- International Health Organization (IHO) - Representative on the Board. IHO is an NGO that works with health in developing countries, primarily in South Asia (2001-2003)
- Harvard University South Asian Association (SAA) - President, Publicity Chair, Freshman Representative. SAA is the 2nd largest cultural organization at Harvard University; consists of over 200 members (2001-2003)
- AIDS in India Conference - Organizer. Harvard School of Public Health (December 6, 2001)

Volunteer Work

- Organizer- Cinderella Dreams Dress Drive (VCU) (2009)
- Organizer- Women in Science Medical Career Day for middle and high school girls (VCU) (2008-09)
- Organizer- Toys for Tots Drive (VCU) (2008)
- Crossover Clinic (2006)
- Organizer- National Gandhi Day of Service (NGDOS) (2002)
- Harvard University's Refugee Youth Tutoring Program (2001)

Membership in Professional Societies

- Society for Neurosciences- Student member (2008-present).
- American Physician Scientist Association (APSA) (2006-present)
- American Academy for the Advancement of Science (AAAS)/Science Program for Excellence- Sponsored member (2006, 2007).